ANKARA UNIVERSITY

GRADUATE SCHOOL OF NATURAL AND APPLIED SCIENCES

Ph. D. THESIS

DESIGN AND CONSTRUCTION OF A SOLAR POWERED AERATION SYSTEM FOR FISH FARMS

Yohannes Berhane GEBREMEDHEN

DEPARTMENT OF AGRICULTURAL MACHINERY AND TECHNOLOGIES ENGINEERING

ANKARA
2016

THESIS APPROVAL

The thesis entitled “Design and Construction of a Solar Powered Aeration System for Fish Farms” prepared by Yohannes Berhane GEBREMEDHEN has been accepted as a DOCTOR OF PHILOSOPHY DISSERTATION under Ankara University Graduate School of Natural and Applied Sciences department of Agricultural Machinery and Technologies Engineering with the approval of the following jury members on 20/05/2016.

Supervisor: Asst. Prof. Dr. Mehmet Ali DAYIOĞLU

Jury Members:

Head: Prof. Dr. Mustafa VATANDAŞ
Ankara University, Department of Agricultural Machinery and Technologies Engineering

Member: Asst. Prof. Dr. Mehmet Ali DAYIOĞLU
Ankara University, Department of Agricultural Machinery and Technologies Engineering

Member: Prof. Dr. Hasan Hüseyin ATAR
Ankara University, Department of Fisheries and Aquaculture

Member: Prof. Dr. Türkan AKTAŞ
Namık Kemal University Department of Biosystem Engineering

Member: Prof. Dr. Can ERTEKİN
Akdeniz University Department of Agricultural Machinery and Technologies Engineering

Approved by:

Prof. Dr. İbrahim DEMİR
Graduate School Head A.

ETHICS

I declare that this thesis is prepared according to the thesis writing guidelines of Ankara University, Graduate School of Natural and Applied Sciences. All the information provided in this thesis that I prepared are true and accurate. I adhered to scientific ethics in conducting the research and collecting data. I cited all the references that are used in this thesis.

May, 20, 2016

Yohannes Berhane GEBREMEDHEN

ÖZET

Doktora Tezi

BALIK ÇİFTLİKLERİ İÇİN GÜNEŞ ENERJİLİ HAVALANDIRMA SİSTEMİNİN TASARIMI VE PROTOTİP İMALATI

Yohannes Berhane GEBREMEDHEN

Ankara Üniversitesi
Fen Bilimleri Enstitüsü
Tarım Makinaları ve Teknolojileri Mühendisliği Anabilim Dalı

Danışman: Yrd. Doç.Dr. Mehmet Ali DAYIOĞLU

Türkiye iç sularında yapılan su ürünleri üretiminde balık ölümlerinin temel nedeni çözünmüş oksijen yetersizliğidir. Sudaki çözünmüş oksijen eksikliği sabaha karşı ve beslenme sırasında oluşmaktadır. Sudaki çözünmüş oksijen seviyesi azaldıkça, balıkların solunum ve beslenme etkinlikleri, büyüme hızıyla birlikte azalmakta ve balıklar hastalıklara karşı daha hassas olmaktadır. Su ürünleri yetiştiriciliğinde kullanılan havuzlar genellikle elektrik hattı olmayan uzak alanlarda bulunmaktadır. Balık çiftlikleri için alternatif enerji kaynağı olarak güneş enerjisi sistemleri kullanılabilir.

Bu tezin amacı, balık çiftlikleri için güneş enerjisi ile çalışan prototip bir havalandırma sistemi tasarlamak ve imal etmektir. Sistem karmaşık mekanik sistem, kullanmadan hidrodinamik ilkelere dayalı olarak, yenilikçi venturi enjektör düzenlemesiyle tasarlanmıştır. Sistem model ve deneylerden alınan sonuçlara göre geliştirilmiştir. En uygun venturi büyüklüğü ve düzenlemesi, difüzör boyutu ve meme çapı hava-su akış testlerine göre belirlenmiştir. Balık havalandırma sistemi için iki prototip, Prototip I ve Prototip II geliştirilmiştir. Havalandırma sisteminde 1” x ¾” x 1” venturi enjektörler kullanılmıştır. Havalandırma sistemi; dalgıç pompa, boru ve armatürlerle bağlanan venturi enjektörler, galvaniz çelik şasi üzerine yerleştirilmiş PV güneş panelleri, jel aküler, şarj kontrol cihazı, pompa kontrol cihazı, oksijen sensörü, su sıcaklık sensörü ve otomatik kontrol biriminden oluşmaktadır. Prototip I’de 150 W’lık seri bağlanmış iki mono-kristal güneş paneli 24 derecelik eğim açısıyla güneye bakacak şekilde yerleştirilmiştir. Güneş paneli, kontrol panosu ve aküler sabittir. Prototip II’de sistemin tüm bileşenleri yüzer platform üzerine yerleştirilmiştir. 245 W’lık poli-kristal güneş paneli yüzer platformun üzerindeki şasiye yatay olarak bağlanmıştır. Her iki prototipte güneş panellerinden toplanan enerji 12 V @ 100 Ah kapasiteli iki jel aküde depolanmıştır.

Geliştirilen havalandırma sisteminin performans parametreleri değişken durumlu ASCE prosedürüne göre belirlenmiştir. 300 W’lık nominal güçte havalandırma sisteminin oksijen transfer katsayısı 5.55 h^{-1} ’dir. %70, %80 ve %90 oksijenle doyma seviyeleri için geçen zaman sırasıyla 20, 21 ve 28 dakikadır. ASCE tarafından kabul edilen standart oksijen transfer hızı (SOTR), standart havalandırma etkinliği (SAE) ve standart oksijen transfer etkinliği (SOTE) havalandırma sisteminin farklı güç tüketimleri için saptanmıştır. En iyi SOTR, SAE ve SOTE değerleri sırasıyla 0.197 kgO_2/h, 0.96 kgO_2/kWh ve % 10.7’dir. Bir saatte 2.1 kg oksijeni emme yeteneğine sahip olan havalandırma sistemi suya çözünmüş olarak bir saatte 0.2 kg oksijen transfer etmektedir. Havalandırma sistemi nominal güçte çalıştırılırken 1 kg oksijen transfer etmek için 6 MJ enerji tüketmiştir. Havalandırma sisteminin otomasyonu Arduino geliştirme kartı, DO ve su sıcaklık sensörleri ile sağlanmıştır. Prototip II havalandırma sistemi Ankara Üniversitesi Çifteler Su Ürünleri Araştırma ve Uygulama İşletmesi alabalık havuzlarında başarılı şekilde test edilmiştir.

Mayıs 2016, 114 sayfa

Anahtar Kelimeler: Havalandırma sistemi, Su ürünleri yetiştiriciliği, Çözünmüş oksijen konsantrasyonu, Güneş enerjisi, Otomatik Kontrol.

ABSTRACT

Ph. D. Thesis

DESIGN AND CONSTRUCTION OF A SOLAR POWERED AERATION SYSTEM FOR FISH FARMS

Yohannes Berhane GEBREMEDHEN

Ankara University
Graduate School of Natural and Applied Sciences
Department of Agricultural Machinery and Technologies Engineering

Supervisor: Asst. Prof. Dr. Mehmet Ali DAYIOĞLU

The main cause of fish deaths in the inland water aquaculture in Turkey is usually the lack of dissolved oxygen. The dissolved oxygen deficiency of water occurs usually at dawn and during feedings. As dissolved oxygen level in water decreases, the respiration and feeding activities of fishes, as well as growing rate decrease, and they become more susceptible to diseases. Artificial aeration systems are required for sustainable fish production. Fishponds used in aquaculture are usually located in remote areas where grid electric supply lines do not exist. Solar energy systems can be used as an alternative energy for fish farms.

The objective of this dissertation is to design and construct a prototype aeration system that will be driven by PV solar electricity for fish farms. The system was designed with an innovative arrangement of venturi injectors based on hydrodynamic principles without complex mechanical components. The system was developed based on theoretical fundamentals and findings obtained from modeling and experimental works. The best venturi size and arrangement, and diffusor size and nozzle diameter were determined from water-air flow tests. Two prototypes namely, Prototype I and Prototype II were developed for aquaculture aeration system. Venturi injectors of 1" x ¾" x 1" were used in the aeration system. The aeration system consists of a submersible pump, venturi injectors that are connected to pipes and fittings, PV panels that are mounted on galvanized steel frames, battery, charge controller, pump controller, oxygen sensor, water temperature sensor, data acquisition and automatic control units. In Prototype I, two mono-crystalline solar panels with 150 W connected in series were placed facing south with a tilt angle of 24 degree. The other components including solar panel, control box and batteries are stationary. In Prototype II, all components of the system were placed on a floating platform. A poly-crystalline solar panel of 245 W was horizontally attached to a frame on the floating platform. The energy collected by the panels was stored in two gel batteries of 12 V @ 100 Ah capacities for both Prototypes.

Performance parameters of the aeration system were determined according to non-steady state ASCE procedures. Oxygen transfer coefficient of aeration system at nominal power of 300 W is 5.55 1/h. The times elapsed for saturations of 70%, 80% and 90% are 20, 21 and 28 minutes, respectively. Performance parameters including standard oxygen transfer rate (SOTR), standard aeration efficiency (SAE) and standard oxygen transfer effectiveness (SOTE), which are defines by ASCE, were determined for different power consumptions of the aerator. The highest SOTR, SAE and SOTE values of the venturi aeration system are 0.197 kgO_2/h, 0.96 kgO_2/kWh and 10.7%, respectively. The aeration system which is capable of sucking 2.1 kg oxygen per hour transfers 0.2 kg of oxygen per hour as dissolved from into water. The aeration system consumes an energy amount of 4.2 MJ to produce one kg of oxygen when operated at optimum power. The automation of the aeration system is provided by an Arduino development board, DO and water temperature sensors. Prototype II was successfully tested in trout fish farm at Çifteler Aquaculture Research and Development Unit of Ankara University.

May 2016, 114 pages

Key Words: Aeration system, Aquaculture, Dissolved oxygen concentration, Solar energy, Automatic control

ACKNOWLEDGEMENT

I am deeply grateful to my thesis supervisor Asst. Prof. Dr. Mehmet Ali DAYIOĞLU, whose enthusiasm, creative ideas, assistance and guidance greatly contributed to this thesis work. He and his family have been like a family for me throughout my stay here in Turkey. Had it been in the absence of his great support and advice it would have been extremely difficult for me to stay and attend my study. He had been always positive, honest and supportive in all aspects of my life during my PhD study.

I would like to thank members of the thesis advisory committee Prof. Dr. Mustafa VATANDAŞ and Prof. Dr. Hasan H. ATAR for their assistance throughout this research work. They were positive and supportive even by coming to the site of the research during their holidays.

This thesis was carried out with the support of TÜBITAK under a project number of 114O095 that I am extremely thankful for the support.

I am indebted to all the members of the department of Agricultural Machinery and Technology Engineering of Ankara University for their support to attend my study and conduct this thesis work. I am also thankful to workers of the mechanical workshop of the department as well as Ankara University, Faculty of Agriculture, Fishery Products Research & Application Centre in Çifteler (Eskişehir) for their support during the construction and testing of the Aerator.

I would like to thank also the University of Ankara, Turkey Scholarships and the Turkish people and government for the chance and support to pursue my PhD study in Turkey.

At last but not least my deepest gratitude goes to my family, specially my wife Eliza Tadesse who is always on my side.

Yohannes Berhane
Ankara, May 2016

CONTENTS

LIST OF SYMBOLS

A	Surface area (m^2)
C	Dissolved oxygen concentration (mg/L)
C_l	Oxygen in gas and liquid film (mg/L)
C_m	Measured dissolved oxygen concentration (mg/L)
C_{in}	Oxygen entering to water (mg/L)
C_{out}	Oxygen leaving from water (mg/L)
C_s	Saturation dissolved oxygen concentration (mg/L)
C_t	Dissolved oxygen concentration at time t (mg/L)
C_{20}	Dissolved oxygen concentration (mg/L) at 20 ^{O}C
C_s^*	Dissolved oxygen concentration (mg/L) at infinity time of aeration
C_t	Dissolved oxygen concentration at time t (mg/L)
DO	Dissolved oxygen (mg/L)
E	Equation of time
EC	Energy consumption (kWh, J)
EC_w	Electric conductivity of water (S/m)
H'	Henry's constant ($Pa \cdot mg/L$)
I	Current (A)
I_b	Beam radiation (W/m^2)
I_d	Diffused radiation (W/m^2)
I_o	Total solar irradiance (W/m^2)
I_{pmax}	Current at maximum power (A)
I_s	Total solar radiation (W/m^2)
I_{sc}	Short circuit current (A)
K_{La}	Oxygen transfer coefficient (h^{-1})

K_{LaT}	Oxygen transfer coefficient at a temperature of T (h^{-1})
K_{La20}	Oxygen transfer coefficient at a temperature of 20 ^{O}C (h^{-1})
L_{loca}	Local latitude (degrees)
n	Number of days
n_b	Number of battery
m_a	Air mass flow rate (kg/h)
$\dot{m}_o$	Oxygen mass flow rate (kg/h)
OIF	Oxygen injection factor (kgO_2/kWh)
OTF	Oxygen transfer factor (kgO_2/kWh)
OTR	Oxygen transfer rate (kg/h)
P	Power (W)
P_{atm}	Atmospheric pressure (Pa)
P_g	Partial pressure in gas (Pa)
P_l	Partial pressure in liquid (Pa)
P_{O2}	Oxygen partial pressure (Pa)
$P_{1,2}$	Pressure at points 1,2 (Pa, kPa)
Q_w	Volumetric water flow rate (m^3/h)
Q	Flow rate (m^3/h, L/h)
RH	Relative humidity (%)
SAE	Standard aeration efficiency (kgO_2/kWh)
SOTE	Standard aeration effectiveness (%)
SOTR	Standard oxygen transfer rate (kg/h)
T	Temperature (°C)
t	Time (s, min, h)
T_a	Air temperature (°C)

T_w	Water temperature (°C)
V	Volume (m^3, L), voltage (V)
v	Velocity (m/s)
V_b	Battery voltage (V)
V_{oc}	Open circuit voltage (V)
V_{pmax}	Voltage at maximum power (V)
v_w	Wind velocity (m/s)
β	Angle of tilt (degrees)
η	Oxygen transfer efficiency (%)
δ	Solar angle of declination (degrees)
ξ_b	Deep of discharge efficiency
σ	standard deviations
γ	Surface azimuth angle (degrees)
γ_s	Solar azimuth angle (degrees)
Φ	Latitude (degrees)
η_b	Battery efficiency
ρ	Density (kg/m^3)
θ’	Angle of incidence (degrees)
θ	Temperature coefficient
θ_z	Zenith angle (degrees)
ω	Solar hour angle (degrees)

Abbrivations

AC	Alternative current
ADC	Analog digital converter
AE	Aeration efficiency

Ah	Ampere hour
ASCE	American Society of Civil Engineers
CSC	Circular stepped cascade
DC	Direct current
DO	Dissolved oxygen
EC	Electric conductivity
I2C	Inter integrated circuit
OD	Oxygen deficit
OTF	Oxygen transfer factor
OIE	Oxygen injection factor
OTE	Oxygen transfer efficiency
OTR	Oxygen transfer rate
PAP	Propeller-aspirator- pumps
PCSC	Pooled circular stepped cascade
PSA	Pump sprayer
PTO	Power take off
PV	Photovoltaic
PW	Paddle Wheel
PWM	Pulse Width Modulation
RTC	Real time clock
SAE	Standard aeration efficiency
SOTE	Standard oxygen transfer effectiveness
SOTR	Standard oxygen transfer rate
TA	Turbine aerator
TMY	Typical meteorological year

TÜİK	Türkiye İstatistik Kurumu (Turkey Statistics Agency)
VA	Venturi type aerator
VAPA	Vertical spray pumps aerator

LIST OF FIGURES

LIST OF TABLES

1. INTRODUCTION

Aquaculture and capture fishing supply the world about 154 million tonnes of water products, of which 131 million tonnes is used as food. World fish food supply has grown dramatically in the last five decades, with an average growth rate of 3.2 percent per year in the period 1961–2009, more than the 1.7 percent per year in the world's population growth. Unlike ocean and sea captures, the cage aquaculture sector has grown very rapidly during the last 20 years and is growing rapidly due to the globalization and a growing demand for water products (Anonymous 2014).

Fish production in Turkey has grown from 118 277 tonnes in 2005 to 235 133 tonnes in 2014. Fish production during the last 10 years (2005 - 2014) in Turkey is as shown in table 1.1 (Anonymous 2015). From table 1.1, it can be seen that the cage culture has been grown from 48 033 tonnes in 2005 to 107 533 tonnes in 2014.

According to Coşkun 2014, fish deaths do occur due to shortage of dissolved oxygen in fish cage farms in Turkey.

1.1 Dissolved Oxygen

Dissolved oxygen (DO) is one of the most critical water quality indicators in aquaculture because it influences the living conditions of all aquatic organisms that require oxygen. DO is crucial for fishes, most animals, phytoplankton and plants in the aquatic system.

The atmosphere contains about 21% oxygen. At standard atmospheric pressure (101.325 kPa), the pressure of oxygen in air is 21.28 kPa (101.325 x 0.21). The pressure of oxygen in air drives oxygen into water until the pressure of oxygen in water is equal to the pressure of oxygen in air. This equilibrium state is known as saturation (Boyd 1998). Although the atmospheric air contains 21% oxygen, there is slightly low soluble

oxygen in water. DO is usually expressed in milligrams per liter (mg/L), parts per million (ppm), or percentage of saturation.

Table 1.1 Turkey's water products production [×1000] (tonnes) (Anonymous 2015)

Type of fish	2005	2006	2007	2008	2009	2010	2011	2012	2013	2014
Total	118.277	128.94	139.87	152.19	158.73	167.14	188.79	212.41	233.39	235.133
Cage										
Trout-Rainbow	48.033	56.03	58.43	65.93	75.66	78.17	100.24	111.34	122.87	107.533
Trout salmon										0.45
Trout carp	0.57	0.67	0.6	0.63	0.59	0.4	0.21	0.22	0.146	0.157
Sturgeon	-	-	-	-	-	-	-	-	-	0.017
Tilapia	-	-	-	-	-	-	-	-	-	0.032
Frog	-	-	-	-	-	-	-	-	-	0.05
Sea										
Trout-Rainbow	1.249	1.633	2.74	2.721	5.229	7.079	7.697	3.234	5.186	4.812
Trout salmon										0.798
Bream	27.634	28.463	33.5	31.67	28.362	28.157	32.187	30.743	35.701	41.873
Perch	37.29	38.408	41.9	49.27	46.554	50.796	47.013	65.521	67.931	74.653
Fangri	-	-	-	-	-	-	-	-	-	0.106
Corb	-	-	-	-	-	-	-	-	-	0.039
Regius	-	-	-	-	-	-	-	-	-	3.281
Sinarit	-	-	-	-	-	-	-	-	-	0.113
Black eye	-	-	-	-	-	-	-	-	-	0.008
Pagry	-	-	-	-	-	-	-	-	-	0.075
Tuna	-	-	-	-	-	-	-	-	-	1.136
Mussel	1.5	1.545	1.1	0.196	0.089	0.34	0.005	-	-	-
Others	2	2.2	1.6	1.772	2.247	2.201	1.442	1.364	1.575	-

At sea level, typical DO concentration in saturated fresh water ranges from 14.6 mg/L (or 14.6 ppm) at 0 degrees Celsius to 7.54 mg/L at 30 degrees Celsius (Lawson 2002). The effect of DO on fish life is given in figure 1.1 (Lawson 2002). It is difficult to specify critical DO concentrations according to fish species because of physiological effects. However, as illustrated in figure 1.1, generally, fish feed best, grow fastest, and are healthiest when DO concentrations are above about 5 mg/L (Parker 2012).

The availability of DO frequently limits the activities and growth of aquatic animals. Fish deaths can result from a variety of causes but the most common are weather, fish population, pond vegetation, and the interaction of two or more causes. The critical parameter of these scenarios is oxygen level.

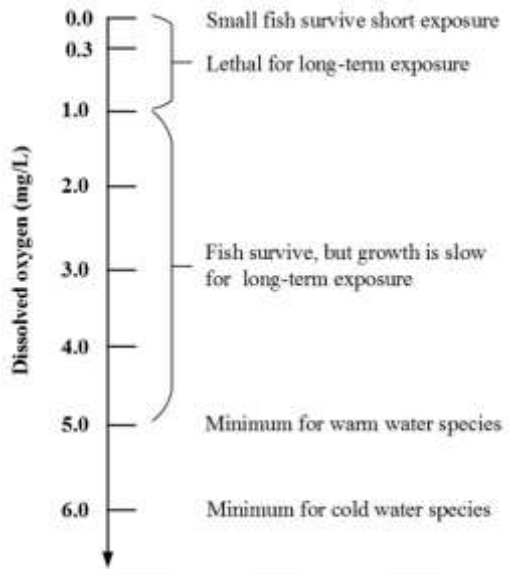

Figure 1.1 Effect of DO level on fish life (Lawson 2002)

Generally, the common causes of oxygen depletion can be listed as follows:

- Oxygen produced during the day may not be enough at night
- Sudden death of algae
- Algae decay consumes oxygen
- Less windy days reduce the diffusion of air from the atmosphere
- Ice cover during winter
- The number of fish in a pond
- Shading of the lower depth by algae
- Lower water transparency
- Turnover (mixing of the upper and bottom layers of the pond/lake).

Low DO concentration levels affect food intake, food conversion rate and yield. A concentration of 4 to 5 mg/L of DO is recommended for good fish health. Concentrations between 2 and 4 mg/L cause stress and a concentration of DO below 2 mg/L results in death of fish (Jensen et al. 1989). The relation of DO with growth rate, food conversion and mortality of fish is given in figure 1.2 (Mallya 2007).

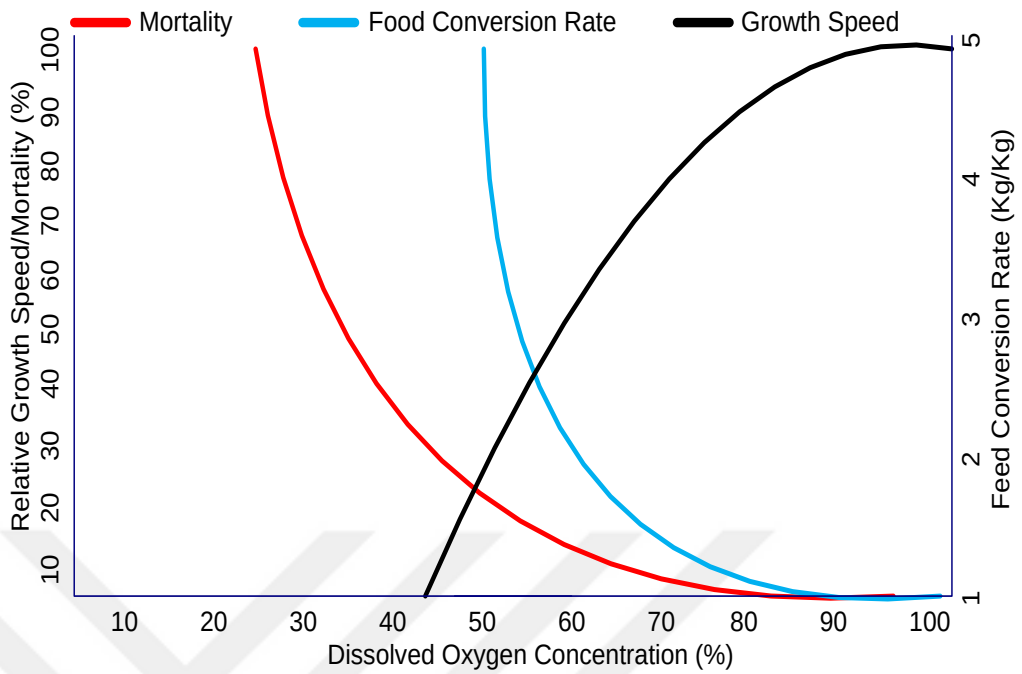

Figure 1.2 Effect of DO on fish growth rate, mortality and feed conversion (Mallya 2007)

The least oxygen concentration in ponds occurs at down specifically between 3 am and 6 am. In addition, most oxygen problems occur from June to September due to the fact that respiration rate of both animals and plants increases with temperature. The typical DO concentration variation in a pond for 24 hours is given in figure 1.3 (Floyd 2011).

DO measurements are carried out mainly by three methods: iodometry, electrochemistry and optic. Iodometry is a method based on chemical principles and it is of high accuracy. However, this method is time-consuming and prone to cause secondary pollution. Therefore, the second method is more popular. Depending on the development of sensor and detection technology, the electrochemistry method realized by DO electrode and detection circuit has more advantages. It is convenient and practical, easy to carry, and costing less time on detection that realized real-time detection. Nowadays with the advancement of sensor technologies, optical DO sensors are being used in some industries.

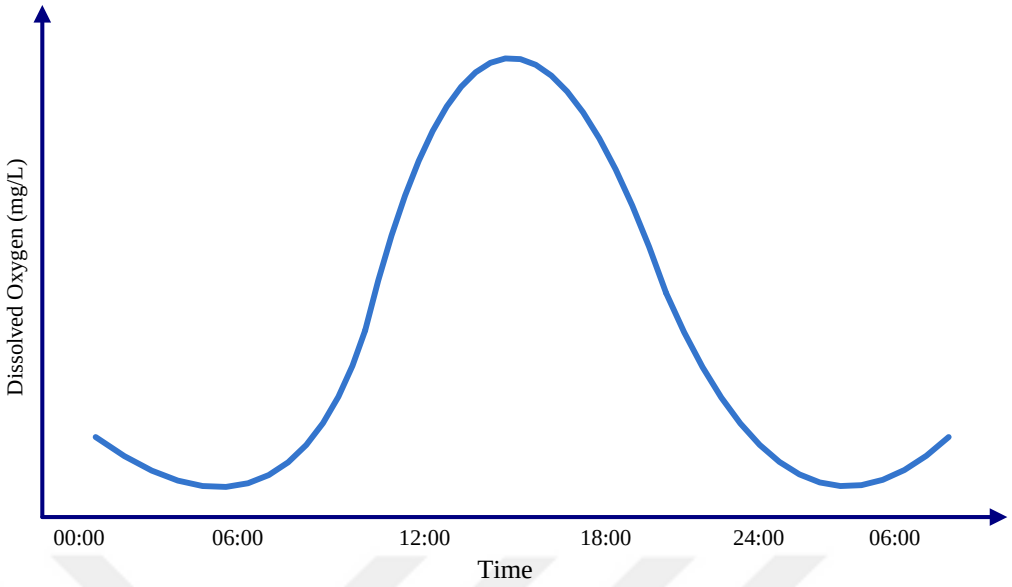

Figure 1.3 DO concentration variations in a pond for 24 hours (Floyd 2011)

Natural oxygen transfer happens by diffusion from the atmosphere to the water and by means of photosynthesis of algae in water during the presence of sun light. A schematic of the natural aeration process is presented in figure 1.4.

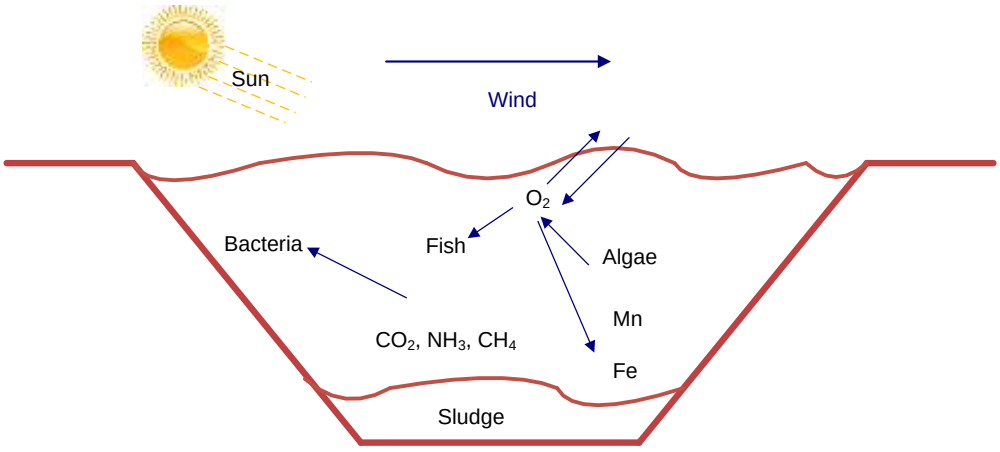

Figure 1.4 Natural aeration

Atmosphere contains vast amount of oxygen, some of which diffuse into water bodies when they are unsaturated with oxygen. Oxygen is lost to the atmosphere when pond water is supersaturated with oxygen. The driving force causing net transfer of oxygen between air and water is the difference in the tension between oxygen in the atmosphere

and oxygen in the water. Once equilibrium is reached, that is, oxygen tensions in air and water are the same, the net oxygen transfer ceases. The diffusion rate of oxygen depends primarily on the oxygen deficit in water, the amount of water surface exposed to the air and the degree of turbulence (Lekang 2013).

The DO gains and losses in ponds are given in table 1.2 and as indicated in table the gains and losses of the DO levels in ponds are very close (Parker 2012). Sometimes oxygen loss is more than oxygen gain. The difference between loss and gain cannot be balanced by natural aeration. Therefore, natural aeration is not enough for sustainable fish production. If the consumption of oxygen by the algae, fish and bacteria exceeds the amount of oxygen produced, oxygen shortage will occur.

In order to prevent oxygen shortage, artificial (mechanical) aeration is required. Mechanical aeration both in the aquaculture and other industries is carried out by machines called aerators.

Table 1.2 Dissolved oxygen balance for ponds (Parker 2012)

Source	Gain (mg/L)	Loss (mg/L)
Photosynthesis	6 – 20	-
Diffusion	1 – 5	1 - 5
Plankton respiration	-	5 -15
Fish respiration	-	2 - 6
Respiration by other organisms	-	1 - 3
Total	7 - 25	9 – 29

1.2 Aerators

Mechanical aeration is the process of adding air from the atmosphere into water to increase the DO concentration of the water body (Mueller et al. 2002). Aeration is very important not only to prevent fish deaths but also to increase production. Aeration is carried out for emergency, supplemental, or continuous cases (Wurts 2010).

Aerators for emergency case are operated temporarily when oxygen falls to or below 3 mg/L during crisis. In this case, aeration is continued until oxygen level is stabilized at 5 mg/L or higher. Supplemental aeration takes place at oxygen depletion times.

Aerators are turned on between 4:00 am and left running until 7:00 am in the morning or until oxygen level get stabilized at 5 mg/L or higher. In continuous aeration, aerators are operated continuously (24 hours daily). Some producers manage high intensity fish farms and run aerators continuously from July to the end of September or until water temperatures dropped to 18 - 20 °C. There are many different types of aerating devices that are used to mix atmospheric oxygen in to ponds in the aquaculture industry. These all types of aerators can be grouped under mechanical aerators, gravity aerators, and air diffusion systems (Lawson 2002). The common aerator types used in the aquaculture industry are the following:

- Paddle wheel (Lekang 2013; figure 1.5 a),
- Spiral paddle wheel (Boyd 1998; figure 1.5 a),
- Propeller aerator (Lekang 2013; figure 1.5 b).
- Vertical spray pumps (Lawson 2002; figure 1.5 c),
- Propeller-aspirator-pumps (Kumar et al. 2010; figure 1.5 d),
- Turbine type aerator (Anonymous 2015; figure 1.5 e)
- Venturi jet aerator (Sulzer 2015; figure 1.5 f)
- Pooled circular stepped cascade (Kumar et al. 2013; figure 1.5 g)
- Inka aerator - compressor, air pump or blower (Lekang 2013; figure 1.5 h).

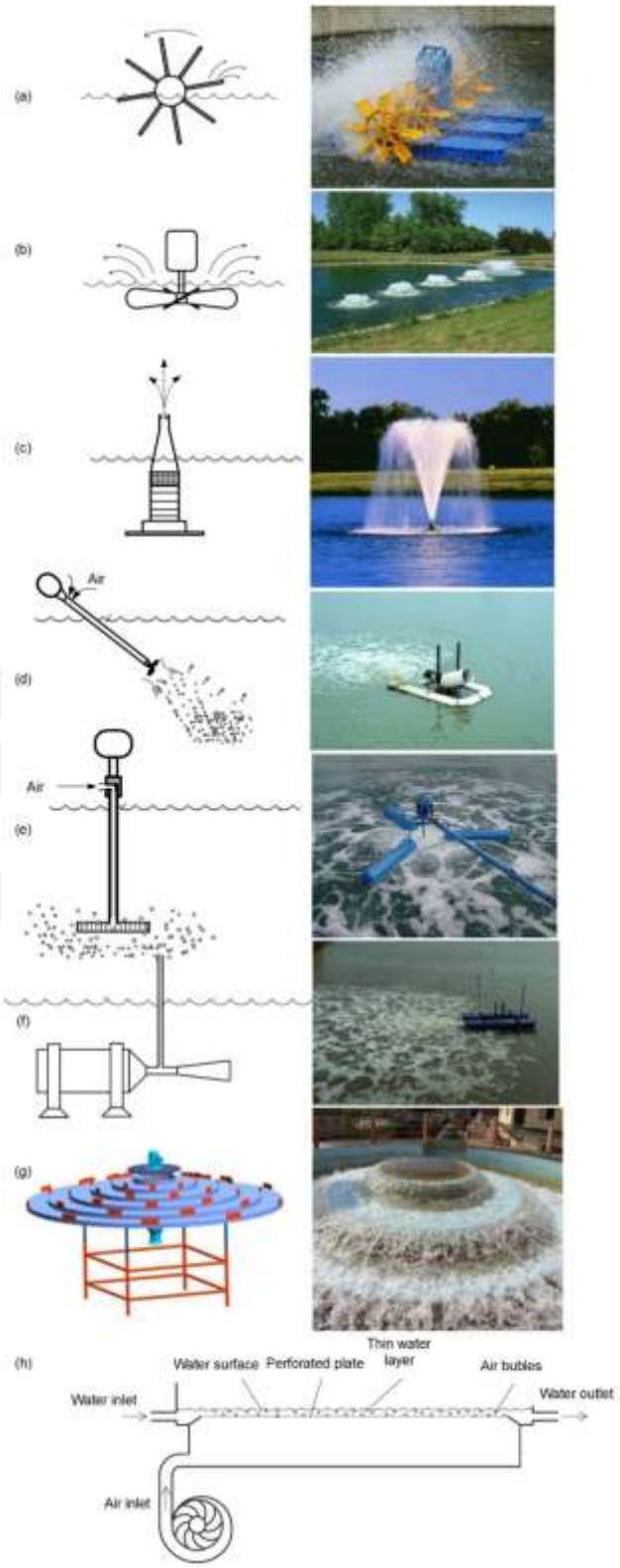

Figure 1.5 Aerator types used in aquaculture industry

In order to operate these aerators, three power sources including grid electric power, tractor power and renewable energy sources (solar and/or wind energy) can be used.

1.3 Objective of dissertation

In relation to aeration, the following gaps are observed in small and medium scale aquaculture farms in Turkey:

- No any aeration system,
- No any DO and water temperature measurement,
- Aquaculture farms are far from electric grids.

The main objective of this dissertation is to design and construct a prototype aeration system to address problems listed above. Aeration system to be developed will be a solar powered venturi type aeration system, which will be automatically controlled by a real time DO concentration and temperature measurements of ponds.

The specific objectives of study are the following:

1. Two types of prototype aerators (Prototype I and Prototype II) will be constructed. Prototype I will be constructed in such a way that, only the air injection part of the aeration system (pump and venturi injectors) will be floating but all the other components such as, solar energy and data acquisition and automation systems will be located outside the water body. In prototype II, all the components of the aeration system will be floating inside the water body.
2. In order to understand the capacity of air suction of venturi system, an ANSYS fluent model will be carried out. The size and type of all the components of the aeration system will then be selected based on the ANSYS simulation results.
3. In this paper the possible optimum fixed and adjustable tilt angles for the solar collectors to be used for prototype I will be determined. This will be carried out by using Typical Meteorological Year (TMY) data set for the province of Ankara with the help of a program written for this purpose using MATLAB software.

4. Water and airflow characteristics of venturi aeration systems will be determined experimentally. Furthermore, performance characteristics of the aeration system will be determined.
5. Since the performance of aeration process is dependent on the environmental conditions, a meteorology station will also be constructed by using latest sensors and data logger technologies.
6. Finally, data acquisition and automation system of the aeration system will be designed by using an Arduino platforms in combination with DO, temperature and power (Current and voltage) sensors.

2. THEORETICAL FUNDAMENTALS

2.1 Principles of Aeration

There is no net transfer of oxygen between air and water if the water is in balance with atmospheric oxygen. When water is unsaturated with oxygen, oxygen will transfer from air to water, and the reverse is true when water is supersaturated with oxygen. The driving force causing oxygen transfer is the difference in oxygen tension in the air and water. At equilibrium, the oxygen tension in air and water are the same, and there is no oxygen transfer. The oxygen deficit (OD) can be expressed as (Lawson 2002):

$$OD = C_s - C_m \tag{2.1}$$

Where C_s is theoretical oxygen saturation concentration under given condition; and C_m is measured oxygen concentration.

Oxygen enters or leaves water at the interface between air and water. Therefore, for the thin film of water in contact with the air, the greater the OD, the faster is the oxygen diffusion through this interface. Turbulence increases the rate of transfer by increasing the contact area of the air and water.

2.1.1 Theory of gas transfer (Henry's Law)

Henry's law describes the amount of a gas in water that can be dissolved as proportional to the partial pressure. Saturation concentration of the DO in the liquid at the gas-liquid interface can be expressed as below:

$$C_s = \frac{P_{O2}}{H'} \tag{2.2}$$

Where P_{O2} represents partial pressure of oxygen in the gas phase (Pa), H' Henry's constant ($Pa \cdot mg/L$).

2.1.2 Two - film theory

According to the two-film theory of Lewis and Whitman, the dissolution of a gas in water occurs in four major steps as illustrated in figure 2.1 (Lawson 2002, Shammas and Wang 2016):

- Oxygen moves from the bulk gaseous phase into the gas-liquid interface,
- Oxygen diffuses through laminar gas film,
- Oxygen diffuses through laminar liquid film,
- Oxygen enters the bulk liquid phase.

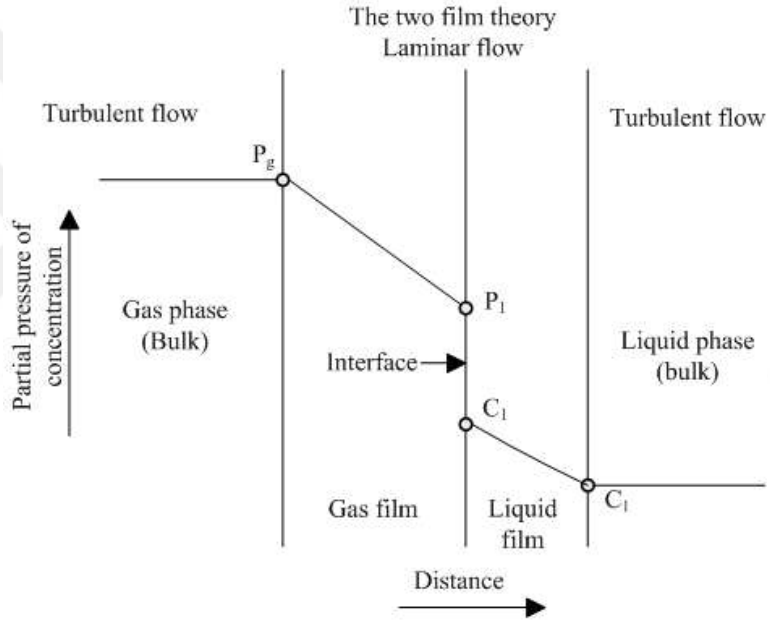

Figure 2.1 Pressure and concentration gradients in gas–liquid interface (Shammas and Wang 2016) P: partial pressure, C: oxygen concentration, g: gas, l: liquid

The oxygen transfer rate is proportional to the differential between existing and saturated concentrations of a gas in water. This relationship can be expressed by a gas transfer model given below (Lawson 2002):

$$\frac{dC}{dt} = \frac{D}{\Delta}\frac{A}{V}(C_s - C_m) \qquad (2.3)$$

Where dC/dt is gas transfer rate (mg/L.s); D diffusion coefficient; Δ the liquid film thickness (m); A area of gas-liquid interface (m^2); V volume of liquid into which the gas is diffusing (m^3); C_s (mg/L) saturation concentration of the gas and C_m (mg/L) gas concentration measured at time t. The rate of gas transfer can be increased by reducing the thickness of the interface film (Δ) or by increasing the value of (C_s- C_m).

The differential between theoretical saturated concentration and actual measured concentration of the gas is the driving force of gas transfer:

- When (C_s-C_m) is positive, gas will transfer from the atmosphere into the bulk water,
- When (C_s-C_m) is negative, gas will transfer from the water to the atmosphere.

The rate of gas transfer can be increased by reducing the thickness of the interface film (Δ) or by increasing the surface area of contact (A). However, it is difficult to measure Δ and A. The ratios (A/V) and (D/Δ) are usually combined with a coefficient called the overall gas transfer coefficient (K_{La}) as follows (Sperling 2007):

$$\frac{dC}{dt} = K_{La}(C_s - C_m) \qquad (2.4)$$

2.2 Factors Affecting Oxygen Transfer

The oxygen transfer rate of the aeration equipment is affected by environmental conditions at the time of operation. Therefore, it is important to measure the factors that affect the oxygen transfer rate. The obtained results can then be changed in to standard conditions (Sperling 2007).

The solubility of oxygen in water bodies is influenced by atmospheric and water variable. The main factors influencing the oxygen transfer rate are temperature, characteristics of water, atmospheric pressure, DO concentration and characteristics of the aerator.

2.2.1 Temperature effect

The solubility of oxygen in water bodies decreases as temperature increase. Consequently, a decrease in transfer rate dC/dt occurs. (Sperling 2007). A detailed table on saturation concentrations of DO in fresh water according to the temperature is given in Appendix 1.

The influence on K_{La} of temperature can be expressed by

$$(K_{La})_T = (K_{La})_{20}\ \theta^{(T-20)} \tag{2.5}$$

Where $(K_{La})_T$ is the oxygen transfer coefficient at temperature T; $(K_{La})_{20}$ the oxygen transfer coefficient under standard conditions; T is temperature (°C). Θ is temperature coefficient, which typically varies from 1.016 to 1.047. In freshwater, Θ value can be used as 1.024 (Lawson 2002).

2.2.2 Salinity effect

Saturation concentration of DO in water bodies decreases as salinity of water increase. The saturation concentrations of DO as a function temperature and salinity are presented again in Appendix 1.

2.2.3 Atmospheric pressure effect

The DO concentrations increase with an increase of barometric pressure. The saturation concentrations of DO as a function temperature and atmospheric pressure are presented in Appendix 2.

2.2.4 Relative humidity effect

The DO concentration increases with a decrease in relative humidity of air. DO concentration with respect to relative humidity is given in Appendix 3.

2.3 Aerator Test Procedure

The unsteady-state method defined by American Society of Civil Engineers (ASCE) is usually used for evaluating the performance of aerators. Unsteady-state tests are conducted by deoxygenating a basin of clean water with chemicals and measuring the change in DO concentration as the water is re-oxygenated by an aerator. Unsteady-state tests are carried out at two stages: (1) de-oxygenation and (2) re-oxygenation (Anonymous 2007). The theoretical chemical requirement for de-oxygenation is 7.88 mg/L of Sodium Sulfite (Na_2SO_3) for 1.0 mg/L of DO. Additionally cobalt chloride ($CoCl_2.6H_2O$) is used at a concentration of 0.1-0.5 mg/L as a catalyzer (Lawson 2002) for each mg/L of DO. Sodium sulfite is added in amounts usually equal to 25 % more of the stoichiometric requirement (Stenstrom et al. 2006). Due to the addition of sodium sulfite catalyzed with Cobalt chloride the DO level of water in a pool is reduced to zero. After de-oxygenating, The DO concentration starts to increase due to the aeration effect of a turned-on aerator and DO concentrations are monitored throughout the re-oxygenation stage.

2.3.1 Performance characteristics of aerator

Three different main performance parameters are used to evaluate the characteristics of aerators (Anonymous 2007):

- Standard oxygen transfer rate (SOTR): SOTR describes the amount of oxygen transferred to water body in kg O_2/h.
- Standard Aeration Efficiency (SAE): SAE is expressed as oxygen transfer per unit power input under standard conditions (0 mg/L, 20°C, and clean water) in SAE is kg O_2/kWh.
- Standard oxygen transfer effectiveness (SOTE): SOTE describes the amount of the injected oxygen that becomes dissolved in water and is expressed in percentage.

The selection of aerators for aquaculture aeration can be done by the oxygen transfer capacity, power requirement and total cost of the systems.

Generally, the factors used for selection of aerator are:

- Fish pond size (surface area and depth)
- Type and availability of energy source
- Cases of aeration (emergency, supplemental or continuous)
- Aerator capacity (performance characteristics)
- Seasonal factors
- Type and number of fish in fish pond.

The SOTR and SAE values for the commonly aerators shown at figure 1.5 are given in table 2.1.

Table 2.1 SOTR and SAE values of some aerators used as current

Aerator type	**SOTR**	**SAE**	**References**
Paddle wheel	2.5 - 23.2	1.1 - 3	Lawson, 2012
Propeller-aspirator- pumps	0.454	0.304	Kumar, 2013
Vertical spray pumps	0.3 – 10.9	0.7 – 1.8	Boyd, 1998
Pump sprayer	11.9 – 14.5	0.9– 1.9	Boyd 1998
Turbine aerator	0.6 – 3.9	1.2 – 1.8	Oxy, 2015
Venturi type	0.09 – 0.31	0.06 – 0.21	Zhu, 2007

2.4 Venturi Effect

Venturi effect is defined as a reduction of the fluid pressure when fluid passes through diminished cross-section of a pipe. By utilizing the venturi effect, air can be transferred from the atmosphere into water without any mechanical action.

Venturi principle that can be used in the design of the aeration system is expressed based on the Bernoulli principle, the flow velocity (V_2) of fluid increases, the pressure (P_2) drops due to diminishing in cross section of a pipe as shown in figure 2.2, when pressure at point (2) drops below atmospheric pressure, air is sucked in from the atmosphere.

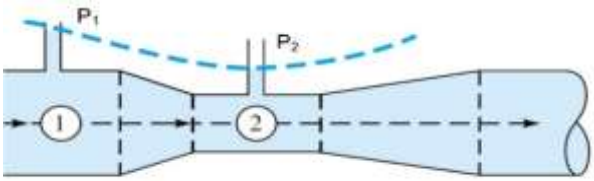

Figure 2.2 Venturi effect principles

According to the continuity equation:

$$A_1V_1 = A_2V_2 \tag{2.6}$$

Where A_1 and A_2 are the areas, V_1, and V_2 are velocities at points (1) and (2), respectively.

According Bernoulli equation, total energy (pressure and kinetic energy) between points (1) and (2) is balanced:

$$\frac{P_1}{\rho} + \frac{V_1^2}{2} = \frac{P_2}{\rho} + \frac{V_2^2}{2} \tag{2.7}$$

Where P_1 and P_2 are pressures at points (1) and (2), ρ is density of the fluid flowing through the venturi.

By combining the continuity and Bernoulli equations, pressure at point 2 (P_2) is calculated as:

$$P_2 = P_1 + \rho\frac{V_1^2}{2}\left(1 - \left(\frac{A_1}{A_2}\right)^2\right) \tag{2.8}$$

When the pressure at point 2 (P_2) is less than the atmospheric pressure, air form the atmosphere will start to flow into the fluid.

2.5 Solar Energy Calculations

In designing of solar energy systems, the amount of solar energy incoming to solar panels is represented as irradiance and insolation. Irradiance is the instantaneous radiant power incident on a surface, per unit area. Usually, it is expressed in Watts per square

meter (W/m^2). Insolation is defined as the integration of the irradiance over a specified period that is typically, hourly, daily, monthly, and yearly. The daily insulations for example are expressed in Watt-hours per square meter per day ($Wh/m^2/day$), kilowatt-hours per square meter per day ($kWh/m^2/day$), Mega Joule per square meter per day ($MJ/m^2/day$ or $kWh/m^2/year$).

The intensity of solar radiation incoming on a plane on the earth varies according to hours of the day and seasons of the year, latitude of location. Incident solar radiation falling on a solar panel can be maximized by using an optimum tilt angle (Yadav et al. 2013). This can be achieved manually or automatically, which determines optimum panel slope angles or using by solar tracking systems. However, tracking systems are more expensive than the fixed ones due to their moving components (Ahmad and Tiwari 2009, Keshavarz et al. 2012).

For this purpose, the geometric relationships between a plane on the earth and the incoming beam solar radiation has to be described by means of solar-earth relationship angles given schematically in figure 2.3 and all the equations from 2.9 to 2.17 are taken from Duffie and Beckman 2013

- Latitude ($-90° \leq \Phi \leq 90°$) is the angular location north or south of the equator, north positive. The latitude angle are usually given in degrees and minutes as the following:

$$\Phi = \Phi_1 + \frac{\Phi_2}{60} \tag{2.9}$$

- Declination ($-23.45° \leq \delta \leq 23.45°$) is the angular position of the sun at solar noon (i.e., when the sun is on the local meridian) with respect to the plane of the equator, north positive as the following according to the day of the year (n):

$$\delta = (57.3) \times 0{,}006918 - 0{,}399912 \times \cos(B)) + (0{,}070257 \times \sin(B)) - (0.006758 \times \cos(2 \times B)) + (0.000907 \times \sin(2 \times B)) - (0.002697 \times \cos(3 \times B)) + (0.00148 \times \sin(3 \times B))) \tag{2.10}$$

$$B = \frac{360}{365}(n - 1) \quad (2.11)$$

- Slope ($0° \leq \beta \leq 90°$) is the angle between the panel plane and the horizontal plane.
- Surface azimuth angle ($-180° \leq \gamma \leq 180°$) is the deviation of the projection on a horizontal plane of the normal to the surface from the local meridian, with zero due south, east negative, and west positive.
- Solar altitude angle (α_s) the angle between the horizontal and the line to the sun, that is, the complement of the zenith angle.
- Zenith angle (θ_z) is the angle between the vertical and the line to the sun, that is, the angle of incidence of beam radiation on a horizontal surface.

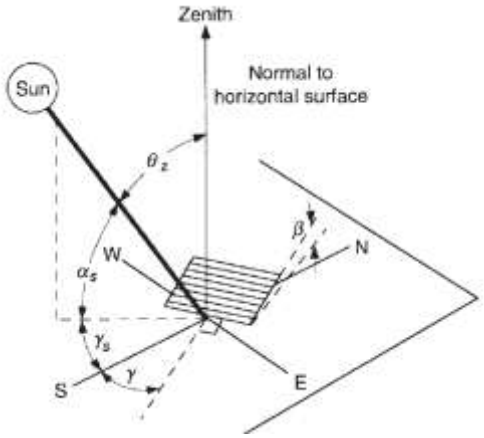

Figure 2.3 Sun - collector relationship (Duffie and Beckman 2013)

- Incidence angle (θ') is the angle between the beam radiation on a surface and the normal to that surface for a solar panel of β tilt angle facing south in the northern hemisphere:

$$\theta' = \cos^{-1}[\sin\delta \sin(\Phi - \beta) + \cos\delta \cos(\Phi - \beta) \cos\omega] \quad (2.12)$$

- Hour angle (ω) is the angular displacement of the sun east or west of the local meridian due to rotation of the earth on its axis at 15◦ per hour; morning negative, afternoon positive:

$$\omega = (\text{Solar time} - 12) \times 15 \quad (2.13)$$

- Solar azimuth angle (γ_s) the angular displacement from south of the projection of beam radiation on the horizontal plane.

The relationship between solar time and standard time must be known to describe the position of the sun. However, two corrections are necessary to convert standard time to solar time:

$$\text{Solar time} - \text{Standard time} = 4 \times (L_{std} - L_{loc}) + E \quad (2.14)$$

- Firstly, the difference between the standard meridian longitude (L_{std}) and the observer's longitude (L_{loc}) is taken into account. The sun takes 4 minutes to transverse 1° of longitude:

$$L_{std} = (\text{Time zone of the area}) \times 15 \quad (2.15)$$

- Second correction is the equation of time (E), which takes into account the disturbances in the earth's rate of rotation:

$$E = 229.2 \times (0000075 + 0.001868 \times \cos(B) - 0.032077 \times \sin(B) - 0.014615 \times \cos(2 \times B) - 0.04089 \times \sin(2 \times B)) \quad (2.16)$$

The total solar radiation incident on a tilted surface consists of mainly two components: beam (I_b) and diffuse radiation (I_d):

$$I_s = \frac{I_b \times \cos(\theta') + I_d \times (1 + \cos\beta)}{2} \quad (2.17)$$

The choice of tilt angle for a solar panel is fundamental for performance of PV panel depends on the tilt angle of the panel with respect to the horizontal plane.

2.6 Planning of Solar Power

In a stand-alone PV system, estimating the energy requirement and evaluating the available solar radiation are the most important tasks. In planning, seasonal and daily

load variations must be known. In order to evaluate daily energy need required for a system, the types and utilization of load types, their power consumptions, daily working hours and appropriate safety factors should be considered by designers as defined at table 2.2.

Table 2.2 Assessing form for total energy requirement related to loads of system

a	b	c	d	e	f = c x d x e
Load	Number	Power consumption (W)	Daily working hours (h/day)	Safety factor	Daily energy need (Wh/day)
1					
2					
3					
…					
Total load		Total power cons.			

The total daily energy requirement (Watt-hour rating-Wh) is evaluated from table 2.2 during assessing of all loads used in system.

The battery should be large enough to store sufficient energy to operate the pump at night and cloudy days. To find out the size of battery, the following steps have to be followed (Foster et. al 2010):

$$\text{Battery Capacity (Ah)} = \frac{(\text{Total daily energy required}) \times (\text{Days of autonomy})}{\eta_b \times \xi_b \times n_b \times V_b} \quad (2.18)$$

Where, η_b is battery efficiency, ξ_b is deep of discharge efficiency, n_b battery number, V nominal battery voltage.

The system must be capable of generating enough power even in the worst climatic condition. The suitable panel sizing is determined by total daily energy requirement and equivalent hours of sunshine.

$$\text{Panel Nominal Power} = \frac{(\text{Total daily energy required})}{(\text{hours of sunshine})} \quad (2.19)$$

The battery type recommended for PV solar system is deep cycle battery. Deep cycle batteries are specifically designed to be discharged to low energy level and rapid recharged or cycle charged and discharged day after day for years.

3. LITERATURE REVIEW

Many studies have been conducted with respect to aerator applications, such as ground water treatments (Ann et al. 2005, Chachuata et al. 2005, Siabi 2008), agriculture (Mukhtar et al. 2010), treatment of municipal wastes (Liu et al. 2011), aquaculture (Boyd and Tucker 1998, Kumar et al. 2010, 2013), food and beverage industry bioreactors (Kadzinga 2015). Although aeration systems are used in different areas, in this section only literatures reviewed in relation to aquaculture including aeration, data monitoring, automation and solar energy technologies are presented.

Boyd and Watten (1989), Tucker and Robinson (1990) said that aeration is required to increase fish yields and profits. They also emphasized that, aerators must be installed when the maximum sustained feeding rate exceeds about 39 kg/ha/day for catfish ponds. Boyd (1998) published a review paper about pond water aeration systems and discussed about aeration principles, type of aerators and performance characteristics of aerators in detail.

Applebaum et al. (2001) implemented solar power for aeration of fishponds. In their work, they used PV solar electricity to power a paddle wheel aerator connected to a permanent magnet DC motor. They tested the aerator for two years and achieved satisfactory results. Figure 3.1 shows the constructed PV system based aeration system.

Moulick et al. (2002) made a prediction of aeration performance of paddle wheel aerators. They studied the effect of geometric and dynamic variables on aeration process based on dimensional analysis. In doing so, they conducted experiments in brick masonry rectangular tanks of dimensions 2.9×2.9×1.6 and 5.9×2.9×1.6 m. The researchers finally come up with simulation equations uniquely correlating SAE, with non-dimensional numbers which can predict the aeration performance of paddle wheel aerators.

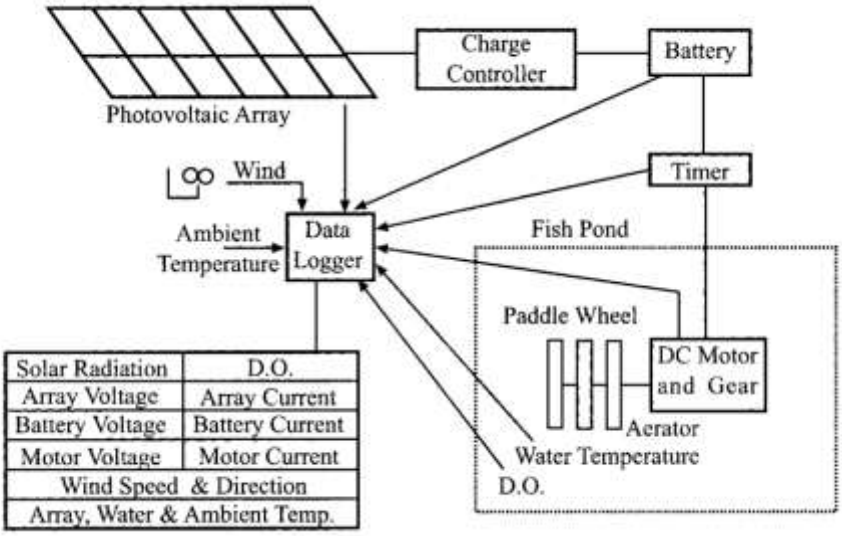

Figure 3.1 Photovoltaic powered paddle wheel aerator (Applebaum et al. 2001)

Laksitanonta and Singh (2003) designed a venturi type aerator and study its performance characteristics and oxygenating capacity. The aerators performance were determined by first removing the DO with the help of sodium sulfite and cobalt chloride chemicals and then re - aerating the water by operating the venturi type aerator. Finally, the researchers concluded that, oxygen improvement can be increased with an increase in volume flow rate of water and the performance of the venturi type aerator at two different depths of the aerator were similar.

Cancino et al. (2004) designed and manufactured a PV solar panel driven high efficiency surface type centrifugal aeration system for fish ponds. The work was carried out by testing 23 different rotor configurations. The different configurations were based on type of propeller, inlet and exit angles of the blades and the rotor's immersion percentage. They found a maximum SAE of 1.805 kg/kWh and concluded that aeration efficiency was directly proportional to Froude number, but was inversely proportional with the speed and diameter of the propeller.

Pearson and Green (2006) made a data acquisition system of DO concentration and temperature measurement at different fishpond depths. A floating system that can carry a maximum of 12 kg load was designed with connecting elements, such as PVC pipes,

90^{o} elbows and T fittings. Sensors were placed inside a housing to prevent environmental effect. Solar panel (12 V, 5 W) and lead acid dry battery (7 Ah) were used to power a data logger and sensors. The system was programmed to make measurements every second and to record the average measurements of 10 seconds. The system was used to measure at a depth of 0.25 to 0.75 m inside a fish pond.

Romaire and Merry (2007) installed a paddle wheel aerator into three fish ponds an make a comparison with three other control fish ponds of the same type. From the research, it had been found that the DO concentrations in control ponds were observed to reach below 3 mg/L during critical times 4 to 5 times more than that of the aerated ponds. A graph of DO plotted for both the non- aerated and aerated ponds is given in figure 3.2.

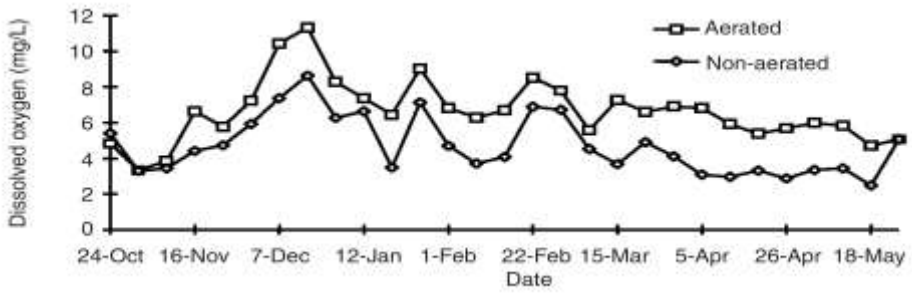

Figure 3.2 DO concentrations for aerated and non-aerated ponds (Romaire and Merry 2007)

Zhu et al. (2007) developed a venturi type - aerator. They tested air injection modules consisting of single and multiple venturies connected in series and parallel. The experimental setup used during the research is schematically given in figure 3.3. From the research, the higher aeration efficiencies were observed for the parallel design of the two modules (0.14 and 0.10 kg O_2/kWh) as compared to those in series design (0.07, 0.06, and 0.06 kg O_2/kWh). In the same way, the oxygenation capacities were also significantly higher for parallel modules (0.22 and 0.15 kgO2/h) than for series modules (0.10, 0.09, and 0.09 kgO2/h).

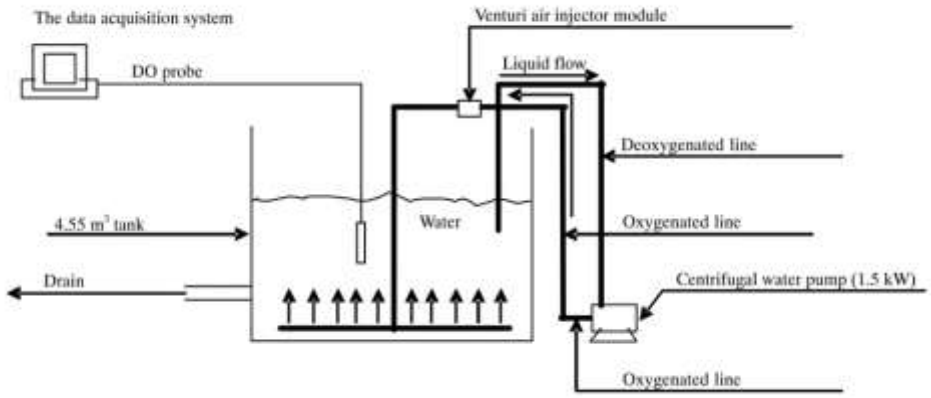

Figure 3.3 Experimental setup for venturi type aeration development (Zhu et al. 2007)

Neelamegam et al. (2008) designed and constructed a microcontroller based data collection system for fish tanks to control the temperature, light, pH and DO of the tanks. The system was effective, quick and cheap. The researchers concluded that by implementing the system, fish growth rate, quantity and quality could be improved.

Ghomi et al. (2009) made an experimental study of nozzle diameters, aeration depths and angles on standard aeration efficiency (SAE) in a venturi aerator. A 1.1 kW submersible water pump with a venturi air injector was used in this study to examine the effects of three factors including nozzle diameter (14, 17 and 20 mm), aeration depth (20, 40 and 60 cm), and aeration angle (0, 22.5 and 45°) on standard aeration efficiency (SAE). The greatest oxygen transfer efficiency in this study was determined by using 14 mm nozzle size, 60 cm depth of aeration, and 45° angle of venturi tube in water aeration.

Kumar et al. (2010) evaluated performance of propeller-aspirator-pump aerator. Aeration experiments were conducted in a brick masonry tank to study the effects of positional angle of propeller shaft, submergence depth and rotational speed of shaft on standard aeration efficiency (SAE) of a propeller-aspirator-pump aerator. As a result, they achieved a maximum SAE of 0.42 kg O_2/kWh.

Dong et al. (2009, 2012) discussed the effect of aeration due to venturi arrangements. Six venturi aerator modules were evaluated and the results indicated that better aeration efficiencies could be achieved by simply changing the way the venturi aerators were connected. Among all the configurations examined, three venturies connected in parallel were able to bring more oxygen into water than the others (Figure 3.4). An increase in liquid flow rate led to an enhancement of the oxygen transfer coefficients, but the improvement was reduced if the liquid flow rate was too high. The oxygen transfer coefficient was found to have a relationship with the depth of diffusing pipes (surface aeration depth) for the surface aeration system and an optimal depth of around 40 cm was obtained from their study. The maximum SAE obtained in this paper was 0.21 kg O_2/kWh for three venturies connected in parallel.

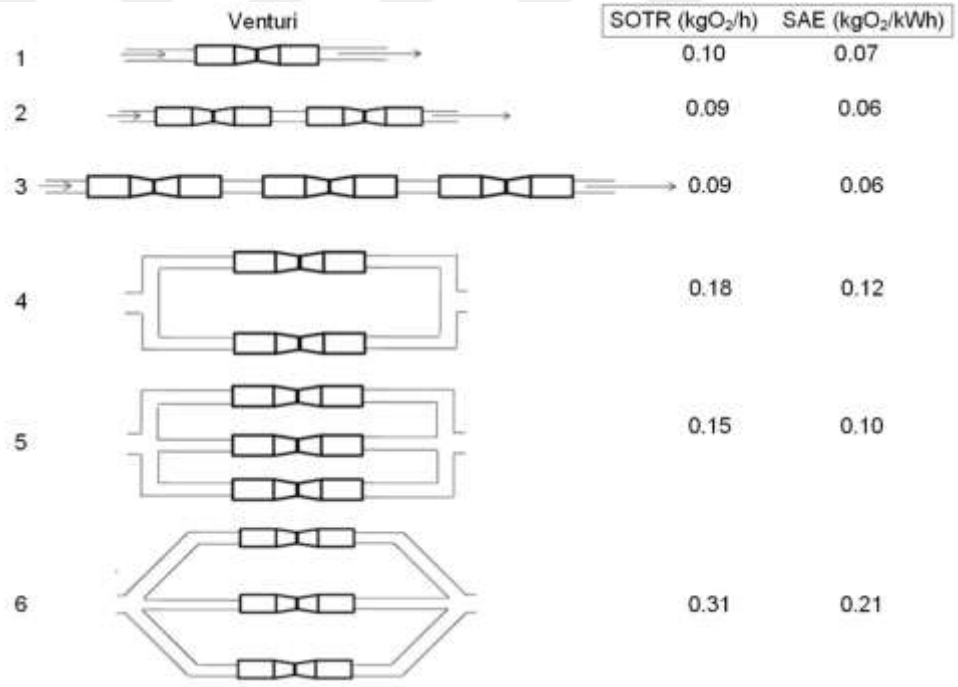

Figure 3.4 Different arrangements of venturies for efficiency improvements (Dong et al. 2012)

Kumar et al. (2013) conducted a research in a brick masonry tank of dimension 4 m × 4 m × 1.5 m to study the design characteristics of pooled circular stepped cascade (PCSC) aeration system. Based on dimensional analysis, non-dimensional numbers related to geometric, dynamic and process parameters were proposed. Simulation equations for oxygen transfer and power consumption were developed. According to the paper, the

SAE of the developed prototype PCSC aerators based on estimated brake power ranged between 2.43 and 3.23 kg O_2/kWh.

Prasetyaningsari and Setiwan (2013) determined the optimum sizing of electric power to support the electricity demand of fish pond aeration system by using HOMER (Hybrid Optimization Model for Electric Renewables) software. Energy load required was varied between 450 Wh/day and 1692 Wh/day. They found that 1 kW as the optimal sizing of photovoltaic, 8 batteries of 200 Ah and inverter 0.2 kW. The least cost of energy (COE) of system was determined as about 0.769 $/kWh.

Brown and Tucker (2014) explored the possibility of using paddlewheel aerators as pumps in split ponds. They analyzed water pumping performance characteristics of a paddlewheel aerator, including the relationships among power input, rotational speed, paddle depth, water velocity, and water flow rate. They also evaluated the effect of pump location on pumping efficiency. They showed that commercial paddlewheel aerators could be modified, operated and located to provide the water flows needed in commercial-sized split ponds. They suggested slow-rotating paddlewheels (which are specifically designed as water pumps) due to advantages of lower investment cost, greater availability, and easy maintenance.

Kumar et al. (2014) developed various types of aeration systems to maintain the desired level of DO concentration in pond water. They made performance evaluations and comparisons of aeration systems of four different types of aerators; paddle wheel aerator, propeller-aspirator-pump aerator, circular stepped cascade aerator and pooled circular stepped cascade aerator. Aeration tests were conducted at Indian Institute of Technology Kharagpur, India. The maximum standard aeration efficiency of 1.65 kg O_2/kWh was estimated for a single hub paddle wheel aerator. In case of propeller-aspirator-pump aerator, the maximum standard aeration efficiency of 0.42 kg O_2/kWh was obtained at a positional angle of 75 degree, rotational speed of 2840 rpm and submergence depth of 0.14 m of propeller shaft. Standard aeration efficiencies based on estimated brake power of the prototype circular stepped cascade and pooled circular stepped cascade aerators ranged between 2.16 to 2.70 kg O_2/kWh and 2.43 to 3.23 kg

O_2/kWh respectively. It had been found that the pooled circular stepped cascade aerator had more standard aeration efficiency compared to the other aerators tested.

Solpico et al. (2014) designed and constructed a 50 W solar PV panel driven air compressor type mini aeration system (Figure 3.5). The aeration system was equipped with DO, temperature and electric conductivity sensors. The measured values were sent out via short message system (SMS) to central server 80 km away in near real time and displayed on a website designed for this purpose. The constructed aeration system was controlled automatically by Arduino platform so that the aerator will be operated every night at 6 AM with the help of solar batteries charged during the day. The researchers concluded that a standalone pond monitoring system could be easily implemented by using Arduino development board.

Figure 3.5 Solar driven floating type aerator (Solpico et al. 2014)

Ma et al. (2015) installed two water-lifting aerators (WLAs) in a stratified, eutrophicated reservoir to investigate its ability to improve the water quality. The results showed that the lower water layer was directly oxygenated by WLAs. The mixing function of WLAs can control algal growth, and its mixed conduction speed gradient can effectively resist cyanobacteria floatation and reduce the competitive advantage of

harmful algae, which changes the quantity and structure of the phytoplankton community. The algal cell density decreased to less than 10 million/L, with cyanobacteria accounting for only 16% of the population in the area of 10 m away from the WLA. The quantity of algae reached to 100 million/L and included Microcystis, which accounted for 91% of the population in the area of 100 m away from the WLA after three weeks of operation. The results can provide direct technical support for reservoir restoration.

Brown et al. (2016) evaluated the circulator performance for four different circulating systems: slow rotating paddle wheel (0.5 to 3.5 rpm for a twin), paddle wheel aerator (12.5 to 56.5 rpm); high-speed screw pump (60 to 240 rpm); an-axial-flow pump (150 to 600 rpm). Water flow rates ranged from 8.6 to 77.6 m^3/min and increased with increasing rotational speed. Power input varied directly with flow rate and ranged from 0.24 to 13.43 kW for all four circulators. Water discharge per unit power input (i.e. efficiency) ranged from 3.5 to 70.9 m^3/kW min for the circulators tested. In general, efficiency decreased as water flow rate increased. Initial investment cost for each circulator and complete system ranged from US $5850 to $22,900 and $15,335 to $78,660, respectively. The least expensive circulator to operate was the twin, slow-rotating paddle wheel, followed by the paddle wheel aerator, high-speeds crew pump, and axial-flow pump. They showed that four different circulating systems could be effectively installed and used to circulate water in split- ponds. However, water flow rate, rotational speed, required power input, efficiency, initial investment cost, and operational expense varied greatly among the systems tested.

4. MATERIAL and METHOD

The design works of the aeration system were started by first modeling a single venturi ANSYS FLUENT package. The modeling was carried out to check weather venturi systems are capable of drawing enough oxygen from the air for the purpose of aeration. The modeling work had also used for the determination of venturi and pump sizes which are big enough for the construction of a prototype aeration system.

Initially, aeration tests related with aeration system designed were carried out in a plastic pool of 4000 L volume at mechanical laboratory by using a 24 V DC power source. Followed by the integration of meteorology station and data logging system were integrated in order to measure and to store variables related to outdoor conditions. Finally, solar powered pool and field experiments were carried out.

4.1 Equipment and Devices

Mechanical and electrical equipment and devices are given in table 4.1. Electronic components, sensors and measurement devices are listed in table 4.2.

4.1.1 Experimental pool

The main experiments in relation to the design and construction of the aeration system were carried out in a plastic swimming pool made up of PVC/PE material with a capacity of 4000 L volume. Both indoor and outdoor experiments were taken place by using this pool. The pool has a diameter of 3.0 m and water depth of 0.76 m.

Table 4.1 Mechanical and electrical tools and equipment

Components	**Characteristics**	**Values**
Submersible pump Lorentz - C-SJ5-8 (Aerator pump)	Maximum power Maximum dynamic head Maximum flow rate Maximum voltage Motor efficiency Weight	300 W 20 m 8 m^3/h 50 V 92 % 12 kg
Pump controller Lorentz -PS150 (Aerator pump controller)	MPPT system Battery connection mode Dry-well and sensor connection system PWM adjustment system	- 12 V-24 V - -
Venturi (Palaplast, Alternatif plastics)	Water inlet x Air inlet x Water and Air mixture outlet	1" x ¾" x 1" 1½" x ¾" x 1½" 2" x 1 x 2"
Experiment pool (Intex)	Diameter Depth Volume	3 m 0.75 m 4 m^3
DC power source (Max Power S 350-24)	In Out	200-240 VAC@ 4.2 A 24 VDC @ 14.6 A
PV solar panels: 2 Type: Monocrystalline (EkoSolar) (Aerator power supply)	Rated Max. Power (P_{max}) Voltage at P_{max} Current at P_{max} Open circuit voltage Short circuit current	150 W 18.72 V 8.01 A 22.64 V 8.8 A
PV solar panel Type: Polycrystalline (Yingli) (Aerator power supply)	Rated Max. Power (P_{max}) Voltage at P_{max} Current at P_{max} Open circuit voltage Short circuit current	245 W 30.2 V 8.11 A 37.8 V 8.63 A
Solar charge controller (Juta 5024Z)	Max. Voltage Max. Current	12/24 V 50 A
Solar batteries: 4 Type: Gel battery (Gold) (Aerator power supply)	Voltage Battery charge rate C- rating	12 V 100 Ah 20
Solar panel (Ekosolar) Type: Monocrystalline (Datalogger power supply)	Rated Max. Power (P_{max}) Voltage at P_{max} Current at P_{max} Open circuit voltage Short circuit current	60 W 17.98 V 3.39A 21.8 3.72 A
Solar battery (Gold) (Datalogger power supply)	Voltage Battery charge rate	12 V 26 Ah
Charge controller (Juta CM20D)	Max. Voltage Max. Current	12 V 5 A

Table 4.2 Electronic components, sensor and measurement devices

Components	**Characteristics**	**Values/Model**
Data logger CR1000 (Campbell Scientific)	Power supply	9.6 - 16 V DC
	Analogue inputs	16 SE, 8 Dif.
	Pulse counter	2
	Input voltage	±5 VDC
	Accuracy (Analogue voltage)	±(0.06%)
	Analogue resolution	0.33 µV
	A/D resolution	13 bit
Meteorology station	Temperature sensor (Texas Instruments)	LMT86LP
	Relative humidity sensor (Honeywell)	HIH5030
	Barometer (Infineon)	KP236N6165
	Pyranometer (Apogee)	SP-110
	Anemometer (Sparkfun)	SEN-08942
	Wind vane (Sparkfun)	SEN-08942
	Rain gage (Sparkfun)	SEN-08942
	Water temperature sensor (Campbell Sci.)	Model 107
DO Sensor, Atlas Scientific - EZO	Full range accuracy	± 0.01 mg/L
	Output	0 to 20 mg/L
	Max Temperature	50 °C
	Max Pressure	690 kPa
	Max Depth	60 m
	Dimensions	16.5 mm X 116 mm
Flow measurement devices	Anemometer	Lutron AM-4204
	pH meter	Lutron PH-207
	EC meter	Lutron CD-4303
	Multimeter	Fluke 189
	Flow meter	Baylan (1½”- 6.5 m^3/h)
A/D converter (Microchip, MCP3425)	Resolution	16 bits
	Gains of	1, 2, 4 or 8
	Comm. protocol	I2C
	Supply voltage	2.7V to 5.5V
Temperature Sensor (Dallas, DS18B20)	Input voltage	3.5 – 5 V
	Measurement range	-55 – 125 °C
	Accuracy	0.5 °C
	Comm. protocol	One wire
Voltage and Current Sense Board (Attopilot)	Maximum Voltage	51.8 V
	Maximum Current	89.4 A
	Analog voltage output	63.69 mV/V
	Analog current output	36.60 mV/A
Arduino UNO Sparkfun Red Board	Microcontroller processor	ATmega32
	Flash memory	32 kB
	Digital input/output pins	14
	Analog inputs	6
	Clock frequency	16 MHz
Relay control board (Robit)	Relay coil voltage	5 V
	Switching current	10 A @ 24 VDC
SD card shield (ITEAD studio)	Supports	SD card (max. 2 GB)
	Compatible with Arduino	5V and 3.3V
Real Time Clock-DS1307	Current consumption	500 nA @ 5 V

4.1.2 Meteorological measurement system

A meteorology station was set up to measure the pool and the environmental variables. The main components of the station are pyranometer, barometer, cup anemometer and wind vane, temperature and relative humidity sensors, rain gage shown in figure 4.2. The data coming from the sensors was stored in a data logger in a time interval of one-minute. The station consists of the different sensors, data logger, solar energy system, housing and connecting elements is given in figure 4.3.

A solar panel of 60 W, a battery of 12 V @ 26 Ah were used to provide power for the meteorological measurement system.

The data logger, solar battery and solar charge controller is also given in figure 4.4.

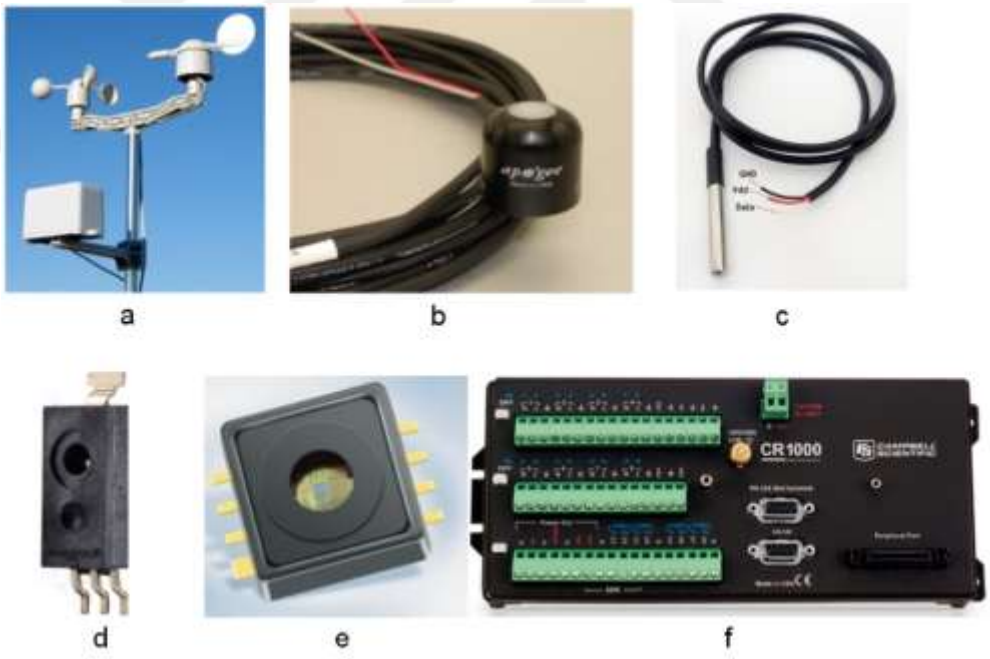

Figure 4.2 The main components for meteorology station

a. cup anemometer, wind vane, rain gage, b. pyranometer, c. LMT86LP temperature sensor, d. humidity sensor, e. barometer and f. CR1000 data logger

Figure 4.3 Meteorology station

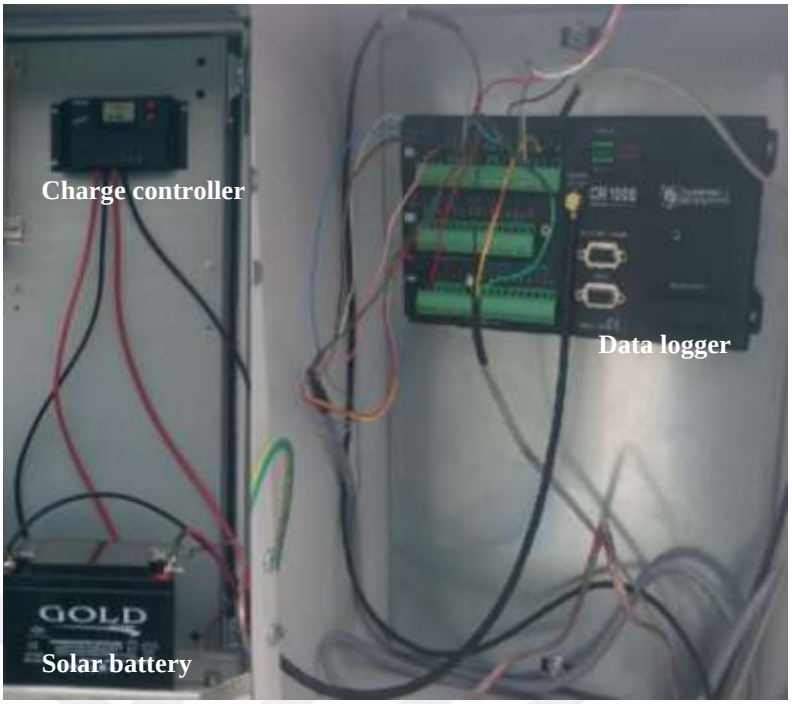

Figure 4.4 Power supply system for meteorology station

4.1.3 Dissolved oxygen measurement and automation

An Arduino Uno development board along with SD and LCD shields was used to fulfill pool measurements and automation (Figure 4.5 a). A DO probe (Atlas Scientific DO V5.0) was used to measure the oxygen amount injected to water body by aerator (Figure 4.5 b). This probe is a galvanic sensor that produces a millivolt (mV) signal directly proportional to the oxygen present in water. Since the maximum signal output of the probe is 36 mV, a MCP3425 single channel Analog Digital (A/D) converter with gain of eight was used (Figure 4.5 c). A waterproof DS18B20 sensor was used to measure water temperature, (Figure 4.5 d). A relay card compatible with Arduino is used for the automation of aeration system (Figure 4.5 e). (Figure 4.5 f) is the current – voltage sensor used in this project.

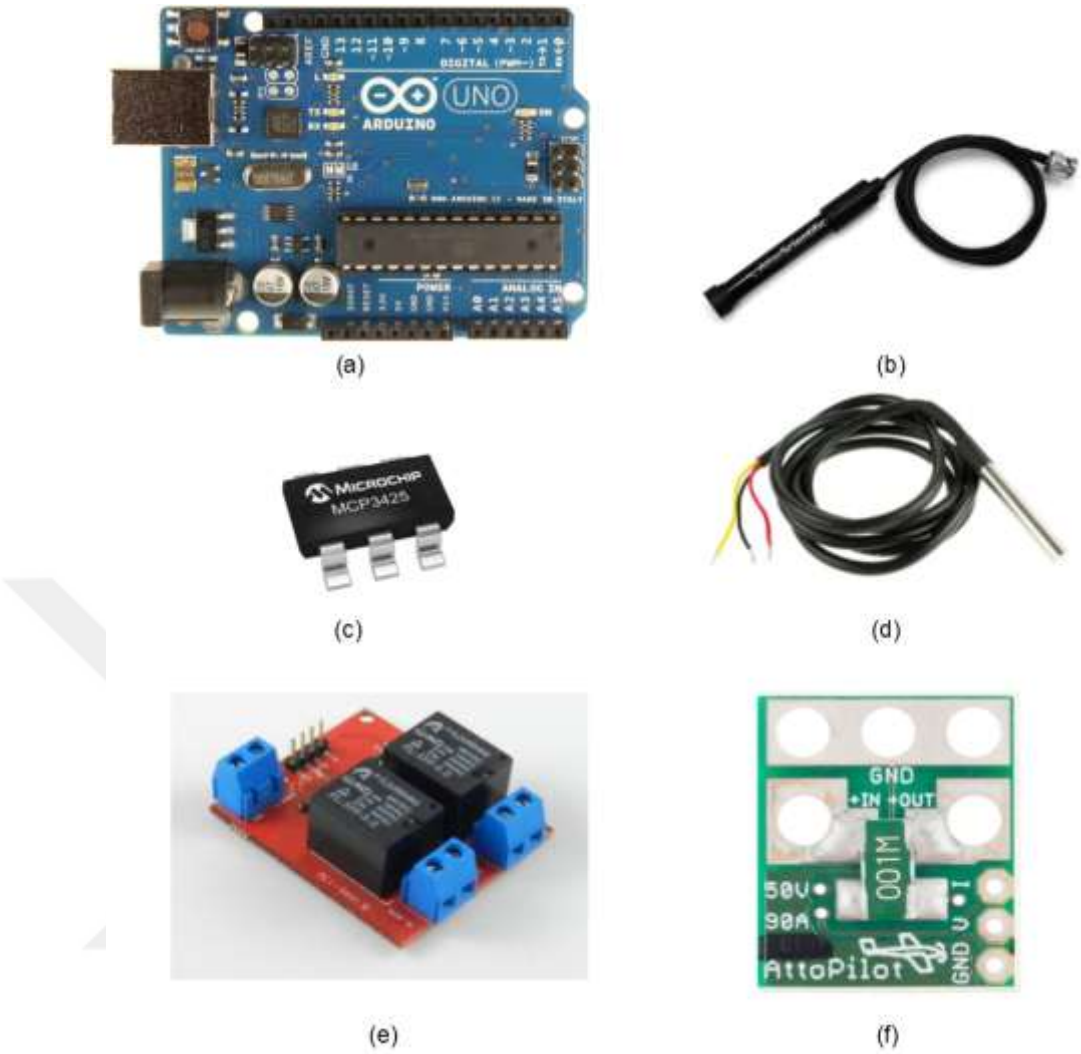

Figure 4.5 Main DO measurement and automation components
a. Arduino Uno development board, b. DO probe, c. A/D converter, d. DS18B20 water Temperature sensor, e. Relay control board, f. AttoPilot Voltage and Current sensor

4.1.4 Power measurement

In order to measure the power consumption of aerator, a power meter based on Arduino Uno to be able to connect with SD card and LCD shields was developed. Power measurement was carried out by using current – voltage sensor (Sparkfun, AttoPilot 50 V – 90 A) that connected between battery and pump controller.

4.2 Method

4.2.1 Venturi modeling and simulation

ANSYS Fluent package was used to simulate the capacity of a single venturi to transfer oxygen from the atmosphere into the water. The following assumptions were taken into account for ANSYS modeling:

- Single 1 inch venturi
- Pressure based
- Steady flow
- Mixture type flow
- Two velocity inlets and one outflow outlet

4.2.2 Water-Air flow tests

The venturi water-air flow tests were done by using a submersible pump, water flow meter, manometer (1), vacuum meter (2), digital anemometer, DO sensor and temperature sensor at a pool test stand shown schematically in figure 4.6.

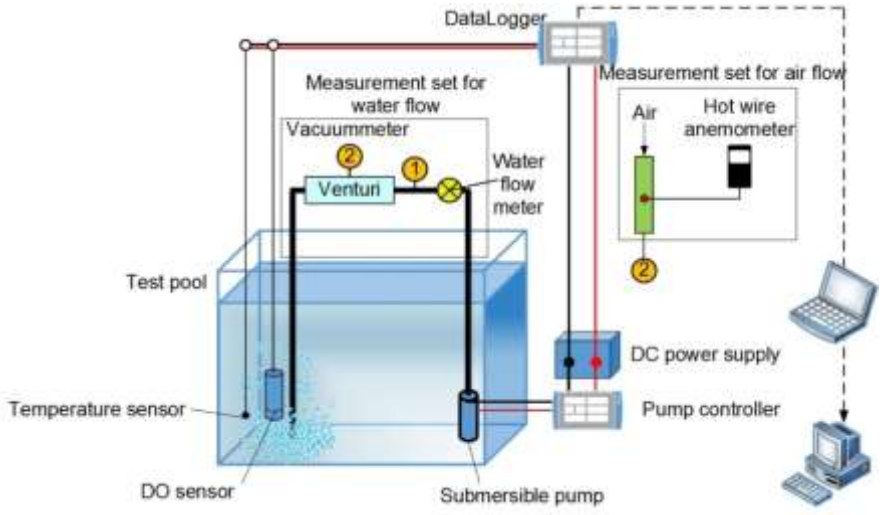

Figure 4.6 Water – air flow test stand

Three different in dimension venturi injectors were used in experiments. They are defined from their nominal diameters ($Ø_{iw}$" x $Ø_a$" x $Ø_{ow}$") listed in figure 4.7. $Ø_{iw,}$ $Ø_a$ and $Ø_{ow}$ show water inlet, air inlet and water air mixture exit diameters, respectively.

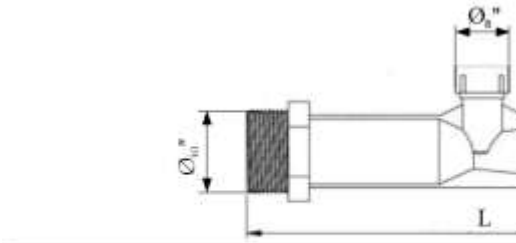

	Ø$_{iw}$"	Ø$_a$"	Ø$_{iw}$"	L(mm)	D$_{i.o}$(mm)	D$_v$(mm)
V$_1$	1 "	¾	1"	230	20	5.0
V$_2$	1½ "	¾	1½"	280	30	7.5
V$_3$	2"	1	2"	375	40	10

Figure 4.7 Three different venturi injectors used in experiments

The vacuum levels created by each venturi for different power and water flow regimes were measured at the test stand. Additionally, the air speeds of provided by venturi injectors were measured for power-flow regimes. After determining the suitable venturi injector dimension, different venturi connection combinations were tested. Then, the air suction capacities for connections of single, double and triple venturi combinations in series and parallel were analyzed. According to analysis results, the venturi type - aeration system was constructed and installed.

4.2.3 Dynamic re-oxygenation method

The unsteady-state test procedure was applied to determine the performance characteristics of aeration system. The standard test steps given by American Society of Civil Engineers (ASCE) were applied to the developed aerator system (Anonymous 2007; Figure 4.8).

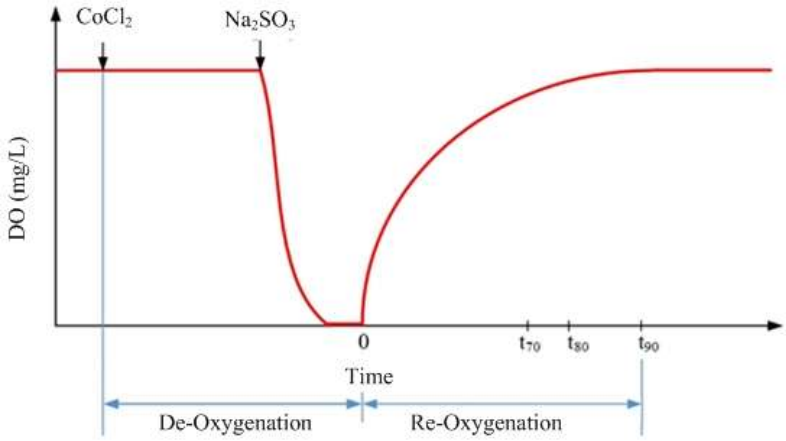

Figure 4.8 Standard test procedure for aerator (Anonymous 2007)

ASCE standard test procedure consists the following six steps:

1. Filling with tap water the test pool
2. Turning on the aerator
3. De-oxygenating by adding of chemicals:
   - Na_2SO_3 of 500 g and $CoCl_2$ of 2 g for water of 4000 L
   - The lowest concentration should be lower than 20% of C_s
4. Re-oxygenating:
   - The highest concentration should be at least 98% of C_s
5. Truncating data measured for true analysis:
   - 20% of C^*_s
   - 80% of C^*_s
6. Converting to standard temperature (20°C) and pressure (101.325 kPa) of the data.

Figure 4.9 shows the experimental layout for performance tests of the aeration system. Performance tests were also conducted in plastic pool of 4000 L filled with clean tap water, which is shown in figure 4.1.

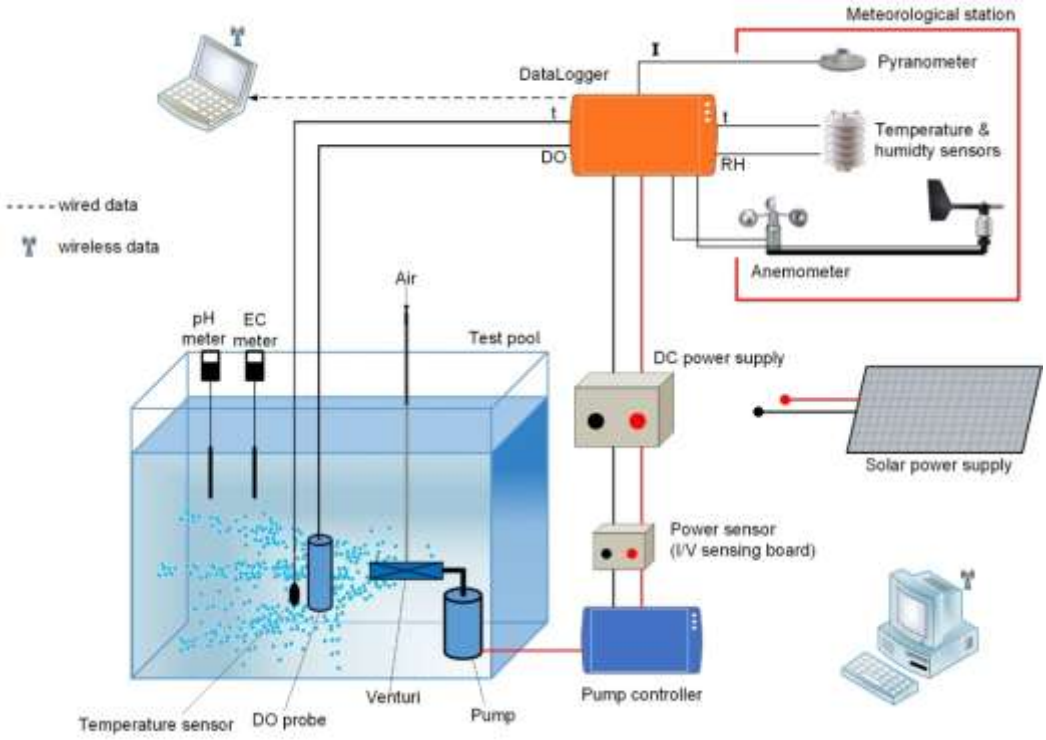

Figure 4.9 Performance test stand

4.2.4 Graphical method for oxygen transfer coefficient determination

By using the unsteady-state test procedure, a mathematical dynamic model that describes oxygen transfer rate in clean water is as shown below (Lekang 2013).

$$\frac{dC}{dt} = K_{La}\,(C_s^* - C_t) \tag{4.1}$$

Where; K_{La} is volumetric mass transfer coefficient (1/min). C_∞ and C_t are saturation DO concentration (mg/L) and measured average DO concentration in the liquid phase at time t, respectively.

By integrating equation (4.1), K_{La} gas transfer rate can be calculated as following:

$$(K_{La})_T = \frac{\ln(C_s^* - C_{t1}) - \ln(C_s^* - C_{t2})}{t_2 - t_2} \tag{4.2}$$

Where C_s^* is equilibrium liquid-phase oxygen concentration, C_{t1} and C_{t2} are measured DO concentrations at time t_1 and t_2 where t_1 and t_2 are initial and final times,

respectively. From equation 4.2, the values (C_s^* – C_{t1}) and (C_s^* – C_{t2}) are the DO deficits.

Graphical method of performance characteristics determination was used for estimating the oxygen transfer coefficient as shown in figure 4.10. The value of K_{La} is usually calculated accurately by plotting the time versus the natural logarithm of the oxygen deficit. The slope of the straight line generated via graphical method equals to K_{La} value (Lawson 2002).

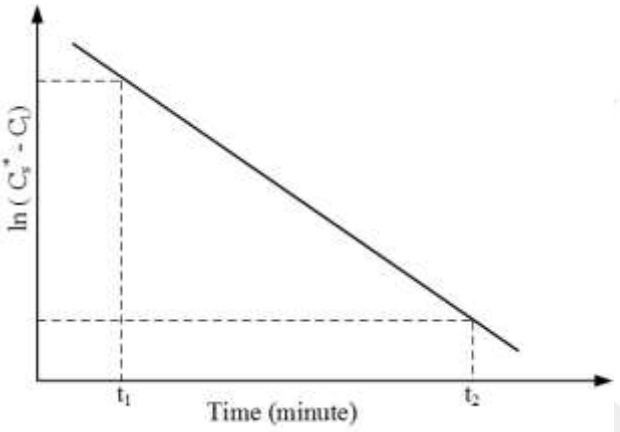

Figure 4.10 Graphical method for determining the overall oxygen transfer coefficient (Lawson 2002)

Since temperature affects viscosity as a result of which affects diffusion rate, values of K_{La} must be corrected for temperature effects. The oxygen transfer coefficient under standard conditions can be calculated by the following equation (Lawson 2002):

$$(K_{La})_{20} = \frac{(K_{La})_T}{\theta^{(T-20)}} \quad (4.3)$$

Where $(K_{La})_T$ is the overall oxygen transfer coefficient at T water temperature (h^{-1}), T the water temperature (°C). Θ was used as 1.024 for fresh water.

4.2.5 Determination of performance parameters

All parameters used to evaluate aerator performance were determined based on standard parameters defined for a water temperature of 20°C and barometric pressure of 1 atmosphere by (Anonymous 2007).

Standard oxygen transfer rate:

The overall oxygen transfer coefficient was used to estimate the standard oxygen transfer rate for an aerator (Kumar et al. 2013):

$$\mathrm{SOTR} = (\mathrm{K_{La}})_{20}(\mathrm{C_s})_{20}(\mathrm{V})(10^{-3}) \quad (4.4)$$

Where; SOTR = standard oxygen transfer rate, kg O_2/h; V = volume of water in test pool, m^3, $(C_s)_{20}$ = DO concentration saturated at standard conditions, (T = 20°C and P_b = 101.325 kPa) = 9.07 mg/L (Appendix 2-3).

Standard aeration efficiency:

Standard aeration efficiency (SAE) can be expressed as kilograms of oxygen transferred per kilowatt per hour as shown by following (Kumar et al. 2014):

$$\mathrm{SAE} = \frac{\mathrm{SOTR}}{\mathrm{P}} \quad (4.5)$$

Where; SAE = standard aeration efficiency (kg O_2/kWh), P = input power in kW.

Standard oxygen transfer effectiveness:

The standard oxygen transfer effectiveness is equal to the oxygen transferred divided by the mass flow rate of oxygen supplied by the aerator (Lawson 2002):

$$\mathrm{SOTE} = \frac{\mathrm{SOTR}}{\dot{\mathrm{m}}} \times 100 \quad (4.6)$$

Where; SOTE = standard oxygen transfer effectiveness, m = mass flow rate (kg/h).

4.2.6 Oxygen transfer model

The amount of oxygen transferred into water by aeration system with numerical model defined between air as a source and water as a sink is given in figure 4.11.

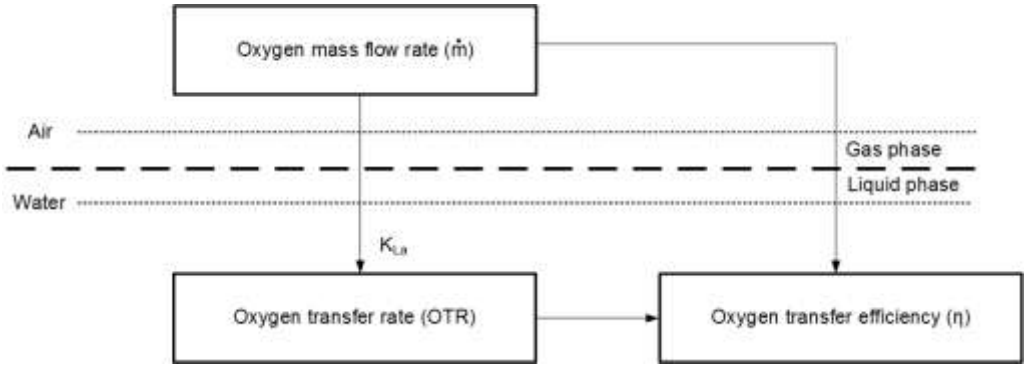

Figure 4.11 Oxygen transfer model

Oxygen mass flow rate ($\dot{m}_o$)

The amount of oxygen sucked by venturi from air is calculated as:

$$\dot{m}_o = 3600.(A.v).\rho.O_{c,w} \quad (4.7)$$

Where; A = venturi air entrance cross sectional area (m^2), v = air velocity (m/s), ρ = air density (kg/m^3), $O_{c,w}$ = oxygen fraction of air by weight (0.233 kg O_2/kg air) .

Oxygen injection factor (OIF)

The oxygen injection efficiency is the ratio of the oxygen mass flow rate to input power:

$$OIF = \frac{\dot{m}_o}{P} \quad (4.8)$$

Oxygen transfer rate (OTR)

The amount of oxygen transferred by venturi is calculated as the following:

$$OTR = C_s.K_{La}.V \times 10^{-3} \quad (4.9)$$

Where, C_s = saturated oxygen concentration at liquid phase (mg/L), K_{La} = overall oxygen transfer coefficient (h^{-1}), V = water volume (m^3).

Oxygen transfer factor (OTF)

The oxygen transfer factor can be defined as ratio of the oxygen transfer rate to power consumption:

$$OTF = \frac{OTR}{P} \quad (4.10)$$

Oxygen transfer efficiency (η)

The oxygen transfer efficiency is ratio of the oxygen transfer factor to the oxygen injection factor:

$$\eta = \frac{\mathrm{OTF}}{\mathrm{OIF}} \times 100 \tag{4.11}$$

Energy consumption

Energy amount requiring for production of oxygen can be calculated from ratio of input power (P) to oxygen transfer rate (OTR):

$$\mathrm{EC} = \frac{\mathrm{P}}{\mathrm{OTR}} \tag{4.12}$$

4.2.7 Power calculation

The wire power, i.e. power consumption, was calculated according to:

$$\mathrm{P} = \mathrm{I} \times \mathrm{V} \tag{4.13}$$

where: P = wire power (W), I = current (A), V = potential difference (V).

4.2.8 Design and installation of solar electricity system

Solar panel tilt angle

In this study, the optimum adjustable and fixed tilt angles of solar panel were estimated by using Typical Meteorology Year (TMY) data set for the province of Ankara. Five different tilt angle types were considered for tilt angle configurations. These configurations are monthly, seasonal (four times a year, Season -1 = January – March, Season-2 = April – June, Season – 3 = July – September, Season – 4 = October - December), semi-annual (twice a year 1^{st} – half = January – June and 2^{nd} – half = July - December), optimum fixed and latitude angle. A MATLAB computer program was used to determine different configurations related to solar panel. The flow chart of a MATLAB program written for this purpose is given in figure 4.12.

Power requirements

According to assessment form given in table 2.2, the required energy for aeration system was calculated by taking rated power of pump as 300 W, critical working time interval (critical oxygen shortage hours 03:00 to 06:00 am = 3 hours) and safety factor (1.2 - Foster et al. 2010). Daily total energy requirement was determined as 1080 Wh as given at table 4.3.

Table 4.3 Daily total energy requirement for pump

a	b	c	d	e	f = c x d x e
Load	Number	Power consumption (W)	Daily working hours (h/day)	Safety factor*	Daily energy need (Wh/day)
Pump	1	300	3	1.2	1080
Total load	1	300			1080

*(Foster et al. 2010)

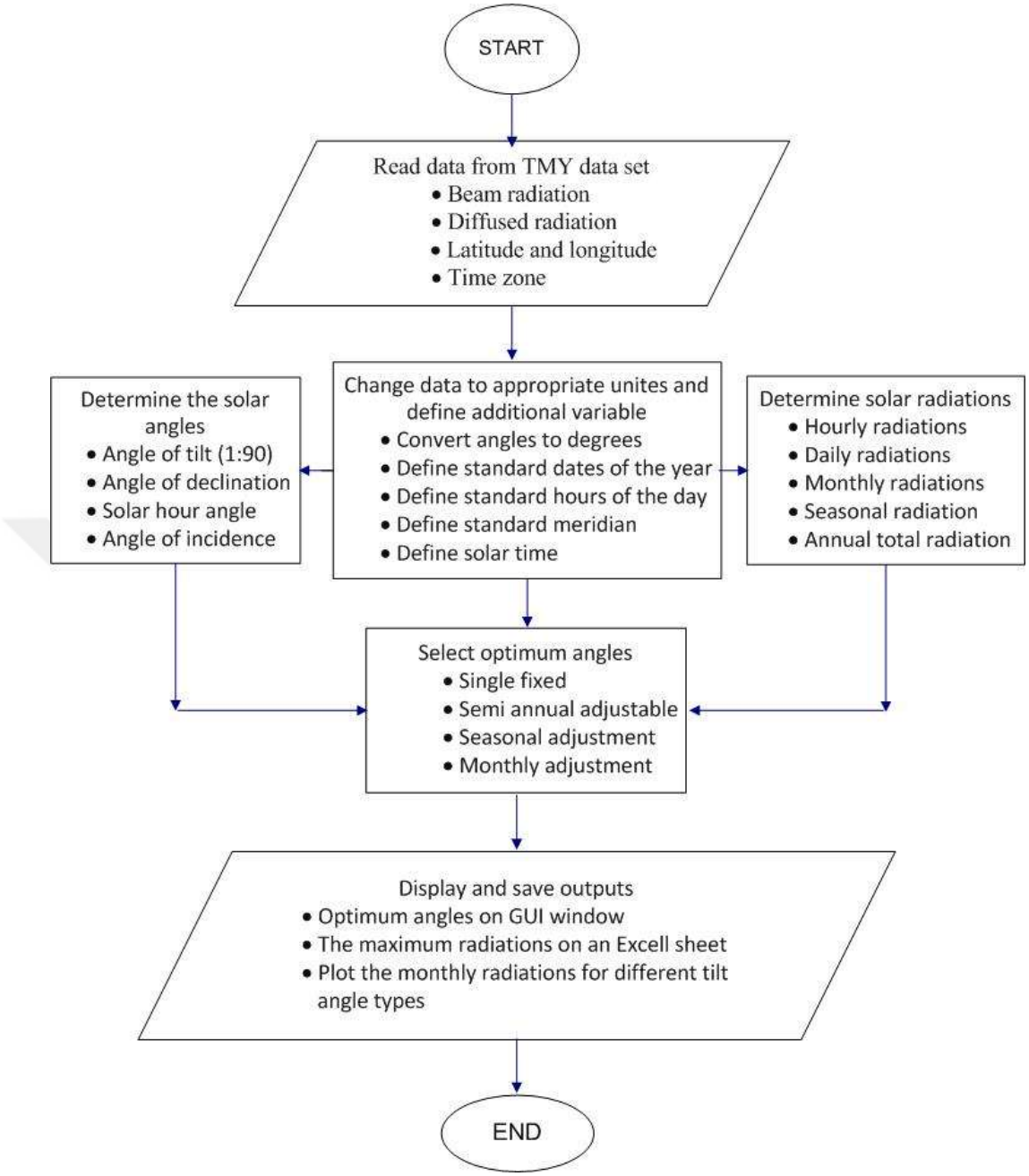

Figure 4.12 Flow chart of MATLAB program for optimum tilt angle determination

In order to meet daily total energy requirement of 1080 Wh, the capacity of battery must be more than 88.2 Ah. In this study, two gel batteries of 100 Ah (12 V) each connected in series were used (Table 4.4).

Table 4.4 Calculated and chosen battery capacities

Battery	n_b	V	η_b*	ξ_b*	Battery capacity calculated (Ah)
Gel type deep cycle	2	12 V	0.85	0.6	88.2
Battery selected					
Gel type deep cycle	2	12 V	-	-	100
Connection (serial)	-	24 V	-	-	100

* (Foster et al. 2010)

In order to calculate photovoltaic panel nominal power, two scenarios for sunshine hours were defined. The critical sunshine hours were taken as 5.4 h and 3.6 h for Ankara and for Scenario I and II, respectively. Nominal powers of panels were determined as 200 W and 300 W, respectively (Table 4.5). By taking sizing results determined for pump, solar panel, batteries, charge control device and pump controller, electrical connections of the aeration system are schematically given in figure 4.13.

Table 4.5 The designed photovoltaic panel nominal power values for aeration system

	Scenario I	Scenario II
Daily total energy requirement = 1080 Wh/day		
Design results		
Critical sunshine hours (h)	4.0*	5.4*
Panel nominal power calculated (W)	270	200
PV panels selected		
Panel type	Monocrystalline	Polycrystalline
Panel number	2	1
Panel nominal power (W)	150	245
Total panel power (W)	300	245
Panel slope (°)	24	0
Panel orientation	South	Horizontal

* Anonymous 2015: http://www.eie.gov.tr/MyCalculator/Default.aspx

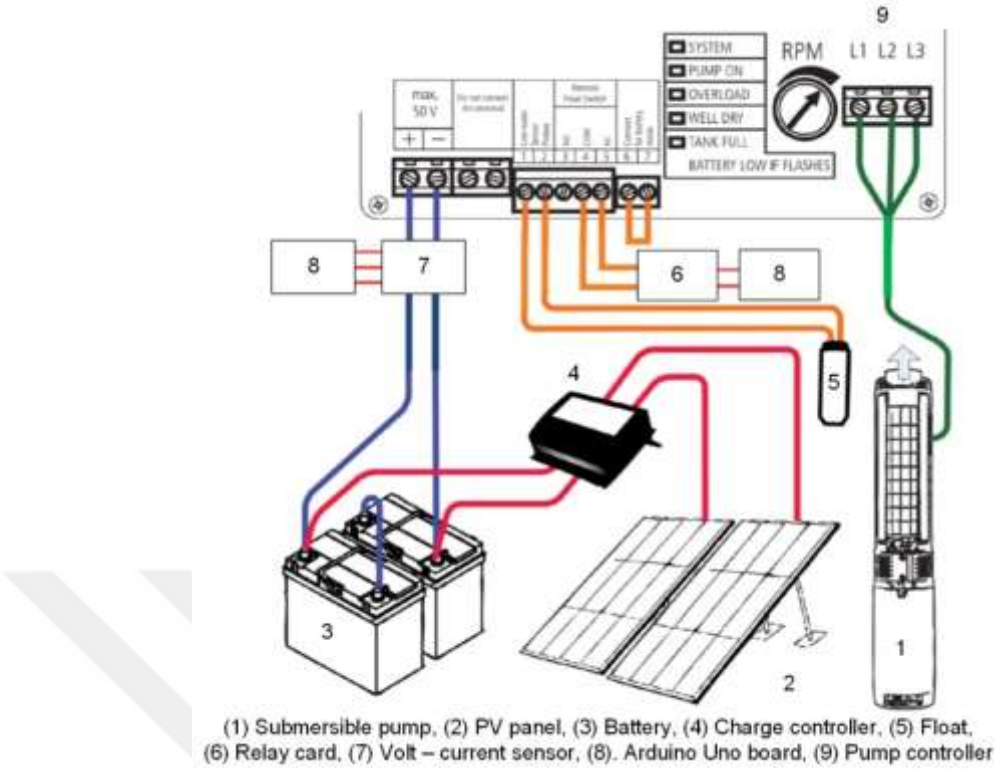

Figure 4.13 Schematic representations of electrical connections of the aeration system

4.3 Prototype Development

Two different prototype aeration systems, Prototype I and Prototype II, were developed, designed, and constructed. Main differences of Prototype I and II are given as summary in table 4.6.

Table 4.6 Main differences of Prototype I and II

	Prototype I	Prototype II
Type	Stationary	Mobile (floating)
PV solar panel	300 W fixed, tilted	245 W mobile, horizontal
Battery	100 Ah @ 24 V, fixed	100 Ah @ 24 V, mobile
Pump	300 W	300 W
Venturi	1 x ¾ x 1” 4 venturi	1 x ¾ x 1” 4 venturi
Measurement device	DO probe Water temperature sensor	DO probe Water temperature sensor

In Prototype I aerator system, only pump and venturi injectors were designed as floating on water inside the pool. Other components including solar energy system pump controller and sensors were fixed next to the water pool. Solar panels were installed with optimum tilt angle facing to the south.

In Prototype II, all components of aeration system were attached on a floating platform. PV solar panel was horizontally bolted on floating platform. For both prototypes a relay board connected between pump controller and Arduino board as shown in figure 4.13 was used for automatic control of Prototype aeration systems.

4.4 Experimental Planning

The main outdoor experimental and test activities were conducted by using the experimental pool on a roof of the building of the Department of Agricultural Machinery and Technologies Engineering of Ankara University shown in figure 4.1.

Firstly, airflow tests of aeration system were performed. Furthermore, pH and EC levels of pool water were also measured during plastic pool experiments.

Secondly, Prototype I was designed and installed according to results of airflow tests. The performance characteristics of Prototype I aeration system were determined in experimental pool conditions.

Thirdly, after designing and installing of Prototype II, it was tested in the experimental pool conditions.

Finally, Prototype II was tested in trout fishponds shown in figure 4.14 at Ankara University, Fishery Products Research and Application Centre in Çifteler (Eskişehir). During experiments, two identical fishponds with size 6 x 10 and at depth of 0.7 m were used. The Prototype aeration system was installed in one of the fishponds, the other fishpond was used for comparison purpose.

Rainbow trout of around 2600 having an average weight of 140 g in each pool were put. Feeding regime and all cultural processing were simultaneously applied. Prototype II was operated for five days between 20/07/2015 to 24/07/2015.

Figure 4.14 Fish ponds used during the field test

The test plan applied in this dissertation is given in table 4.7.

Table 4.7 Experimental planning, targets and variables

Experiments	Target	Variables	Tests
1	Venturi selection and design	• Vacuum [-1, +1 bar]	3
2	Venturi system design and Diffusor design	• Vacuum • Air distribution in water (observation)	20
3	Determination of air-water flow characteristics	• Air velocity [1, 2.5 m/s] • Pump flow rate [0-5 m^3/h] • Pressure [0, 3 bar] • Power consumption [75, 300 W]	6
4	Development of electronic sensing board	• DO sensor [0 – 32 mV] • Temperature sensor [0-50°C]	3
5	Development of power measurement board	• Current [0, 12.5 A] • Voltage [24, 25 VDC]	3
6	Determination of performance parameters • SOTR • SAE • SOTE	• DO [0, 10 mg/L] • Water temperature [18, 25°C] • Water: pH [5-7.1], EC [0.1-0.3 mS/cm] • Current [0, 12.5 A] • Voltage [24, 25 VDC] • Power [75, 100, 150, 200, 250, 300 W]	6
7	Saturation - time tests for aerator • 70 % • 80 % • 90 %	• DO [0, 10 mg/L] • Water temperature [18, 25°C] • Current [0, 12.5 A] • Voltage [24, 25 VDC]	6
8	Setting up of solar energy system • Installing and Construction	• Panel slope [0, 24°]	1
9	Making electrical connections • Panel – charge controller • Battery – charge controller • Pump – pump controller • Battery– pump controller	• Solar panel: 2 x 150 W • Solar panel: 1 x 300 W • Battery: 4 x 100 Ah @ 12 V • Charge controller (24 V @ 50 A] • Pump [300 W, 24 V] • Panel - battery current [0, 15 A] • Pump - battery current [0, 12.5 A] • Panel voltage level [0, 28 V] • Battery voltage level [21, 25 V]	1
10	Prototype development • Prototype I	• PV panel tilted [2 x 150 W] • Battery [2 x 100 Ah @ 12 V] • Pump [75 – 300 W] • 4 Venturi [1” x ¾” x 1”] • DO [0, 10 mg/L] • Water Temperature [18, 25°C],	1
11	Prototype development • Prototype II	• PV panel horizontal [1 x 245 W] • Battery [2 x 100 Ah @ 12 V] • Pump [300 W] • 4 Venturi [1” x ¾” x 1”] • DO [0, 10 mg/L] • Water temperature [18, 25°C]	1
12	Pool experiments	• Prototype I and II	10
13	Fields experiments	• Prototype II	5

5. RESULTS

The design and construction of the aeration system was carried out based on the light of experience from theories reviewed and applications obtained throughout the thesis work.

To realize the objectives of the research, a number of studies mainly water air flow dynamics of pumps and venturies, solar energy systems, data acquisition and automation etc. were put through.

5.1 Modeling and Simulation Results

5.1.1 Solar insolation model

From the optimum adjustable and fixed tilt angle simulation work, the total annual energy to be collected by the five different tilt angle arrangements for Ankara were obtained.

Total annual energy that can be collected by using a tilt angle equals to the latitude of the area is 1773 kWh/m^2. Energy to be collected by monthly adjustment , seasonal adjustment , twice a year adjustment and optimum fixed arrangement of panel tilt angles are 6.9%, 6.3%, 4% and 3.8% more than the energy that can be collected by tilt angle equal to latitude angle, respectively.

A graph of monthly solar insolation that can be collected under Ankara conditions for the different tilt angle configurations is given in figure 5.1.

The optimum angles obtained for Ankara for the four types of adjustments that maximizes insolation collection are given in table 5.1

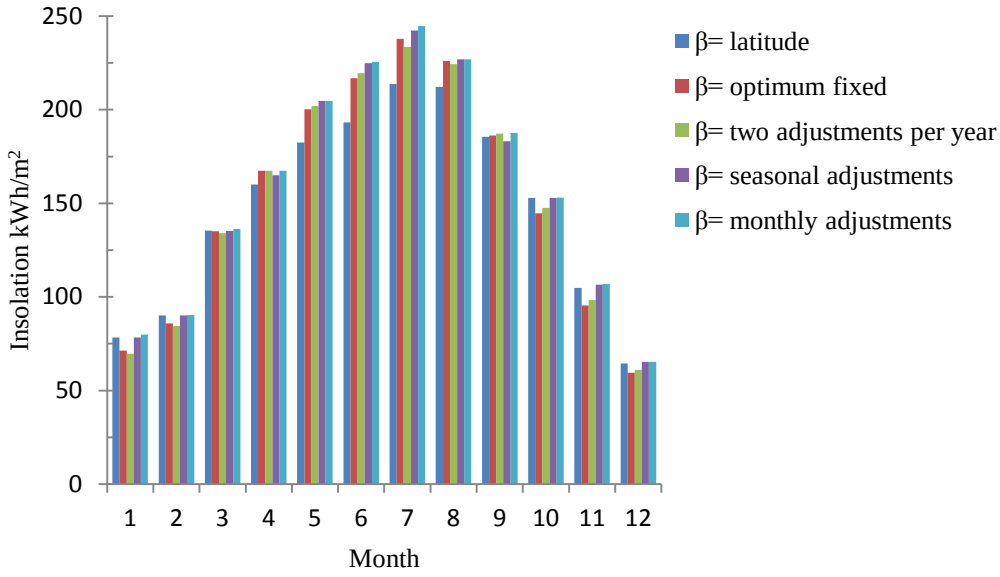

Figure 5.1 Monthly solar insolation (kWh/m^2) for different collector tilt angles for Ankara

Table 5.1 Optimum tilt angles for Ankara

Adjustment Type		**Angle (degrees)**
Monthly	January	53
	February	43
	March	32
	April	21
	May	10
	June	5
	July	8
	August	18
	September	31
	October	44
	November	52
	December	51
Seasonal	Season - 1	41
	Season - 2	11
	Season - 3	18
	Season - 4	48
Half yearly	1st- half	21
	2nd - half	28
Yearly	Single fixed	24

5.1.2 Venturi ANSYS model

The ANSYS model of the 1" venturi was carried out by assuming a pump of 5 m^3/h flow rate capacity and 5 m head to pump water into the venturi water entrance end. As a result of this the air suction capacity of the venturi ANSYS model output are given in figure 5.2 to figure 5.4. From the graphs of velocity and pressure distributions of flow shown in figure 5.2 and 5.3, it can be seen that velocity increased up to 5.9 m/s, but the pressure dropped up to -2.0 Pa at venturi throttle point. This means that, air can be sucked from the atmosphere by using the venturi considered in the simulation with the above mentioned pump type due to the fact that a pressure below the atmospheric pressure is obtained.

The air volume fraction that can be sucked by the system throughout the venturi length was obtained from the ANSYS modeling as shown in figure 5.4 below. The maximum air volume fraction after air is mixed with water was around 0.18. This means that the venturi can yield an 18% air by volume of water - air mixture.

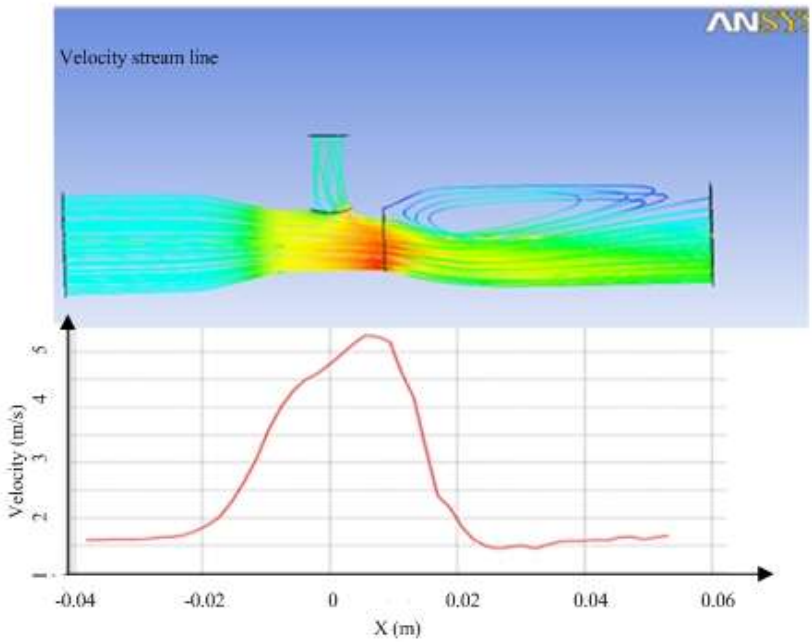

Figure 5.2 Velocity distribution of flow throughout the venturi length

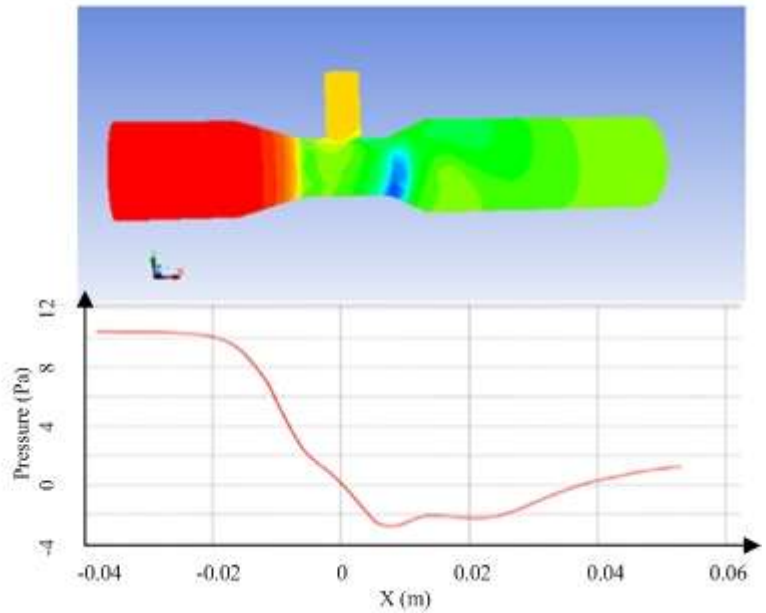

Figure 5.3 Pressure distribution of flow along the venturi length

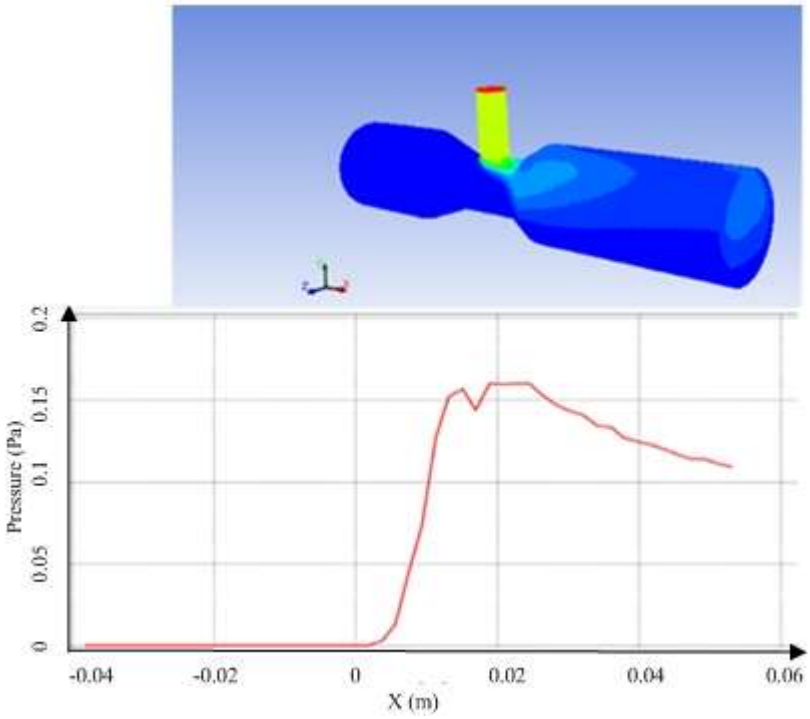

Figure 5.4 Air volume fraction along the venturi length

According to the modeling results obtained from ANSYS fluent package, it was concluded that venturi can be used for aeration. One can also conclude that a pump with a flow rate of 5 m^3/h and a head of 5 m can be used to construct a prototype aerator.

5.2 Venturi Selection

In order to select the best venturi size among the available ones in the market, water – airflow experiments were performed at a test stand shown in figure 4.7. By running a pump with DC power supply, the magnitude of vacuum created for each venturi size was obtained via measurement. The vacuum levels for V_1, V_2 and V_3 venturi injectors measured at point (2) of figure 4.6 were -1.0, bar, -0.8 bar and -0.6 bar, respectively. Because of this, the venturi with maximum vacuum V_1 was selected as it is suitable for the pump capacity used in this research.

Following the selection of venturi size, venturi injectors connected in parallel and series were experimented for maximum air suction purpose. From the experiments, the following results were obtained:

- The performance of venturi injectors connected in series was lower than a single venturi performance.
- Venturies connected in parallel yielded better performance.
- Three venturi injectors connected in parallel-performed better that two venturies connected in parallel.
- Four venturies connected in parallel performed better than three venturies connected in parallel.
- The number of venturies connected in parallel could be increased in line with the pump capacity to increase air suction volume.

5.3 System Design and Construction Results

After determining suitable venturi size, many experimental studies were carried out to develop an efficient venturi, pump and pipes arrangement. During the research, it was

found that the pressure loss was an important factor in the design of venturi aeration system.

The following points were observed to play an important role at the appearance of an innovative venturi aerator design.

- Reducing pressure losses by making connections in line with pump outlet,
- Reducing pressure losses by using reduction fitting at later connections,
- Determining the suitable venturi number with pump capacity.
- Designing a diffuser with suitable diameter to reduce air bubble diameter, so as to increase the amount of oxygen to be dissolved in water

The final configuration of venturi type air injection system developed is given in figure 5.5.

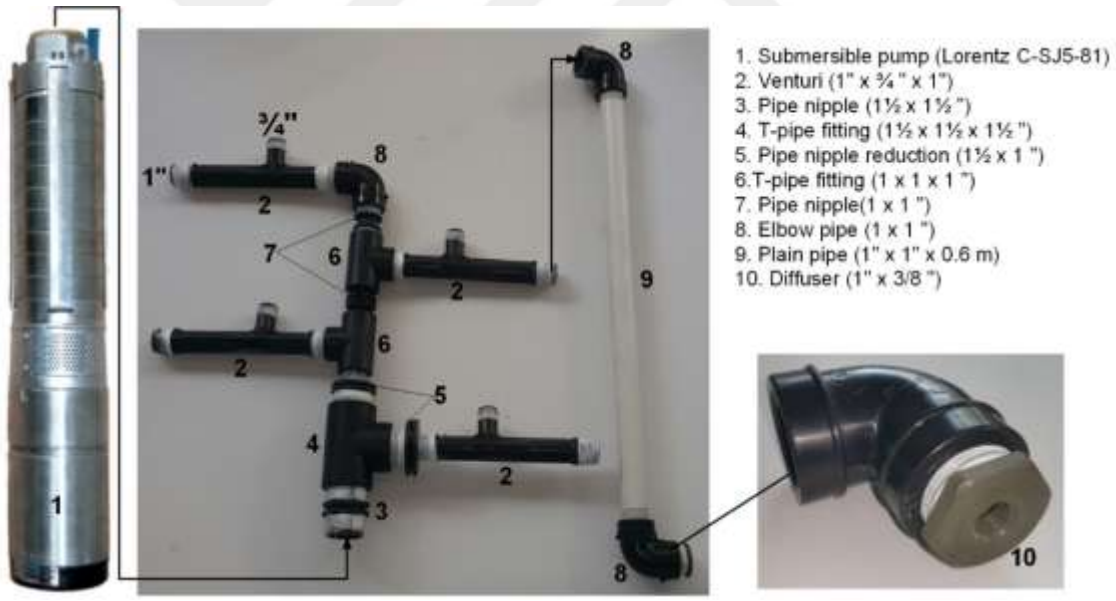

Figure 5.5 Configuration of the developed venturi type - air injection system

5.3.1 Prototype I

Prototype I aeration system consists of a floating part on water and a fixed part installed outside of water body. The floating part consists of flotation panel, submersible pump, venturi injectors, pipe fittings and connection elements. The fixed part includes two

solar panels, two batteries, galvanized steel profiles, charge controller, pump controller and connection elements. As shown in figure 5.6, two polystyrene boards, originally constructed for wall insulation, with a sizes of 0.6 m × 0.6 m and thickness of 50 mm was used as a flotation panel. Two steel plates with sizes of 0.3 x 0.3 m were used to fix the board together. The submersible pump was bolted by using brace clamp profiles, bolts and nuts to a hole drilled at the center of floating system (Figure 5.6).

In Prototype I, two mono-crystalline panels of each 150 W were used as a power supply of aeration system. The two PV panels were connected in series for power of 300 W. PV panels were mounted on adjustable galvanized steel profiles with a tilt angle of 24° (optimum fixed tilt angle for Ankara) facing south as shown in figure 5.7 (a).

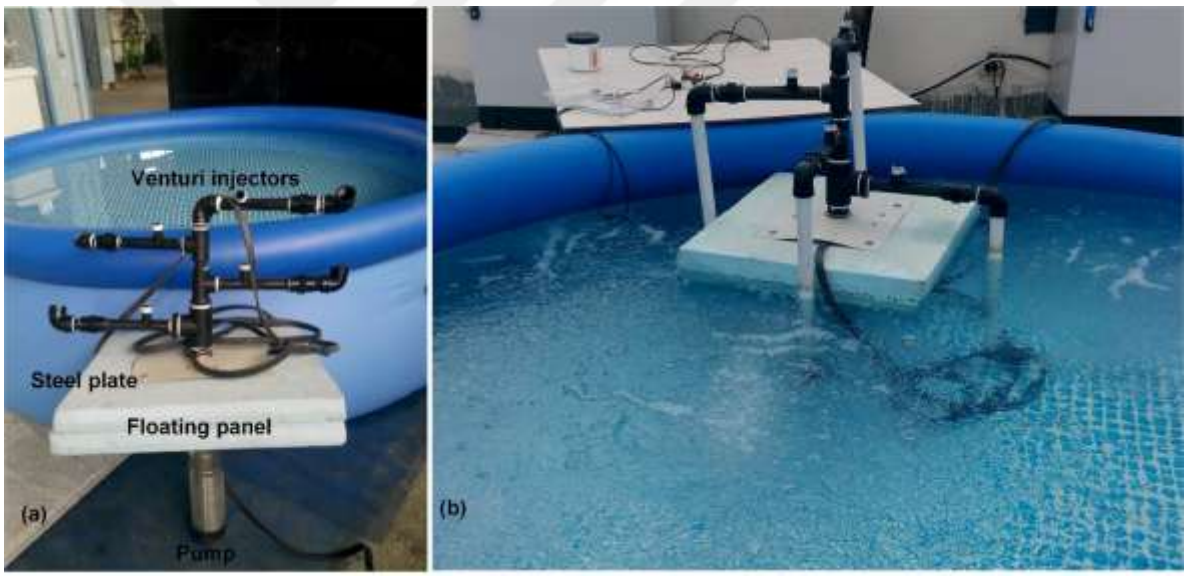

Figure 5.6 Prototype aeration system

a. Prototype I: Venturi injectors and pump, pipe fittings connections b. Pool experiment for Prototype I

Figure 5.7 Energy system for prototype I

a. Adjustable tilted solar panel b. Solar power box and connections

The energy obtained from the two solar panels was stored in two gel batteries of each 100 Ah @ 12 V shown in figure 5.7 (b). Batteries were connected in series to each other so that electrical energy could be stored at a nominal voltage of 24 V. A charge controller was connected between solar panels and battery to protect the batteries during recharging and discharging. Devices such as batteries, charge controller, pump controller were put in waterproof metal housing. The cross sectional area of electrical cables used between panels - charge controller and the charge controller - the pump controller is 4 mm^2. The cross sectional area of cables used to connect the two batteries, and for the connections between battery and charge controller is 16 mm^2 (Figure 5.7b).

5.3.2 Prototype II

Rigid polyurethane foam sandwiched between two corrugated metal plates was used as a floating platform (Figure 5.8). This platform with a size of 1.5 x 1 x 0.2 m was designed in the manner that all components of aeration system will be securely installed. A hole of 120 mm diameter was drilled at the center of the platform for the placement

of the pump. Pump and batteries were fixed on the platform by using galvanized steel hinges, bolts and nuts. Floating platform side faces which are not covered with metal plates were coated with UV-stabilized polymer paint to protect the surfaces from adverse effects of water and sun light.

In Prototype II, one poly-crystalline panel of 245 W was used as power supply of aeration system. The energy obtained from the solar panel was stored in two batteries like that of Prototype I. The batteries were fixed on the floating panel in such a way that the center of gravity of the whole system to be at the center of the system as shown in figure 5.9. Waterproof control boxes were connected vertically on the steel profiles. The total weight of components placed on the platform is approximately 100 kg.

To obtain higher water - air mixing capacity by means of smaller air bubbles, multiple diffusors exit diameters were tested. Finally, the best nozzle diameter of diffusor was determined as 11 mm diameter (Figure 5.5).

Figure 5.8 Floating platform constructed for Prototype II

Figure 5.9 Assembling the components of Prototype II

5.3.3 Electronic measurement and control unit

An electronic control system was constructed by using an Arduino microcontroller, DO and temperature sensors (Figure 5.10). Electronic control unit was programmed according to the critical DO levels, 4 mg/L< DO < 6 mg/L, for trout species. Figure 5.11 shows LabView interface to monitor the real time operation of aeration system during the experimental study. Figure 5.12 shows the algorithm of the automatic control system developed based on Arduino platform.

Figure 5.10 Aeration system control unit

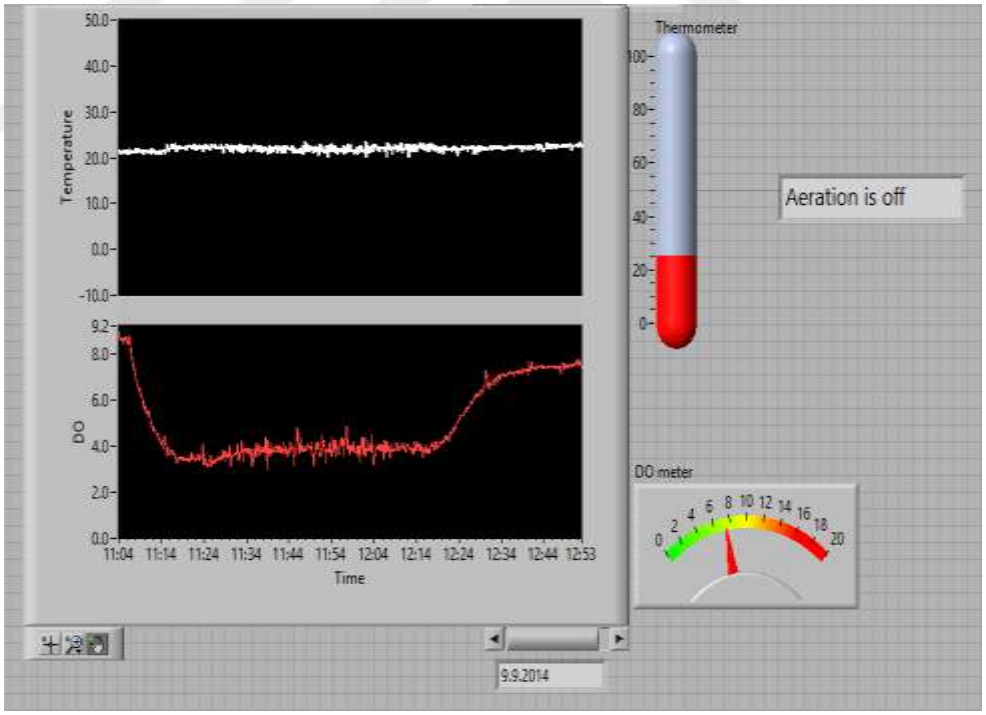

Figure 5.11 LabView interface of aeration system

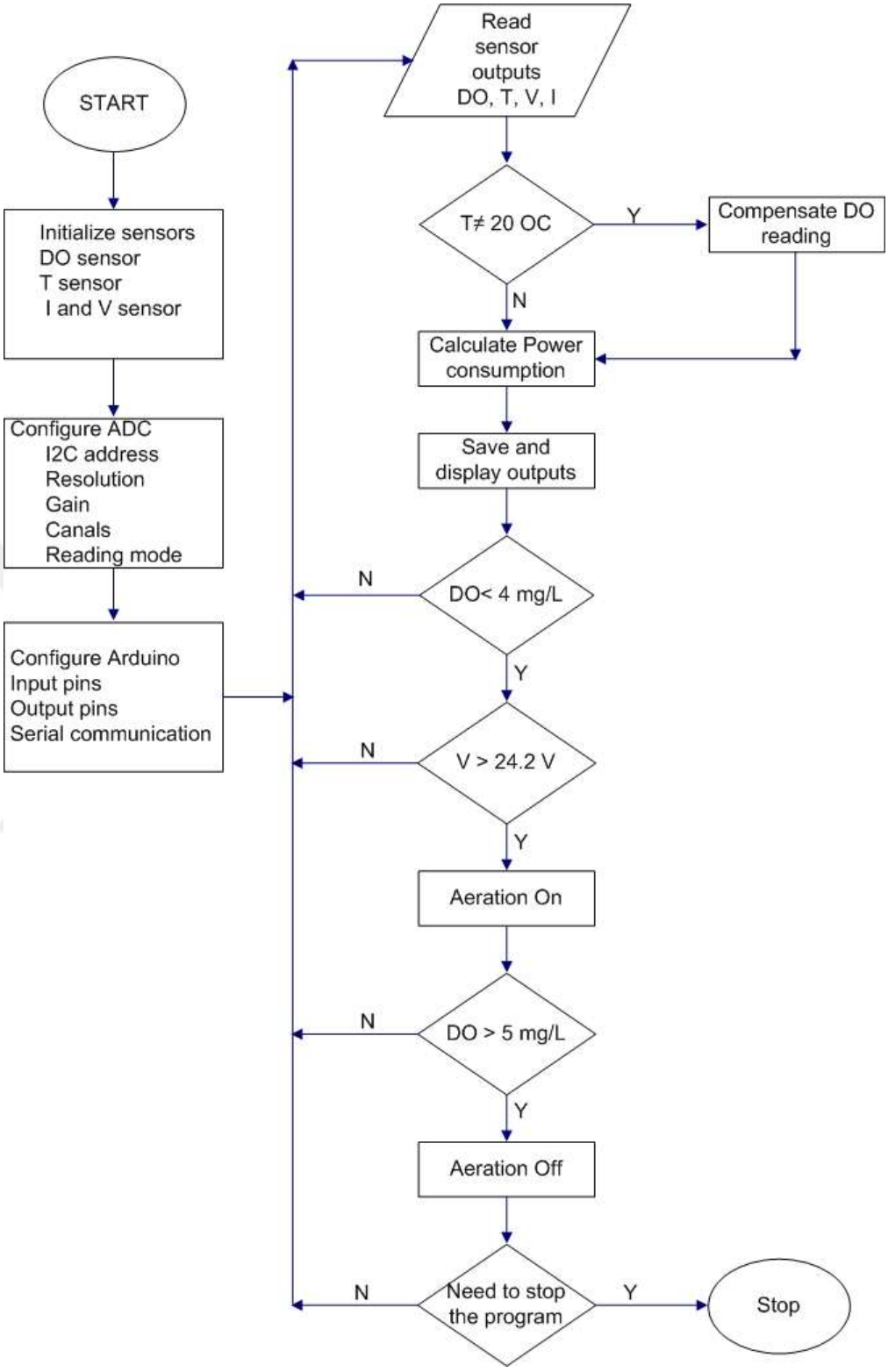

Figure 5.12 Algorithm of automatic control for Prototype II aeration system

5.3.4 Power-meter unit

A power meter was developed by using Arduino Uno, current and voltage sensors. Measured DO, temperature, voltage, current and power data were monitored and recorded by using LCD shield and SD shield for data processing and monitoring (Figure 5.13). All data were stored at one-minute intervals with the help of a real time clock for time stamp.

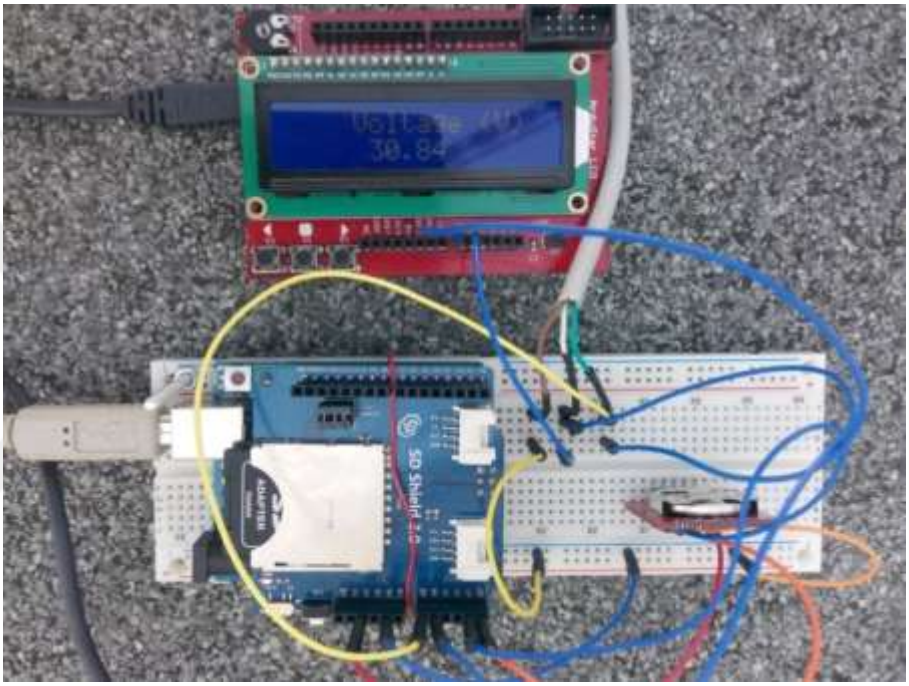

Figure 5.13 Aeration system power meter with SD-RTC- LCD shields

5.4 Meteorological Data

Pool experiments were conducted under the environmental conditions given in table 5.2. Figure 5.14 shows total solar radiation data, as well as water and air temperature data measured during experiments. Total solar radiation changed between 500 and 800 W/m^2, air temperature changed between 20 and 24°C, and water temperature changed between 18 and 22°C during experiments. Figure 5.15 shows a sample text file taken from data recorded by CR1000 data logger.

Table 5.2 Environmental data during performance tests

Tests	T_w (°C)	T_a (°C)	RH (%)	I_o (W/m^2)	P_{atm} (kPa)	v_w (m/s)
1	18	21	59	500-800	91.9	2.3
2	22	24	52	650-900	91.9	1.2
3	18	20	40	200-550	91.9	2.3
4	18	20	41	300-600	91.9	2.2
5	21	22	55	700-900	91.7	0.9
6	21	22	60	650-850	91.7	0.5

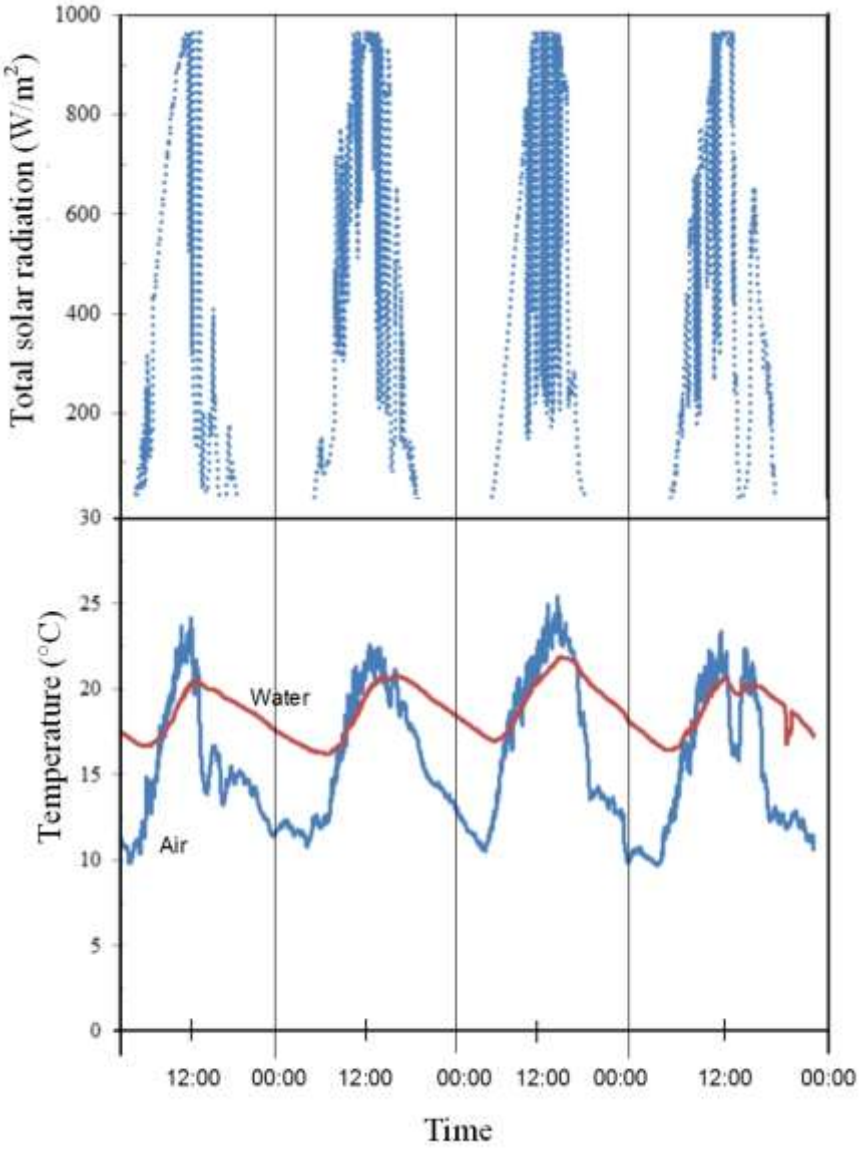

Figure 5.14 Total solar radiation, water and air temperature data

CR1000_Table1

Dosya Düzen Biçim Görünüm Yardım

```
"TOA5","CR1000","CR1000","65909","CR1000.Std.27","CPU:met_test.CR1","43680","Table1"
"TIMESTAMP","RECORD","Ta","RH","Patm","WD","Io","It_Tot","T107","WS","Rain_mm_Tot"
"TS","RN","C","%","kPa","V","W/m^2","kJ/m^2","Deg C","ms","mm"
"","","Smp","Smp","Smp","Smp","Smp","Tot","Smp","Smp","Tot"
"2015-04-27 15:03:00",0,24.61,22.33,91.9,0.455,342.1,20.52781,24.24,0,0
"2015-04-27 15:04:00",1,24.61,22.13,91.9,0.454,345.5,20.72867,24.18,2.123,0
"2015-04-27 15:05:00",2,24.61,22.07,91.9,0.454,346.1,20.76849,24.14,2.09,0.559
"2015-04-27 15:06:00",3,24.61,21.96,91.9,0.454,346.1,20.76849,24.13,1.912,0
"2015-04-27 15:07:00",4,24.61,21.96,91.9,0.454,347.8,20.86872,24.06,2.068,0.279
"2015-04-27 15:08:00",5,24.67,21.98,91.9,0.454,347.8,20.86872,24.04,1.956,0
"2015-04-27 15:09:00",6,24.61,21.9,91.8,0.455,320,19.20149,24.02,2.112,0
"2015-04-27 15:10:00",7,24.61,22.09,91.9,0.454,322,19.32188,24.02,2.101,0
"2015-04-27 15:11:00",8,24.61,22.01,91.9,0.454,325.4,19.52273,23.96,2.034,0
"2015-04-27 15:12:00",9,24.61,22.26,91.9,0.455,328.1,19.68332,23.98,1.99,0
"2015-04-27 15:13:00",10,24.61,22.24,91.9,0.454,329.1,19.74357,23.96,2.112,0
"2015-04-27 15:14:00",11,24.61,22.18,91.9,0.454,330.4,19.82383,23.96,2.179,0
"2015-04-27 15:15:00",12,24.54,22.05,91.9,0.454,331.7,19.90417,24.01,2.145,0
"2015-04-27 15:16:00",13,24.61,21.73,91.9,0.454,333.4,20.00454,24,1.334,0
"2015-04-27 15:17:00",14,24.61,21.06,91.8,0.454,335.4,20.12499,23.96,0.211,0
"2015-04-27 15:18:00",15,24.54,21.34,91.8,0.454,336.1,20.16516,23.89,0.2,0
"2015-04-27 15:19:00",16,24.57,21.26,91.9,0.454,340.4,20.42623,23.87,0.2,0
"2015-04-27 15:20:00",17,24.54,21.41,91.8,0.454,343.4,20.60699,23.84,0.2,0
"2015-04-27 15:21:00",18,24.54,21.43,91.8,0.454,344.8,20.68729,23.8,0.2,0
"2015-04-27 15:22:00",19,24.54,21.51,91.8,0.454,344.8,20.68729,23.75,0.2,0
"2015-04-27 15:23:00",20,24.54,21.6,91.8,0.454,344.8,20.68727,23.73,0.2,0
"2015-04-27 15:24:00",21,24.54,21.94,91.8,0.454,345.5,20.72741,23.7,0.2,0
```

Figure 5.15 Sample data recorded by CR1000 data-logger

5.5 Pool Water Conditions

In addition to the meteorological measurements, the pool water conditions were measured throughout the pool experiments. Figure 5.16 shows the pool test stand and devices used at experiments during testing aeration system in the pool. During performance tests, pool water data such as water temperature, DO concentration, pH and electrical conductivity (EC) were measured. The measured pool data are given as a summary in table 5.2. The daily changes of water temperature are given in figure 5.14.

Table 5.2 Experimental conditions in water pool

	De-oxygenation		Re-oxygenation
	Before	After	After
DO (mg/L)	8-10	0.3 – 0.5	8.0-9.0
pH	7.1	5.0	
EC_w (mS/cm)	2.0	3.0	
Water temperature (°C)	18-22		

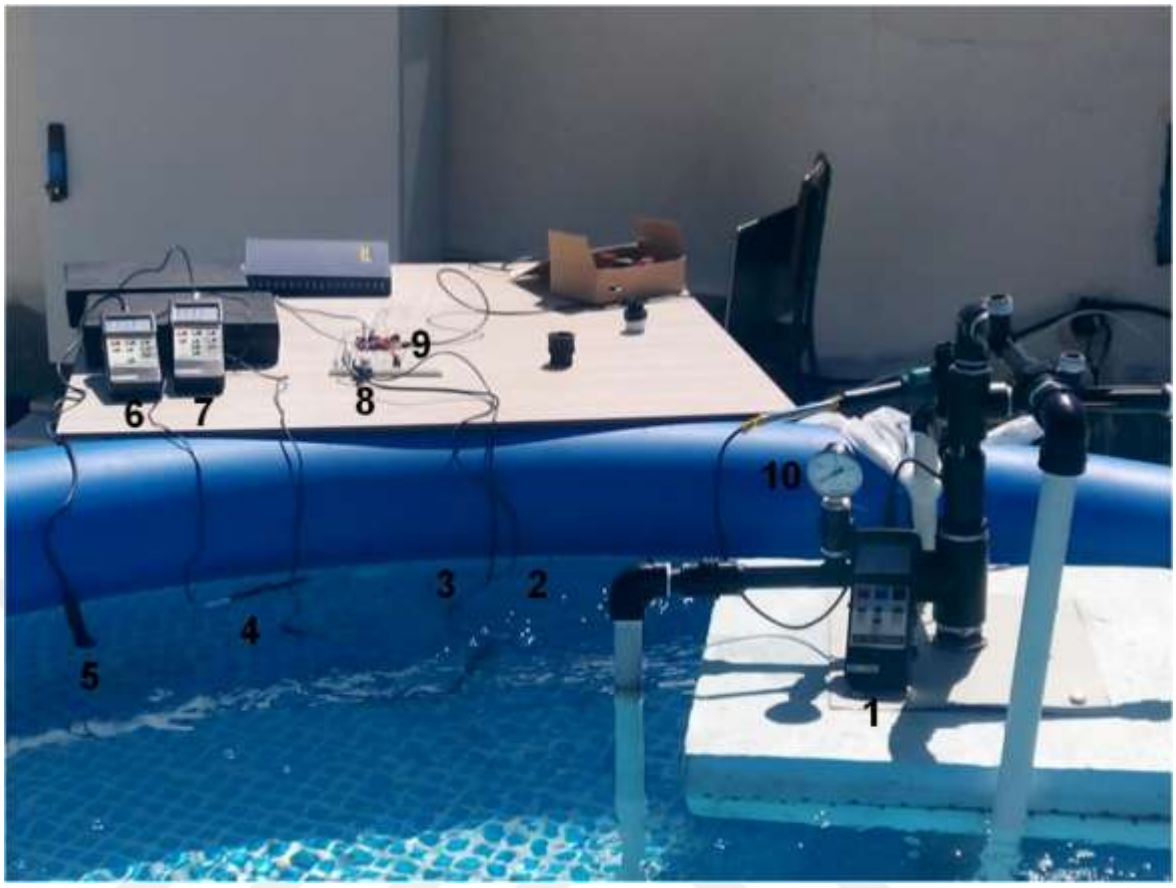

Figure 5.16 Experimental pool test stand

1.Anemometer, 2. DO probe, 3. Water temperature sensor, 4,7. pH probe-device,
5,6. EC sensor-device, 8. Measurement card (Temperature – DO), 9. Arduino Uno

5.6 Test Results

Two prototype aeration systems, Prototype I and Prototype II were tested one by one in plastic pool shown in figure 5.17 (a) and (b). Pool experiments include water-air flow and aerator performance tests. Both water-air flow and aerator performance tests were conducted with six power regimes of the pump including 75, 100, 150, 200, 250, and 300 W.

Figure 5.17 Prototypes pool tests
a. Prototype I, b. Prototype II

5.6.1 Water – Air flow data

Water flow rate and venturi suction air velocity were measured by using water flow meter and hot wire anemometer respectively at test assembly shown in figure 5.18 and figure 5.19 for six different power regimes (75, 100, 150, 200, 250 and 300 W). Power measurements were performed by using power meter shown in figure 5.13 of page 61.

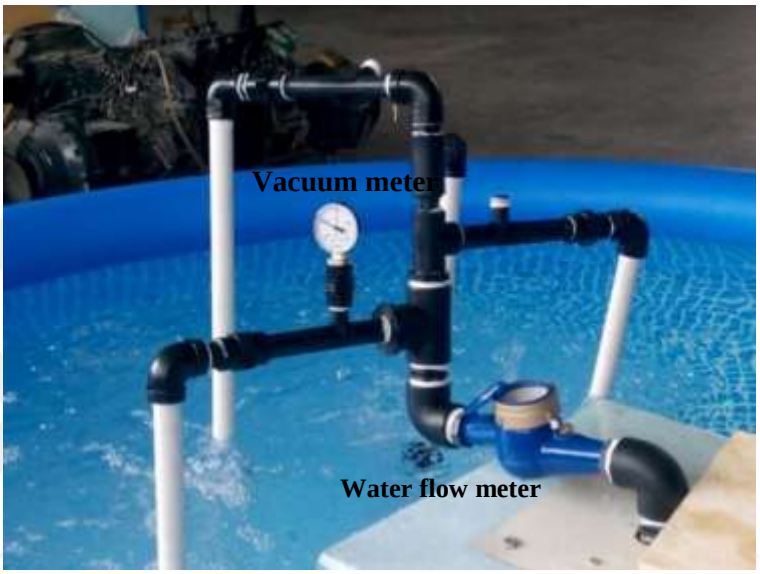

Figure 5.18 Water-flow rate and vacuum measurements

During the aeration system flow measurements, the performance of all the four venturies in the system gave similar vacuum level (- 1.0 bar) and air suction speed. The airflow rates were calculated from measurement data for single venturi and four venturies as shown in table 5.3. It presents water flow rates (Q_w), air velocities (v_a), air flow rates (Q_a) provided for different power consumptions (P). When operating the pump at power levels between 75 and 300 W, water flow rate changed between 3 and 5 m^3/h and air velocity measured with the help of the hot wire anemometer changed between 1 and 2.3 m/s. Airflow rates calculated for a system with single venturi changed between 0.82 – 1.88 m^3/h, and between 3.27 – 7.51 m^3/h for a system with four venturi injectors.

Figure 5.19 Air suction velocity measurement by using hot wire anemometer

Table 5.3 Measurements taken during water and airflow tests

P (W)	Q_w (m^3/h)	v_a (m/s)	$Q_{a,\,single}$ (m^3/h)	$Q_{a,\,4}$ (m^3/h)
75	3.0	1.0	0.82	3.27
100	3.6	1.3	1.06	4.25
150	4.0	1.5	1.23	4.90
200	4.5	1.7	1.39	5.55
250	4.7	2.0	1.63	6.53
300	5.0	2.3	1.88	7.51

5.6.2 Dissolved oxygen concentration data

Firstly, Prototype I was tested based on the ASCE standard to determine standard performance parameters under different pool conditions and power regimes. Test procedure including de-oxygenation and re-oxygenation processes is shown in figure 5.20 as an example for the power consumption of 150 W. As it can be seen from figure 5.20, the de-oxygenation process takes approximately 10-15 minutes after the addition of oxygen removal chemicals. The oxygen concentration decreases up to nearly zero.

However, the re-oxygenation process takes longer time that that of the de-oxygenation process. DO concentrations were measured in 1 minute time intervals.

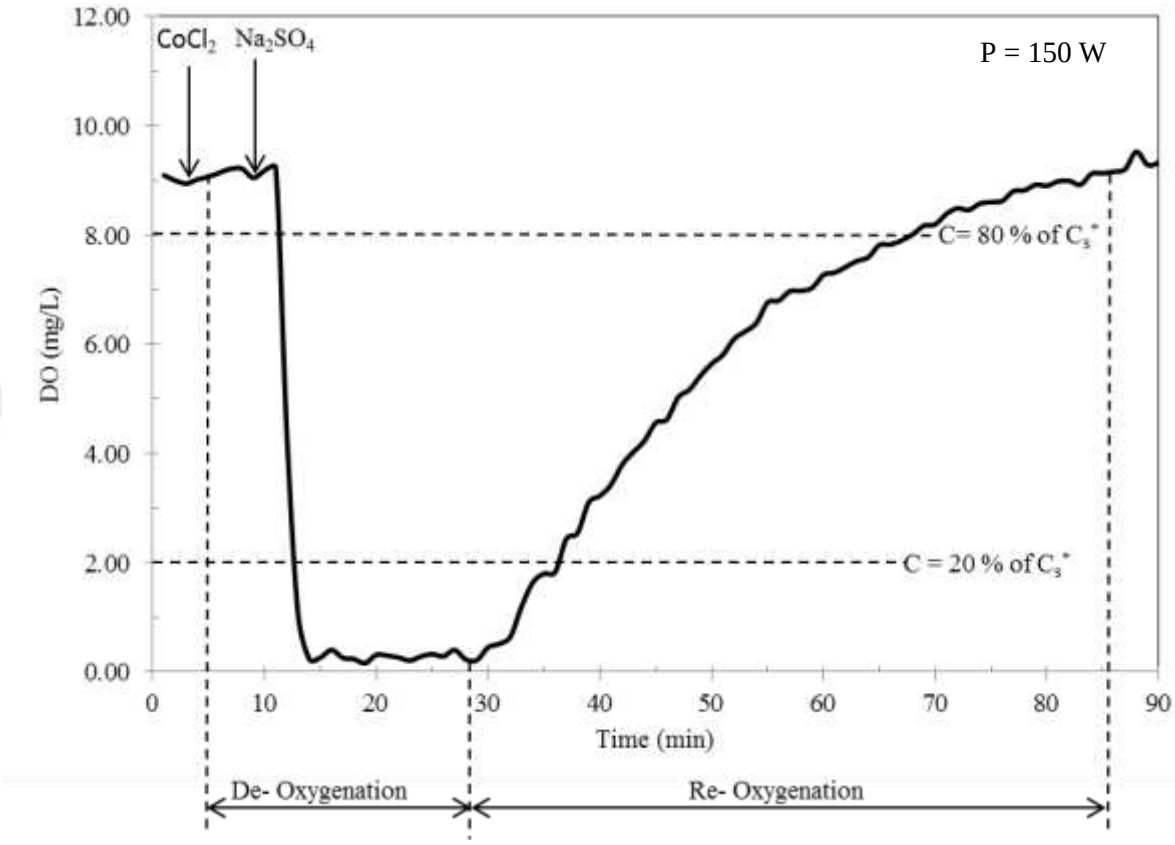

Figure 5.20 DO variations with time for de-oxygenation and re-oxygenation processes

Figure 5.21 shows dissolved-oxygen variation with time for different power regimes during re-oxygenation processes. As it can be seen from the graph, the lower the power consumption the longer is the time required to reach equilibrium concentration. DO concentrations and the elapsed times for saturations of 70%, 80% and 90% at different power regimes are presented in table 5.4.

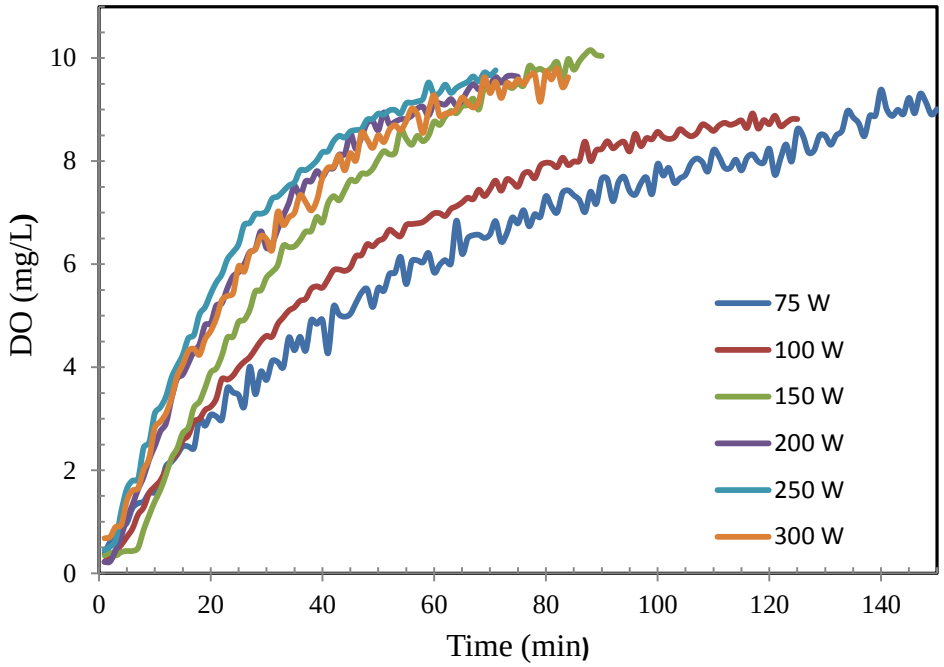

Figure 5.21 Variations of time versus DO for different power consumptions

Table 5.4 DO and the elapsed time* (minutes) for saturations of 70%, 80% and 90%

Power (W)	DO (mg/L)		
	70 %	80 %	90 %
75	6.3 (65)	7.2 (82)	8.1 (110)
100	6.1 (38)	6.95 (43)	7.8 (64)
150	5.9 (23)	6.7 (25)	7.6 (34)
200	6.0 (22)	6.85 (24)	7.7 (30)
250	6.1 (21)	7.0 (22)	7.9 (29)
300	6.1 (20)	6.9 (21)	7.8 (28)

* Values in the parentheses at right side indicate as minute of time elapsed

The elapsed times were between 28 and 110 minutes for the minimum and maximum power consumptions, respectively, while reaching from zero to 90% DO saturation concentration. At input power of 300 W, the elapsed times for saturations of 70%, 80% and 90% took 20, 21 and 28 minutes, respectively. The full DO data obtained during the performance test for 150 W power with their oxygen deficit and natural logarithmic values (to be used for performance characteristics determination by using the graphical method) is given in table 5.5.

Table 5.5 Results of an aeration test for P = 150 W at pool scale of 4 m^3

Time Elapsed (min)	DO (mg/L)	Oxygen deficit (mg/L)	Ln (Oxygen deficit)
1	0.45	8.15	2.10
2	0.51	8.09	2.09
3	0.65	7.95	2.07
4	1.20	7.40	2.00
5	1.64	6.96	1.94
6	1.80	6.80	1.92
7	1.83	6.77	1.91
8	2.44	6.16	1.82
9	2.54	6.06	1.80
10	3.10	5.50	1.71
11	3.22	5.38	1.68
12	3.43	5.17	1.64
13	3.80	4.80	1.57
14	4.03	4.57	1.52
15	4.24	4.36	1.47
16	4.56	4.04	1.40
17	4.63	3.97	1.38
18	5.03	3.57	1.27
19	5.17	3.43	1.23
20	5.42	3.18	1.16
21	5.65	2.95	1.08
22	5.81	2.79	1.03
23	6.10	2.50	0.92
24	6.24	2.36	0.86
25	6.39	2.21	0.79
26	6.76	1.84	0.61
27	6.80	1.80	0.59
28	6.97	1.63	0.50
29	6.98	1.62	0.48
30	7.03	1.57	0.45
31	7.27	1.33	0.29
32	7.31	1.29	0.26
33	7.42	1.18	0.17
34	7.53	1.07	0.07
35	7.59	1.01	0.01
36	7.82	0.78	-0.248
37	7.83	0.77	-0.261
38	7.90	0.70	-0.357
39	8.01	0.59	-0.528
40	8.17	0.43	-0.844
41	8.19	0.41	-0.892
42	8.39	0.21	-1.561
43	8.49	0.11	-2.207
44	8.60	0.00	-

5.6.3 Overall oxygen transfer coefficients

In order to determine the overall oxygen transfer coefficient of aerator, the graphical method shown in figure 4.10 was applied. For this purpose, data of logarithmic oxygen deficit were calculated by using equation (4.2). The graph of the elapsed time versus logarithmic oxygen deficit is shown in figure 5.22. For better accuracy, data below 20% and above 80% of measured oxygen concentrations were truncated (Figure 5.20 and Figure 5.22). For input power of 150 W, DO concentrations at saturations of 20% and 80% were 1.72 mg/L and 6.88 mg/L, respectively (ln[1.72] = 0.542; ln[6.88] = 1.929). The elapsed times for these saturations were 6 and 28 minutes, respectively. The time difference was 22 minutes and logarithmic oxygen deficit was 1.387. The overall oxygen transfer coefficient that is the ratio logarithmic oxygen deficit to time difference or the slop of the line in the graph was calculated as 0.0635 min^{-1}.

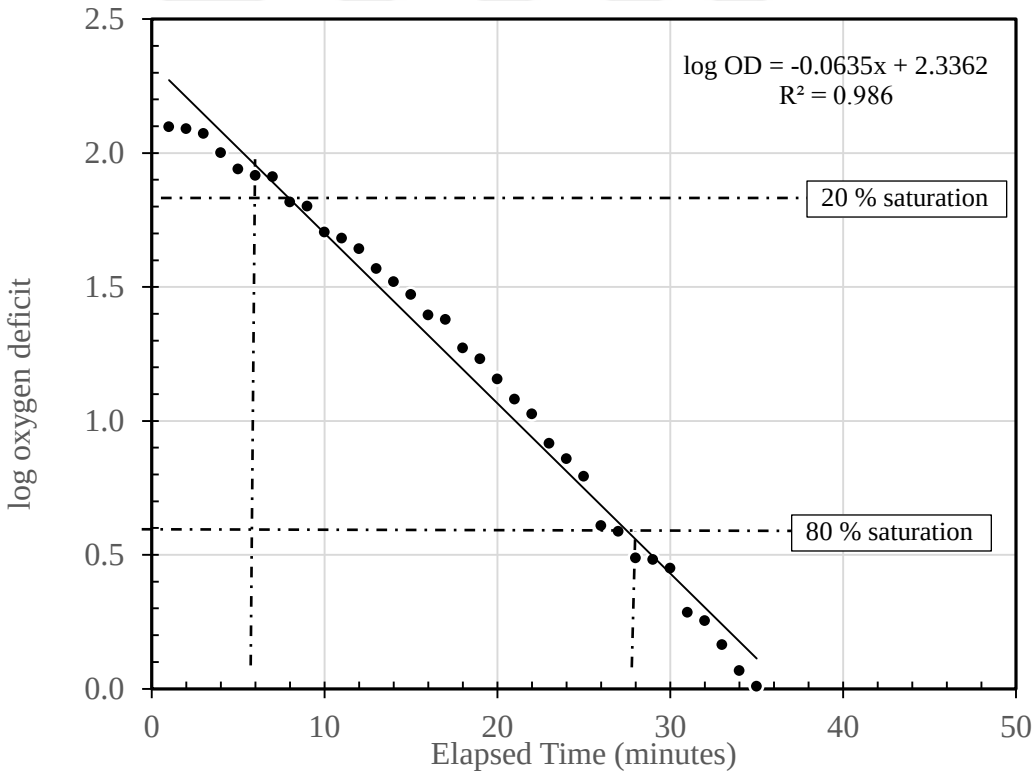

Figure 5.22 Logarithmic oxygen deficit graph for an input power of 150 W

Standard oxygen transfer coefficients $(K_{La})_T$ corrected by using equation (4.3) were calculated. For different water temperatures, coefficients $(K_{La})_T$ at power inputs are also given in table 5.6. Oxygen transfer coefficients $(K_{La})_T$ changed between 1.1 and 5.55 h^{-1}. Standard oxygen transfer coefficient ($(K_{La})_T$) changed between 1.15 and 5.42 h^{-1}. It is observed that oxygen transfer coefficient increases as power increases.

Table 5.6 Oxygen transfer coefficients

P (W)	T_w (°C)	K_{LaT} (min^{-1})	K_{LaT} (h^{-1})	K_{La20} (h^{-1})
75	18	0.0183	1.10	1.15
100	22	0.0397	2.38	2.27
150	18	0.0630	3.78	3.96
200	18	0.0693	4.16	4.36
250	21	0.0815	4.89	4.78
300	21	0.0925	5.55	5.42

Results related to oxygen transfer coefficients obtained in this research were compared with results of a study conducted by Dong et al. (2012) for venturi arrangements given in figure 3.4. According to Dong et al. (2012)'s six different venturi arrangements for input power of P=1500 W, K_{La} oxygen transfer coefficients are between 3.31 h^{-1} and 12.92 h^{-1}. According to Kumar et al. (2014)'s study for input power of P=360 W, K_{La} oxygen transfer coefficient is 1.53 h^{-1} for propeller aspirated pump (PAP) aerator.

5.6.4 Performance test results

Data obtained from aeration performance tests shown in figure 5.23 a, b were used for calculating SOTR, SAE and SOTE. Aerator performance parameters were first obtained for nonstandard conditions (experimental conditions) and changed to standard performance values.

Figure 5.23 Prototype performance test a. prototype I and b. prototype II

Standard performance parameters

Performance parameters including standard oxygen transfer rate (SOTR), standard aeration efficiency (SAE) and standard oxygen transfer effectiveness (SOTE), which are accepted by ASCE, were determined for power consumptions of aerator (Table 5.7).

Table 5.7 Standard performance parameters of aerator

Power consumption (W)	SOTR (kgO_2/h)	SAE (kg O_2/kWh)	SOTE (%)
75	0.042	0.560	4.7
100	0.082	0.820	7.0
150	0.144	0.960	10.7
200	0.158	0.790	10.3
250	0.174	0.696	9.6
300	0.197	0.657	9.4

SOTR values varied between 0.042 kg O_2/h for 75 W and 0.197 kg O_2/h for 300 W. SOTR values increased with an increase in input power (Figure 5.24). However, SAE values increased from 0.56 kg O_2/kWh to 0.96 kg O_2/kWh, and then decreased to 0.66 kg O_2/kWh (Figure 5.24). The highest SAE values were obtained for 150 W of input power. SAE value at the maximum power of 300 W was 0.66 kgO_2/kWh. SOTE changed from 4.7% to 10.7% in parallel with SAE (Figure 5.25).

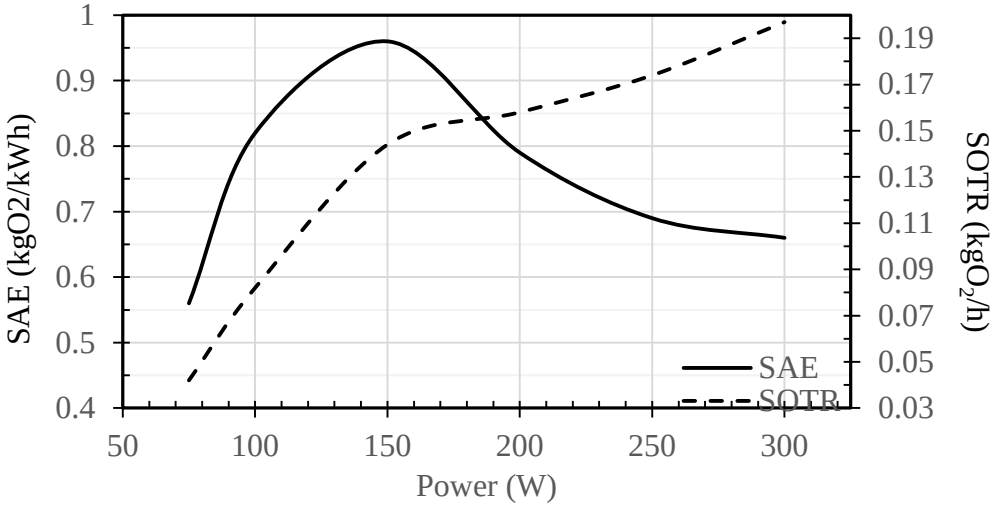

Figure 5.24 Variations of SAE and SOTR with power

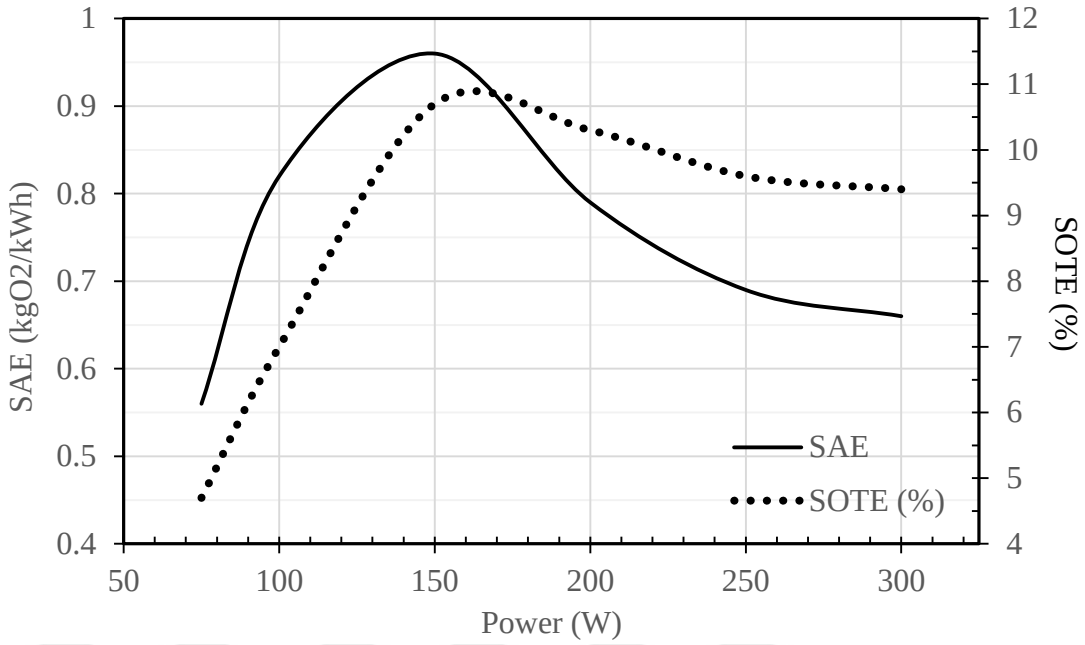

Figure 5.25 Variations of SAE and SOTE with power

SOTR and SAE values according to input powers for different aerator types (V: venturi, PAP: propeller aspirator pump, PCSC: pooled circular stepped cascade pump, CSC: circular stepped cascade pump, PW: paddle wheel) are presented in table 5.8. By comparing the results for different power regimes, it can be seen that performance values of the developed aeration system are higher than results obtained by Zhu et al (2007), Kumar et al. (2010), Dong et al. (2012), Kumar et al. (2013) and Kumar et al. (2014) for other all aerators excluding paddle wheel (PW) surface type aerator. Furthermore, SOTR values are between 0.055 kgO_2/h (Module 3) and 0.204 kgO_2/h (Module 6), SAE values are between 0.082 and 0.306 kgO_2/kWh for different venturi module configurations given by Dong et al. (2012) as shown in figure 3.4. For input power of P=1500 W, the best SOTR and SAE values of Dong et al. (2012) are 0.306 kgO_2/h and 0.204 kgO_2/kWh, respectively. For input powers of P = 150 W and P = 300 W, SAE values of the present aeration system are five times and three times higher than those of Dong et al. (2012), respectively.

Table 5.8 Comparisons of SOTR and SAE according to input power aerator types

Sources	Aerator type	P (W)	SOTR (kg O_2/h)	SAE (kg O_2/kWh)
Prototype I[a]	V	150[b]	0.144	0.960
Prototype I[a]	V	300[c]	0.197	0.660
Prototype II[a]	V	300[c]	0.200	0.670
Zhu et al (2007)	V	1500	0.100	0.070
Zhu et al (2007)	V	1500	0.220	0.140
Kumar et al. (2010)	PAP	361	0.150	0.420
Dong et al. (2012)	V	1500	0.306	0.204
Kumar et al. (2013)	PCSC	186	0.161	0.867
Kumar et al. (2013)	CSC	186	0.135	0.726
Kumar et al. (2013)	PW	746	2.600	3.485
Kumar et al. (2013)	PW	1492	5.000	3.351
Kumar et al. (2013)	PAP	1492	0.454	0.304
Kumar et al. (2014)	PAP	400	0.112	0.280
Kumar et al. (2014)	CSC	160	0.135	0.844

a. Aerator developed in this dissertation
b. Input power was adjusted as P = 150 W
c. Full power.

Typical performance parameters

In addition to the standard performance parameters given above, all the typical performance parameters were calculated from measurement results by using application model defined in figure 4.11. Firstly, water flow rate of pump and air flow rate of venturi were measured. Table 5.9 shows water temperatures (T_w), atmospheric pressure of location (P_{atm}),water flow rate (Q_w), total oxygen mass flow rate (m_o), oxygen transfer rate (OTR), oxygen transfer factor (OTF) and oxygen utilization effectiveness (η) for different power regimes.

Table 5.9 Typical performance parameters determined for prototype aerator

P (W)	T_w (°C)	P_{atm} (kPa)	Q_w (m^3/h)	m_o (kg O_2/h)	OTR (kg O_2/h)	OTF (kg O_2/kWh)	η (%)
75	18.2	91.9	3.0	0.913	0.0378	0.504	4.14
100	21.9	91.9	3.6	1.188	0.0754	0.754	6.35
150	18.0	91.8	4.0	1.370	0.1299	0.866	9.48
200	18.1	91.9	4.5	1.551	0.1430	0.715	9.22
250	20.9	91.7	4.7	1.827	0.1582	0.633	8.66
300	21.0	91.7	5.0	2.102	0.1796	0.599	8.54

When circulating water with flow rate of 5 m^3/h at a power level of 300 W, the velocity of air entering the venturi was 2.3 m/s that, the airflow rate was 1.88 m^3/h for. The total air mass flow rate by the four venturies was 9 kg per hour; total oxygen mass flow rate was 2.1 kg/h. The oxygen injection efficiency of the aeration system was 7 kg O_2/kWh. The oxygen transfer rate was 0.18 kg O_2/h, the oxygenation efficiency was 0.6 kg O_2/kWh. Oxygen utilization effectiveness was 8.5% (for 300 W power). From the total oxygen injected by venturi aeration system, only 4% to 9.5% of it was transferred into water for different power inputs. The rest was discharged into the atmosphere.

Figure 5.26 shows volumetric water flow rate versus variations of air mass and oxygen mass flow rate. Figure 5.27 shows changes in oxygen transfer rate and oxygen transfer factor according to volumetric water flow rate**.** Figure 5.28 shows changes in oxygen mass flow rate and oxygen injection factor according to power.

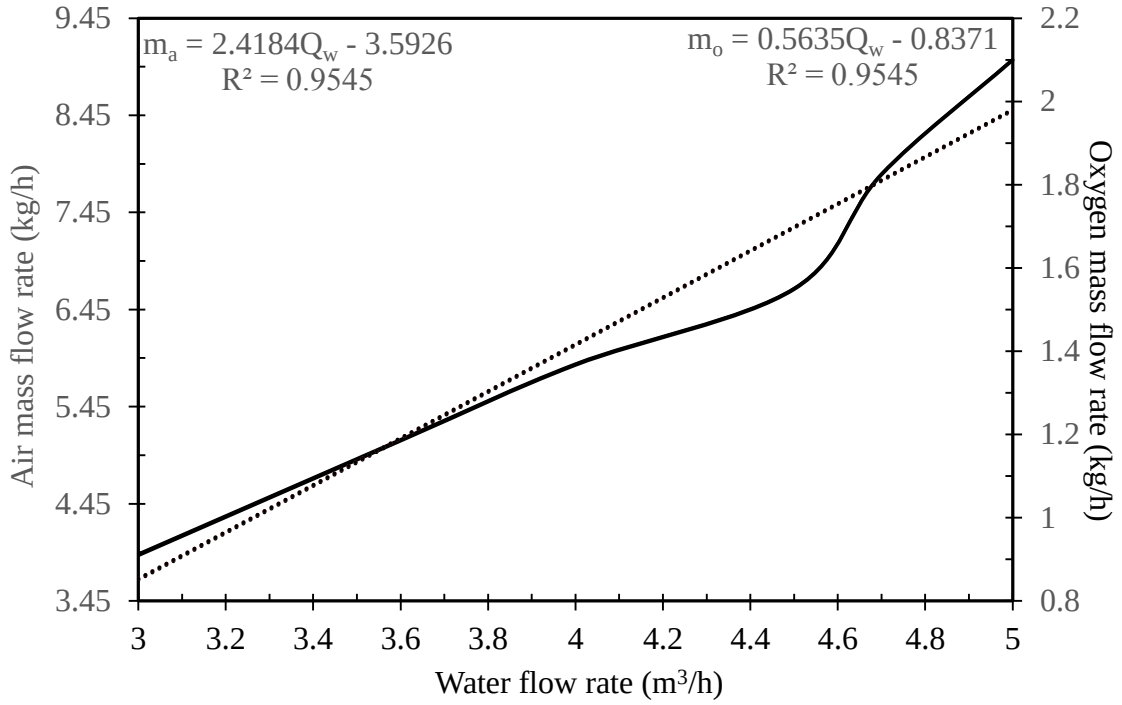

Figure 5.26 Changes in air mass and oxygen mass flow rates according to volumetric water flow rate

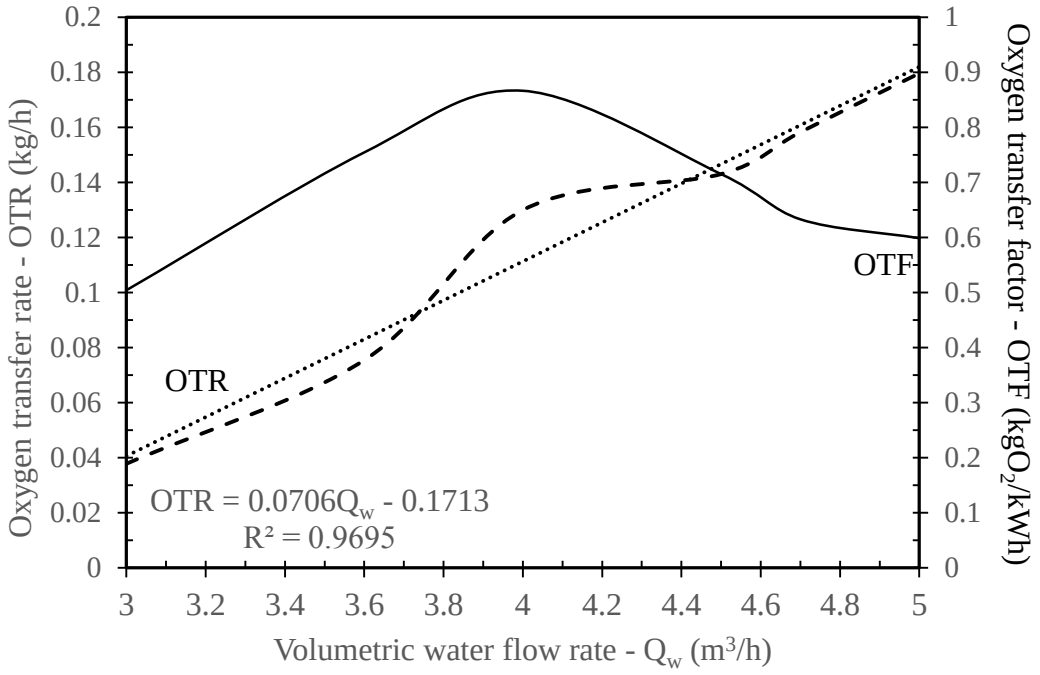

Figure 5.27 Changes in oxygen transfer rate and oxygen transfer factor according to water flow rate

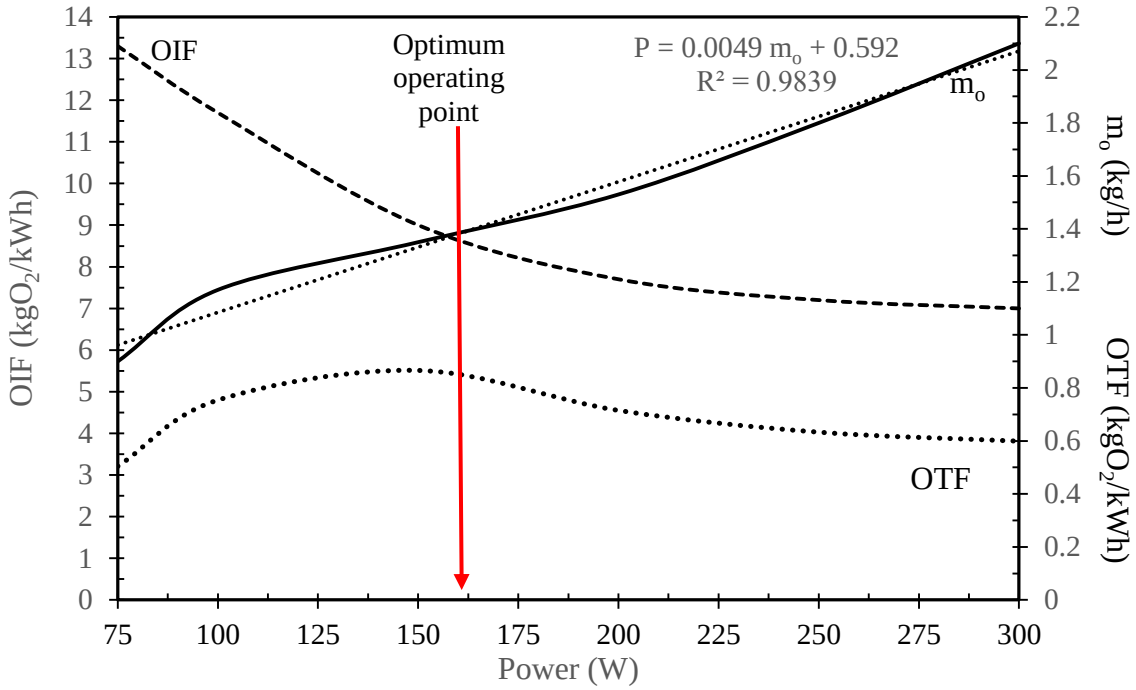

Figure 5.28 Changes in oxygen injection factor - oxygen mass flow rate - oxygen transfer factor according to power consumption

Energy consumption

The energy consumption per kg of DO production for the Prototype aerator was calculated in kWh and MJ. According to power inputs and water flow rates, changes in energy consumption are presented in table 5.10. Energy consumptions of aerator system developed in this dissertation varied between 4.2 and 6.0 MJ of energy per kg O_2.

Table 5.10 Energy consumptions of venturi type aerator

P (W)	Q_w (m^3/h)	OE (kg O_2/kWh)	EC (kWh/kg O_2)	EC (MJ/kg O_2)
75	3	0.504	1.98	7.14
100	3.6	0.754	1.33	4.77
150	4	0.866	1.15	4.16
200	4.5	0.715	1.40	5.03
250	4.7	0.633	1.58	5.69
300	5	0.599	1.67	6.01

5.6.5 Trout fish farm test findings

Protype II (floating platform aeration system) was tested in between 20-24 July 2015 at trout production ponds in Çifteler of Ankara University (Eskişehir). Tests were made using two similar ponds having sizes of 6 x 10 m at depths between 0.5 and 1 m. Around 2600 Rainbow trout fish with an average weight of 140 g each were placed in each pond. The Prototype aerator was placed in one of the ponds but the other pond was used for control. Water temperature and DO concentrations were measured in both ponds. Figure 5.29 shows fishponds and aerator used during the tests. Feeding regimes and all cultural operations for both ponds were similar and performed simultaneously.

The average temperature and DO concentration of the water entering trout pond was 19.3°C and 4.23 mg/L, respectively. Figure 5.30 shows variations in water and air temperatures. Figure 5.31 shows changes in DO concentration of both ponds.

Figure 5.29 Prototype II during field test

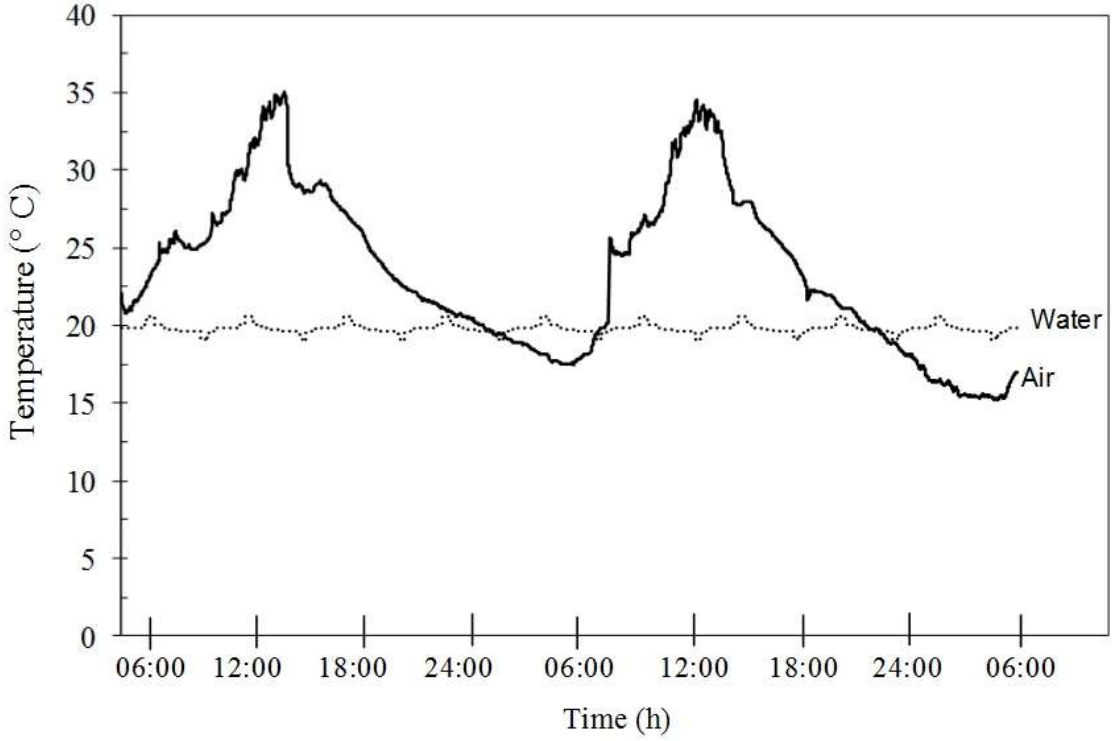

Figure 5.30 Variations in water and air temperatures at pond environment

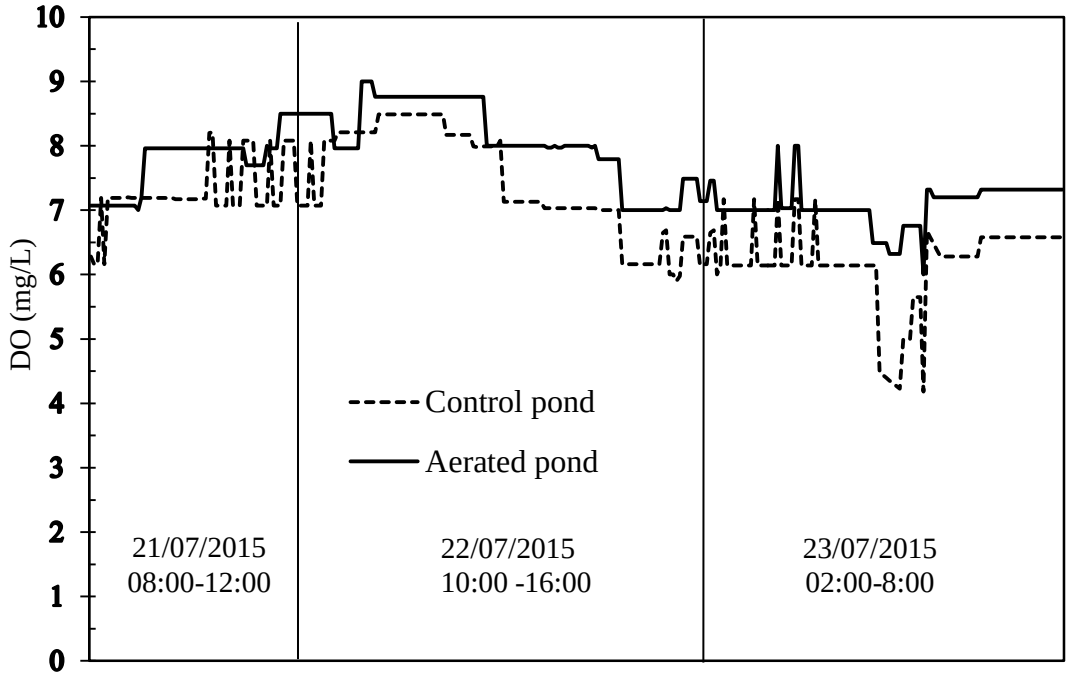

Figure 5.31 Changes in DO concentration of the both ponds water

The minimum concentrations of DO occur just before sun rise and the maximum concentration is just before sun set. DO concentrations of the water in the entrance of the canal were measured to be 3.5 to 6 ppm throughout one day. Due to the prototype aeration system the DO concentration was observed to increase by 1.5 – 2.0 mg/L.

During the testing period it had been observed that, there were fish deaths in all non-aerated ponds during the night time due to oxygen shortages. It had been observed that between 3 to 12 fish dies overnight. Meanwhile fish deaths didn't occurred in the aerated pond during the test period.

6. CONCLUSIONS and RECOMMENDATIONS

In commercial scale aquaculture, DO concentration and water temperature must be always measured, and controlled. DO shortages usually occur few hours before sunrise. DO concentrations have a direct effect on the degree of comfort of aquatic animals for sustainable production with in high stocking densities in intensive aquaculture. Artificial aeration requires for sustainable aquaculture production and preventing fish deaths due to DO shortage.

The main objective of this thesis is to design and construction a prototype solar energy driven venturi type - aeration system for fishponds. Furthermore, the system was designed to be able to measure DO concentrations and temperatures of pond water at real time and automatically control the operation of system.

Two prototype aerator systems based on nominal power of 300 W were designed: Prototype I and Prototype II. Prototype aerators were constructed based on theoretical fundamentals and experimental results of aeration system in which critical points like flow pressure and energy losses were taken into consideration.

Prototype I aeration system consists of a floating part and a fixed part. The floating part involves flotation panel, submersible pump, venturi injectors, pipefittings and various fasteners. The fixed part includes two solar panels of 300 W (2 x 150 W), two batteries galvanized steel profiles, various fasteners, charge controller and pump controller.

It is difficult to reach every part of ponds for aeration from shore that the floating type aerator is the best alternative. Solar PV panel driven floating type aerators will avoid electric wirings and other connecting parts with the shore.

Prototype II aeration system was constructed as a floating system. Prototype II consists of same components with Prototype I. However, components of all the system were fastened on the floating platform made from polyurethane. In addition, one poly-crystalline solar panel of 245 W was used for power requirement.

The system can work as long as there is solar radiation during the day. Furthermore, it can work continuously for 6 hours in the absence of solar radiation during the night. This means that it can work for three days during the night for two hours per night or two nights for three hours per night in the absence of any solar radiation during these days.

Venturi type injectors were used for oxygen injection to suck air from the atmosphere into water. These injectors work only due to hydrodynamic principles without any extra mechanical components. According to modeling and experiment results, specific solutions to minimize pressure losses were carried out during construction of the system. In order to improve system efficiency, venturi arrangement and nozzle exit diameter were determined. Pump - venturi arrangements and nozzle exit diameters were taken in to account for efficient performance. The smaller the size of bubble diameter is the larger the efficiency of aerator. The optimum nozzle - exit diameter was determined. In addition, the minimum possible lengths of pipe as well as minimum connecting parts are used for minimum pipe and fittings pressure losses.

Performance parameters including standard oxygen transfer rate (SOTR), standard aeration efficiency (SAE) and standard oxygen transfer efficiency (SOTE), which are accepted by ASCE, were determined for aerators developed as Prototype.

It has been understood from this project that an aerator with higher standard oxygen transfer rate is not always the most efficient one when we consider its energy consumption (standard aeration efficiency). As a result of this aerators can be operated at high SOTR when energy is not a problem. For example, a solar or wind energy driven aerator can work at its maximum oxygen transfer capacity during the times when wind and solar radiation are in excess. But if there is energy scarcity it is better to operate at the best SAE. For solar driven aerators the aerator can be on at maximum oxygen transfer rate during the day time in the summer and it is better to operate it at its highest standard aeration efficiency during the night and winter time.

An oxygen transfer model was defined for aerators. The oxygen transfer rate (OTR), oxygen transfer factor (OTF) and oxygen transfer efficiency (η) values were calculated from measurement results.

During this dissertation study, it has been understood that the name standard aeration efficiency (SAE) that is used almost in all literatures in the area of aeration does not exactly match with its meaning. First of all the main parameter for the determination of SAE is not air but oxygen, its unit is kg O_2/kWh. Additionally, the word efficiency is not an appropriate technical term. Efficiencies are usually expressed with no unit in fractional number with a maximum ideal value of unity (it can also be expressed in percentages). But for the case of SAE the value can be any value of above or below unity. It is not also without a measuring unit.

Due to the above two reasons, it is recommended to re-name the SAE. In doing that the term aeration must be replaced with oxygen and the word efficiency must be changed. In this dissertation work it is suggested to use Standard Oxygen Transfer Factor (SOTF) in place of SAE.

Aquaculture farms are usually far away from electric grids that, solar energy is the best feasible alternative among other energy resources. One of the main problems of solar energy in many fields of application is the fact that the availability of solar radiation when it is needed. For example heating loads required and solar radiation magnitudes are out of phase. That means heating of buildings is necessary during the winter time but the solar radiation at winter times is low; but there is the highest solar radiation during the summer where cooling is not necessary. Whereas aeration and solar radiation availability are in phase that aeration is usually required during the months of June to September where there is high solar radiation available during this time.

The designed solar energy floating type aerators can also be easily constructed for any scale. This can be done by either selecting large sized components like the pump, venturi solar panels battery etc. or by manufacturing multiple aerators of the same size.

From the solar radiation modeling one can conclude that, installation of solar collectors with optimum fixed tilt angles has a significant advantage in energy gain. More Significant energy gain can also be harvested by making timely adjustments of angles of tilt. The more number of the adjustments per year the better are the energy benefits.

From the ANSYS venturi model and experimental works, it can be concluded that a venturi type aeration system fulfills satisfactory result for aeration of small and medium fish farms for following reasons and advantage over other conventional aerator types:

- No any moving parts and no damage on fishes
- Low friction, low maintenance
- Designing for any size (small, medium, large)
- Low cost solution
- Low energy consumption
- Environmental friendly
- DO and water temperature measurement
- Automatic control.

From this research, it can be understood that dissolved oxygen measurement can be successfully achieved by using cheaply available DO measuring probe and signal conditioning circuit. The automation of aerators can be provided in a flexible way and low cost by measuring DO and temperature levels via electronic platforms based on ARM.

Generally, a full monitoring and control system can be implemented to fish farms and for other areas where aeration is required. Since aeration process is affected by environmental condition, the meteorology data need for efficient system monitoring and control.

Medium and small scale farmers do not produce fish during the hot season due to the fact that the hotter the water the lower is the dissolved oxygen content. But by implementing an aerator, the fish production season can be increased. These aerator

systems can also be used for prevention of algal blooming at both fishponds and natural water areas.

The constructed type solar energy driven aerators can have additional advantages for effluent treatment purposes when it is compared with aquaculture applications. This is due to the fact that effluent treatment of factory wastes can takes please at any time where there is energy available but DO shortages for fish farms are usually occurred during night where the aerator will perform by battery powers.

Furthermore, very important application of this venturi type aerator is for purification of ground waters to remove metals (Iron and Manganese) and unnecessary gasses. The advantage of using it to this type of application is that the pump used in the system to pump water out of the ground will also be used for aeration purpose at the same time, that is, no need of additional power and additional pumping system.

REFERENCES

Ahmad, M.J. and Tiwari, G.N. 2009. Optimization of Tilt Angle for Solar Collector to Receive Maximum Radiation. The Open Renewable Energy Journal, 2, 19 – 24.

Ann, T.L., John, J.S. and Linda, P.W. 2005. Iron and Manganese in Household Drinking Water, Cornell Cooperative Extension, 3, New York USA.

Anonymous. 2007. Measurements of Oxygen Transfer in Clean Water. American Society
of Civil Engineers (ASCE), Virginia, last accessed: 30/09/2013.

Anonymous. 2015. http://www.eie.gov.tr/MyCalculator/Default.aspx, last accessed: 13/12/2015.

Anonymous. 2014. The state of world fisheries and aquaculture. Rome, Italy, last accessed: 01/01/2015.

Anomymous. 2015. turbine aerator, http://www.oxyturbine.com/, last accessed: 30/08/2015.

Anonymous. 2015. Türkiye su ürünleri istatistikleri. http://www.tuik.gov.tr/, last accessed: 01.08.2015.

Applebaum, J., Mozes, D., Steiner, A., Segal, I., Barak. M., Reuss, M. and Roth, P. 2001 Aeration of fish ponds by photovoltice power. Progress in photovoltaic research and applications, 9, 295 – 301.

Boyd, C.E. 1998. Pond water aeration systems, Aquacultural Engineering, 18, 9–40.

Boyd, C.E. and Tucker, C.S. 1998. Pond aquaculture water quality management, Kluwer Academic Publishers.

Boyd, C.E. and Watten, B.J. 1989. Aeration systems in aquaculture, Reviews in Aquatic Science, 1: 425–472.

Brown T.W. and Tucker, C.S. 2014. Pumping Performance of a Modified Commercial Paddlewheel Aerator for Split-Pond Aquaculture Systems, North American Journal of Aquaculture, 76 (1), 72-78

Brown, T.W., Tucker, C.S. and Rutland, B.L., 2016. Performance evaluation of four different methods for circulating water in commercial-scale, split-pond aquaculture systems, Aquacultural Engineering, Volume 70 (1), Pages 33-41

Cancino, B., Roth, P. and Reub, M. 2004. Design of high efficiency surface aerators part one. Aquacultural Engineering, 31, 83–98.

Chachuata, B., Rocheb, N. and Latifi, M.A. 2005. Optimal aeration control of industrial alternating activated sludge plants. Biochemical Engineering Journal, 23, 277–289.

Coşkun, F. 2014. Su ürünleri yetiştiricileri sektör raporu. Ankara.

Dong, C., Zhu, J. and Miller, C.F. 2009. Evaluation of six aerator modules built on venturi air injectors using clean water test. Water science and technology, IWA Publishing, 1353- 1359. Science

Dong, C., Zhu, J., Wu, X. and Miller, C.F. 2012. Aeration efficiency influenced by venturi aerator arrangement, liquid flow rate and depth of diffusing pipes. Environmental Technology, 33 (11), 289 – 1298.

Duffie, J.A. and Beckham, W.A. 2013. Solar Engineering of Thermal Processes. Wiley, 1- 178, New Jersey, USA

Floyd, R.F. 2011. Dissolved oxygen for fish production. Florida Cooperative Extension Service, Institute of Food and Agricultural Sciences, New York, USA.

Foster, R., Ghassemi, M. and Costa, R. 2010. Solar Energy. Taylor and Francis Group: CRC press, Chicago, USA.

Ghomi, M.R., Sohrabnejad, M. and Ovissipour, M.R. 2009. An experimental study of nozzle diameters, aeration depths and angles on standard aeration efficiency (SAE) in a venturi aerator. Water practice and technology, 4 (3), 1-8.

Kadzinga, F. 2015. Venturi Aeration of Bioreactors. Master's thesis. University of Cape Town, Cape Town, South Africa.

Keshavarz, S.A., Talebizadeh, P., Adalatia, S., Mehrabian, M.A. and Abdolzadeh, M. 2012. Optimal Slope-Angles to Determine Maximum Solar Energy Gain for Solar Collectors Used in Iran. International Journal of Renewable Energy Resource, 2, 665 – 673.

Kumar, A., Moulick, S., Singh, B.K. and Mal, B.C. 2013. Design characteristics of pooled circular stepped cascade aeration system, Aquacultural Engineering, 56, 51– 58.

Kumar, A., Moulick, S. and Mal, B.C., 2014. Performance Evaluation of Different Aeration Systems for Aquaculture, 2014 ASABE – CSBE/SCGAB Annual International Meeting, Montreal, Quebec Canada, July 13 – 16, 2014 Paper, Paper Number: 141902230, 1-12

Kumar, A., Moulick, S. and Mal, B.C. 2010. Performance evaluation of propeller-aspirator-pump aerator, Aquacultural Engineering, 42, 70–74.

Laksitanonta, S. and Singh, G. 2003. Development of a Venturi Aerator for Aquaculture Pond. ASAE Annual International Meeting, Las Vegas, Nevada, USA.

Lawson, B.T. 2012. Fundamentals of Aquacultural Engineering. Kluwer Academic Publishers, Massachusetts, USA.

Lekang, O.I. 2013. Aquaculture engineering. John Wiley & Sons, New York, USA.

Liu, C., Li, S. and Zhang, F. 2011. The oxygen transfer efficiency and economic cost analysis of aeration system in municipal wastewater treatment plant. Energy Procedia, 5, 2437–2443.

Mallya, Y.J. 2007. The effect of dissolved oxygen on fish growth in aquaculture. UN-Fisheries Training Program, Iceland.

Ma, W.X., Huang, T.L. and Li, X., 2015. Study of the application of the water-lifting aerators to improve the water quality of a stratified, eutrophicated reservoir, Ecological Engineering, Volume 83, Page: 281-290.

Moulick, S., Mal, B.C. and Bandyopadhyay, S., 2002. Prediction of aeration performance of paddle wheel aerators. Aquacultural Engineering, 25 (4), 217–237.

Mueller, A.J., Boyle, W.C. and Popel, H.J. 2002. Aeration: Principles and Practice. CRC Press, New York, USA.

Mukhtar, S., Borhan, M.S., Rahman, S. and Zhu, J. 2010. Evaluation of field scale aeration system in an anaerobic poultry lagoon. Applied Engineering in Agriculture, 26(2), 307-318.

Neelamegam, P., Kumaravel, S. and Raghunathan, R. 2008. Microcontroller Based Distributed Monitoring System for Fresh Water Fish Aquaculture. Instrumentation Science and Technology, 36: 515–524.

Parker, R. 2012. Aquaculture science, Delmar Cengage Learning, New York, USA.

Pearson, P.R. and Green, B.W. 2006. A Device to Continuously Monitor Dissolved Oxygen and Temperature at User-Selected Depths and Locations in Culture Ponds. North American Journal of Aquaculture 68:253–255.

Prasetyaningsari, A. and Setiwan, A.A. 2013. Design optimization of solar powered aeration system for fish pond in Sleman Regency, Yogyakarta by HOMER software, Energy Procedia, 32, 90 – 98.

Romaire, R.P. and Merry, G.E., 2007. Effects of Paddlewheel Aeration on Water Quality in Crawfish Ponds, Journal of Applied Aquaculture, 19(3), 61-75.

Shammas, N.K. and Wang. L.K., 2016. Water engineering: hydraulics, distribution, and treatment, John Wiley & Sons, Inc.

Siabi, W.K. 2008. Aeration and its application in ground water purification. 33rd WEDC International conference, Accra, Ghana.

Solpico, D.B. Libatique, N.J. Tangonan, G.L. Cabacungan, P.M. Girardot, G. Macaraig,R.M. Perez,T.R. and Teran, A. 2014. Solar Powered Field Server and Aerator Development for Lake Palakpakin. Journal of Advanced Computational Intelligence and Intelligent Informatics, 18(5), 755 -763.

Sperling, V.M., 2007. Basic Principles of Wastewater Treatment: Biological Wastewater Treatment Volume 2, 212 pages, IWA Publishing, UK

Stenstrom, M.K, Leu, S.Y. and Jiang, P., 2006. Theory to Practice: Oxygen Transfer and the New ASCE Standard. Proceedings of WEFTC 2006, pp 4838-4852

Sulzer, 2015. Aerator Type ABS Venturi Jet, http://www.sulzer.com/en/-media/Documents/ProductsAndServices/Pumps_and_Systems/Compressors_and_Aeration/ProductInformation/ABS_Venturi_Jet_Aerator/Venturi_Jet_TDS.pdf, last accessed 30/08/2015.

Tucker, C.S. and Robinson, E.H. 1990. Channel catfish farming handbook.Van Nostrand Reinhold.

Wurts, A.W. 2010. Guideline for producing food size channel catfish. Kentucky state University cooperative extension program, Kentucky, USA.

Yadav, A.K. and Chandel, S.S. 2013. Tilt angle optimization to maximize incident solar radiation. Renewable and Sustainable Energy Reviews, 23, 503 – 514.

Zhu, J.,Miller, J.F., Dong, C., Wu, X., Wang, L. and Mukhtar, S. 2007. Aerator module development using venturi air injectors to improve aeration efficiency. Applied Engineering in agriculture, 23(5): 661-667.

APPENDIX

Appendix 1 Oxygen Solubility in Water at Different Temperatures and Salinity

Table 1 The solubility of oxygen (mg/L) in water at different temperatures and salinity from moist air at 101.325 kPa (Lawson, 2002)

t (°C)	Salinities (g/l)							
	0	5	10	15	20	25	30	35
0	14.6	14.11	13.64	13.18	12.74	12.31	11.9	11.5
2	13.81	13.36	12.91	12.49	12.07	11.67	11.29	10.91
4	13.09	12.67	12.25	11.85	11.47	11.09	10.73	10.38
6	12.44	12.04	11.65	11.27	10.91	10.56	10.22	9.89
8	11.83	11.46	11.09	10.74	10.4	10.07	9.75	9.44
10	11.28	10.92	10.58	10.25	9.93	9.62	9.32	9.03
11	11.02	10.67	10.34	10.02	9.71	9.41	9.12	8.83
12	10.77	10.43	10.11	9.8	9.5	9.21	8.92	8.65
13	10.52	10.2	9.89	9.59	9.29	9.01	8.73	8.47
14	10.29	9.98	9.68	9.38	9.1	8.82	8.56	8.3
15	10.07	9.77	9.47	9.19	8.91	8.64	8.38	8.13
16	9.86	9.56	9.28	9	8.73	8.47	8.21	7.97
17	9.65	9.36	9.09	8.82	8.55	8.3	8.05	7.81
18	9.45	9.17	8.9	8.64	8.39	8.14	7.9	7.66
19	9.26	8.99	8.73	8.47	8.22	7.98	7.75	7.52
20	9.08	8.81	8.56	8.31	8.07	7.83	7.6	7.38
21	8.9	8.64	8.39	8.15	7.91	7.68	7.46	7.25
22	8.73	8.48	8.23	8	7.77	7.54	7.33	7.12
23	8.56	8.32	8.08	7.85	7.63	7.41	7.2	6.99
24	8.4	8.16	7.93	7.71	7.49	7.28	7.07	6.87
25	8.24	8.01	7.79	7.57	7.36	7.15	6.95	6.75
26	8.09	7.87	7.65	7.44	7.23	7.03	6.83	6.64
27	7.95	7.73	7.51	7.31	7.1	6.91	6.72	6.53
28	7.81	7.59	7.38	7.18	6.98	6.79	6.61	6.42
29	7.67	7.46	7.26	7.06	6.87	6.68	6.5	6.32
30	7.54	7.34	7.14	6.94	6.76	6.57	6.39	6.22
31	7.41	7.21	7.02	6.83	6.64	6.47	6.29	6.12
32	7.29	7.09	6.9	6.72	6.54	6.36	6.19	6.03
33	7.17	6.98	6.79	6.61	6.43	6.26	6.1	5.94
34	7.05	6.86	6.68	6.51	6.34	6.17	6.01	5.85
35	6.93	6.75	6.58	6.4	6.24	6.07	5.91	5.76
36	6.82	6.65	6.47	6.31	6.14	5.98	5.83	5.68
37	6.72	6.54	6.37	6.21	6.05	5.89	5.74	5.59
38	6.61	6.44	6.28	6.12	5.96	5.81	5.66	5.51

Appendix 2 Concentration of DO with Atmospheric Pressure and Temperature

Table 2 DO (mg/L) with atmospheric pressure and temperature at 100% RH (Honeywell, 2013)

	P_{atm} (kPa)									
t(°C)	105.325	103.325	101.325	99.325	97.325	95.325	93.326	91.326	89.326	88.659
0	15.2	14.9	14.6	14.3	14	13.7	13.4	13.2	12.9	12.6
1	14.8	14.5	14.2	13.9	13.6	13.3	13.1	12.8	12.5	12.2
2	14.4	14.1	13.8	13.5	13.3	13	12.7	12.4	12.2	11.9
3	14	13.7	13.4	13.2	12.9	12.6	12.4	12.1	11.8	11.6
4	13.6	13.4	13.1	12.8	12.6	12.3	12.1	11.8	11.5	11.3
5	13.3	13	12.8	12.5	12.2	12	11.7	11.5	11.2	11
6	12.9	12.7	12.4	12.2	11.9	11.7	11.4	11.2	10.9	10.7
7	12.6	12.4	12.1	11.9	11.6	11.4	11.2	10.9	10.7	10.4
8	12.3	12.1	11.8	11.6	11.4	11.1	10.9	10.7	10.4	10.2
9	12	11.8	11.6	11.3	11.1	10.9	10.6	10.4	10.2	9.94
10	11.7	11.5	11.3	11	10.8	10.6	10.4	10.1	9.92	9.69
11	11.5	11.2	11	10.8	10.6	10.4	10.1	9.91	9.69	9.47
12	11.2	11	10.8	10.5	10.3	10.1	9.9	9.68	9.47	9.25
13	10.9	10.7	10.5	10.3	10.1	9.89	9.68	9.47	9.26	9.04
14	10.7	10.5	10.3	10.1	9.88	9.67	9.46	9.26	9.05	8.85
15	10.5	10.3	10.1	9.87	9.67	9.46	9.26	9.06	8.86	8.65
16	10.3	10.1	9.85	9.65	9.45	9.26	9.06	8.86	8.66	8.46
17	10	9.84	9.65	9.46	9.26	9.07	8.87	8.68	8.48	8.29
18	9.83	9.64	9.45	9.26	9.07	8.88	8.69	8.5	8.31	8.12
19	9.63	9.45	9.26	9.07	8.89	8.7	8.51	8.33	8.14	7.95
20	9.44	9.25	9.07	8.89	8.7	8.52	8.34	8.15	7.97	7.79
21	9.26	9.08	8.9	8.72	8.54	8.36	8.18	8	7.82	7.64
22	9.07	8.9	8.72	8.54	8.37	8.19	8.01	7.84	7.66	7.48
23	8.91	8.73	8.56	8.39	8.21	8.04	7.86	7.69	7.52	7.34
24	8.74	8.57	8.4	8.23	8.06	7.89	7.72	7.55	7.38	7.2
25	8.58	8.41	8.24	8.07	7.9	7.74	7.57	7.4	7.23	7.06
26	8.42	8.26	8.09	7.92	7.76	7.59	7.43	7.26	7.1	6.93
27	8.28	8.11	7.95	7.79	7.62	7.46	7.3	7.14	6.97	6.81
28	8.13	7.97	7.81	7.65	7.49	7.33	7.17	7.01	6.85	6.69
29	7.99	7.83	7.67	7.51	7.35	7.2	7.04	6.88	6.72	6.57
30	7.85	7.7	7.54	7.38	7.23	7.07	6.92	6.76	6.61	6.45
31	7.72	7.56	7.41	7.26	7.1	6.95	6.8	6.64	6.49	6.34
32	7.58	7.43	7.28	7.13	6.98	6.83	6.68	6.53	6.38	6.22
33	7.46	7.31	7.16	7.01	6.86	6.71	6.57	6.42	6.27	6.12

Appendix 3 Concentration of DO with Relative Humidity and Temperature

Table 3 DO (mg/L) with relative humidity and temperature (Honeywell, 2013)

t (°C)	DO (100% R.H.)	DO (0% R.H.)
0	14.6	14.66
1	14.19	14.26
2	13.81	13.89
3	13.44	13.53
4	13.09	13.18
5	12.75	12.85
6	12.43	12.54
7	12.12	12.23
8	11.83	11.94
9	11.55	11.66
10	11.27	11.4
11	11.01	11.14
12	10.76	10.9
13	10.52	10.66
14	10.29	10.44
15	10.07	10.22
16	9.85	10.01
17	9.65	9.82
18	9.45	9.63
19	9.26	9.45
20	9.07	9.27
21	8.9	9.11
22	8.72	8.95
23	8.56	8.8
24	8.4	8.65
25	8.24	8.51
26	8.09	8.37
27	7.95	8.24
28	7.81	8.12
29	7.67	8
30	7.54	7.88
31	7.41	7.77
32	7.28	7.66
33	7.16	7.56
34	7.05	7.46

CURRICULUM VITAE

Name **:** Yohannes Berhane GEBREMEDHEN

Place of Birth **:** Axum, Ethiopia

Date of birth **:** 02/09/1980

Marital status **:** Married

Foreign language : English and Turkish

Educational background

High school: Axum comperhensive high school (1998)

BSC: Addis Ababa University Department of Mechanical Engineering (2004).

MSC: Addis Ababa University Department of Mechanical Engineering (2007).

Work experience

Axum University department of Mechanical Engineering in (2008 - present)

Publications

YOHANNES, B. G. 2014. Determination of Optimum Fixed and Adjustable Tilt Angles for Solar Collectors by Using Typical Meteorological Year data for Turkey. International journal of renewable energy research, Vol.4, No.4.

ANKARA ÜNİVERSİTESİ
FEN BİLİMLERİ ENSTİTÜSÜ

DOKTORA TEZİ

GENİŞ ÖZET

BALIK ÇİFTLİKLERİ İÇİN GÜNEŞ ENERJİLİ HAVALANDIRMA SİSTEMİNİN TASARIMI VE PROTOTİP İMALATI

Yohannes Berhane GEBREMEDHEN

TARIM MAKİNALARI VE TEKNOLOJİLERİ MÜHENDİSLİĞİ ANABİLİM DALI

ANKARA
2016

1.GİRİŞ

Son yıllarda, dünya'da su ürünleri yetiştiriciliği ve avcılıktan elde edilen 154 milyon ton su ürününün 131 milyon tonu gıda amaçlı kullanılmaktadır. Dünya balık arzı son 50 yılda, yıllık %1.7'lik nüfus artışına karşın, % 3.2'lik ortalama büyüme hızıyla dikkat çekmektedir. Okyanus ve deniz avcılığı dışında, kafes su ürünleri sektörü son 20 yılda küreselleşme ve su ürünleri için artan talep nedeniyle hızla büyümektedir .

Türkiye'de balık üretimi 2005'den 2014'e 118 277 tondan 235 133 tona artmıştır. Bu dönemde kafes balık üretimi ise 48 033 tondan 107 533 tona yükselmiştir.

Kültür balıkçılığı alanında, 2012 verilerine göre, 1791 adet tatlı suda, 372 adet denizde üretim yapan olmak üzere toplam 2163 adet işletme faaliyet göstermektedir. Alabalık üretimi yapılan küçük ve orta ölçekli bu işletmelerin çoğunda birçok teknik eksiklikler sonucu sürdürülebilir üretim sağlanamamaktadır.

Türkiye'de özellikle durgun olan iç sularda yapılan kültür balıkçılığında balık ölümleri ile çok sık karşılaşılmaktadır. Genellikle, balık ölümleri suda çözünmüş oksijen seviyelerinin düşük olmasından kaynaklanmaktadır. Balığın büyümesini ve gelişimini etkileyen en önemli faktör suda çözünmüş oksijen konsantrasyonudur.

Türkiye Su ürünleri istatistikleri verilerine göre, iç sularda yaklaşık 450 milyon adet alabalık yetiştirildiği söylenebilir. Balık çiftliklerinde oksijen yetersizliğinden kaynaklanan kayıplar ekosistem dinamikleri, mevsim değişimleri, su kaynaklarındaki yosun ve fitoplankton yoğunluğu, aşırı balık stok yoğunluğu, yanlış yemleme gibi birçok faktöre bağlı olarak her yıl değişmektedir. Oksijen yetersizliğinin neden olduğu balık ölümlerinin %1 – 3 arasında olması durumunda, ortaya çıkacak ekonomik kaybın yılda 40 milyon TL olabileceği, stok yoğunluğunun arttırılamamasından kaynaklanan toplam ekonomik kaybın ise 100 milyon TL'ye kadar çıkabileceği tahmin edilmektedir.

Türkiye'nin iç sularındaki küçük ve orta ölçekli balıkçılık işletmelerinin çoğunda tespit edilen eksiklikler aşağıda sıralanmıştır:

1) Suda çözünmüş oksijen konsantrasyonu ölçümleri yapılmamaktadır.

2) Havalandırma sistemi yoktur.

3) Elektrik şebekesinden uzak noktalarda alternatif bir enerji kaynağı mevcut değildir.

Bu tez çalışmasında, yukarıda sıralanan tespitlere göre, küçük ve orta ölçekte üretim yapan balık çiftlikleri için su sıcaklığı ve sudaki çözünmüş oksijen miktarını ölçen, oksijen seviyesi düşünce otomatik olarak devreye giren, güneş enerjisi ile çalışan bir havalandırma sistemi geliştirilmiş ve prototip imalatları yapılmıştır.

2. MODEL ve SİMÜLASYON

Havalandırma sisteminin tasarımında ANSYS Fluent yazılım paketi kullanılarak venturi modeli oluşturulmuş, hava hızı ve basınç karakteristikleri simüle edilmiştir.

Tez çalışmasında Şekil 4.7'de gösterilen farklı büyüklüklerdeki üç plastik venturi enjektör modülü kullanılmıştır. V1, V2 ve V3 venturi enjektörleri şekil 5.16 ve 5.18'de gösterilen deney standında hava hızı ve vakum verileri esas alınarak test edilmiştir. En yüksek hava emme basıncı geliştiren V1, modülü havalandırma sisteminin imalatında kullanılmıştır.

Güneş panelinin Ankara koşullarında farklı eğim açıları, Matlab 2010b programı kullanılarak, yıllık, mevsimlik, yılda iki konum ve her ay için hesaplanmıştır. Sonuçlar esas alınarak, deneylerde kullanılan paneller güneye dönük olarak 24° (yıllık) eğim verilerek ayarlanmıştır.

3. SİSTEM TASARIMI ve KONSTRÜKSİYON

Yenilikçi bir havalandırma sisteminin tasarımında aşağıda sıralanan noktalar önemli rol oynamıştır:

- Pompa çıkış hattın kalınarak uygun bağlantılar ile basınç kayıpları azaltılmıştır.

- Pompa çıkışıyla aynı çaplarda nipel ve T-boru bağlantıları kullanılarak basınç kayıpları azaltılmıştır.
- Sonraki bağlantılarda uygun kademeli redüksiyon bağlantıları yapılmıştır.
- Pompa kapasitesi ile uygun venturi sayısı belirlenmiştir.
- Suda çözünecek oksijen miktarını arttırmak için uygun çaplı difüzör ve meme çapı saptanmıştır.

Geliştirilen havalandırma sisteminin pompa ile en uygun bağlantı şekli ile boru ve bağlantı parçalarının çapları aşağıdaki şekilde verilmiştir.

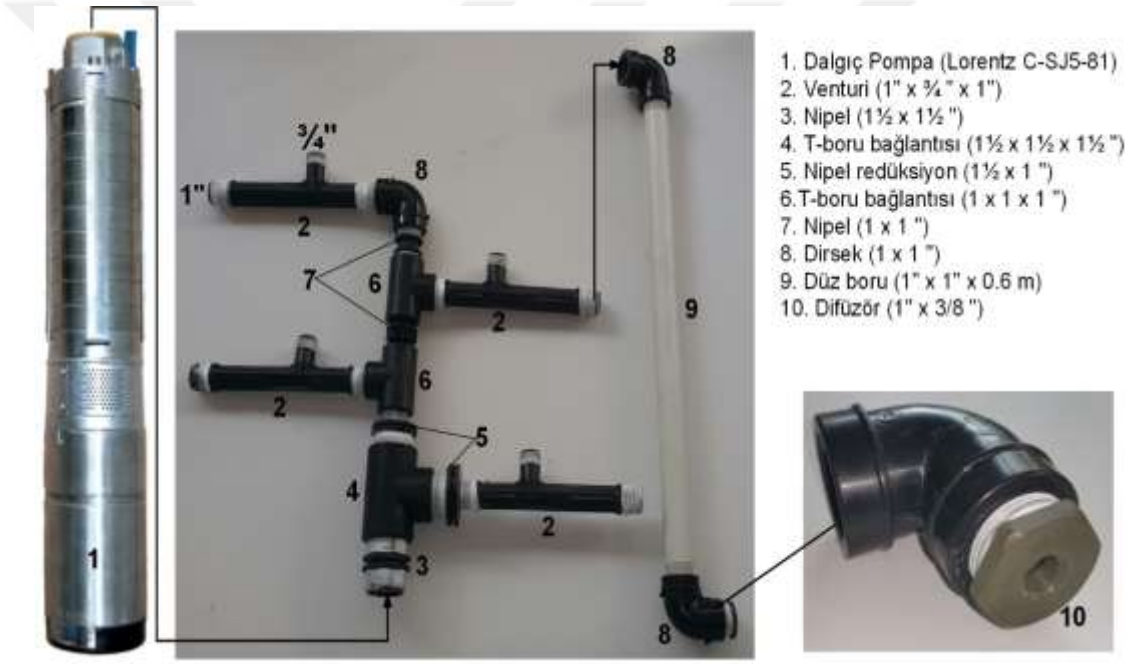

Şekil 1 Geliştirilen venturi enjeksiyon sistemi bağlantıları (Figure 5.5)

4. VERİ TOPLAMA CİHAZI ve METEOROLOJİ İSTASYONUNUN KURULUMU

Çevresel koşullardaki sıcaklık, bağıl nem, atmosfer basıncı, toplam güneş ışınımı, rüzgar hızı, rüzgar yönü, yağmur, su sıcaklığı değişimlerinin ölçümü için bir meteoroloji istasyonu tasarlanmıştır. Yüksek hassasiyete sahip yeni nesil sıcaklık (LMT86LP), bağıl nem (HIH5030), atmosfer basıncı (KP236N6165) sensörlerinin prob üzerine montajı ve kablo bağlantıları yapılmıştır. Bu sensörlerin güneşin direkt ışınımından etkilenmemesi

ve laminer akış sağlanması için özel olarak tasarlanmış 0.2 m çapında paslanmaz çelik güneş siperi imal edilmiştir. Meteoroloji istasyonuna yerleştirilen tüm sensörlerin CR1000 veri toplama cihazlarına bağlantıları yapılmış ve sensörlerin teknik özelliklerine göre 1 dakikalık aralıklarla ölçüm yapacak şekilde programlanmıştır. Meteoroloji istasyonundaki tüm sensörler ve CR1000 veri toplama cihazının güç gereksinimi güneş enerjisinden sağlanmıştır. Burada 60 W monokristal güneş paneli, 12 V 20 Ah kuru akü ve şarj kontrol cihazı kullanılmıştır.

Şekil 2 Meteoroloji istasyonu (Figure 4.3)

5. GÜNEŞ PANELİ ve AKÜ BAĞLANTILARI

Güneş paneli, akü ve şarj kontrol cihazı arasındaki bağlantılar aşağıdaki şekilde gösterildiği gibi yapılmıştır. PV güneş paneli ile şarj kontrol cihazı arasında kablo bağlantılarında kesit alanı 4 mm^2 ve akü bağlantılarında kesit alanı 16 mm^2 olan özel UV dayanıklı solar kablo kullanılmıştır:

1. Mono-kristal panel: 2 × 150 W=300 W'lık iki panel seri olarak bağlanmıştır. Galvaniz çelik delikli profiller kullanılarak eğim açısı 24° olarak ayarlanmıştır.
2. Poli-kristal panel: 245 W nominal güce sahip panel eğim açısı 0° olarak bağlanmıştır.
3. Akü bağlantıları: İki adet 12 VDC jel akü 24 VDC @ 100 Ah akü kapasitesi elde etmek için seri olarak bağlanmıştır.
4. Şarj kontrol cihazı: Akülerin şarj-deşarj işlemlerinin güvenilir aralıkta çalışması için uygun bağlantılar yapılmış ve çalışma aralıkları programlanmıştır.

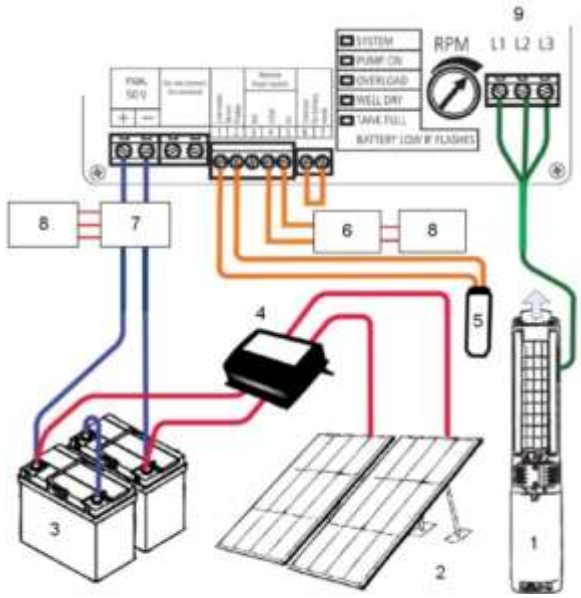

Şekil 3 Elektriksel bağlantıların şematik gösterimi (Figure 4.13)

1.Dalgıç pompa, 2. PV panel, 3. Akü, 4. Şarj kontrol cihazı, 5. Şamandıra, 6. Röle kartı, 7. Volt-akım sensörü, Jel akü, 8. Arduino Uno kartı, 9. Pompa kontrol cihazı

6. PROTOTİP GELİŞTİRME

Havalandırma sistemi venturi tip enjektörler kullanılarak hidrodinamik esaslara göre tasarlanmıştır. Pompa ve V1 (1" x ¾" x 1") venturi modülleri arasında 1" - 1½" PE boru ve bağlantı parçaları (T, dirsek, manşon, nipel, redüksiyon) iki prototip geliştirilmiştir. Her iki prototip için aynı bağlantıya sahip yukarıda gösterilen venturi sistemi kullanılmıştır.

Prototip I: Pompanın ve venturi sisteminin aşağıdaki şekilde gösterildiği gibi su içinde yüzdürülmesi amaçlanmıştır. 50 mm kalınlığında iki adet 0.8 x 0.8 m büyüklünde ekstrüde polistren yalıtım paneli kullanılmıştır. Büyüklüğü 0.3 x 0.3 m olan boyalı iki sac plaka arasında iki yüzdürme paneli üst üste yerleştirilerek pompa arasında cıvatalı sağlam bağlantılar yapılmıştır. Prototip I uygulamasında güneş paneli, kontrol panosu ve aküler sabittir. Seri bağlanmış 300 W (2 × 150 W) PV monokristal güneş paneli aşağıdaki şekilde gösterildiği gibi yatayla 24° açı yapacak şekilde güneye dönük yerleştirilmiştir. Güneş panellerinden gelen enerji 12 V 100 Ah kapasiteli 2 adet jel aküde depolanmıştır.

Şekil 4 Prototip I (Figure 5.6)

(1) Jel akü (100 Ah @ 12 V)
(2) Şarj kontrol cihazı (24 V @ 50 A)
(3) Pompa kontrol cihazı

Şekil 5 Açı ayarlı monokristal güneş panelleri ve konstrüksiyonu (Figure 5.7)

Prototip II: Sistemin tüm bileşenlerinin aşağıda gösterildiği gibi su üstünde yüzecek şekilde taşınması amaçlanmıştır. Yüzdürme platformu olarak ölçüleri 1.5 × 1 × 0.2 m olan iki tarafı galvaniz ve boyalı saç arasına yerleştirilmiş poliüretan sandviç panel kullanılmıştır. Prototip II uygulamasında sistemin tüm bileşenleri yüzer platform üzerine yerleştirilmiştir. Gücü 245 W olan polikristal PV güneş paneli platform üzerine yatay olarak bağlanmıştır. Güneş panellerinden gelen enerji, ikişer seri olarak bağlanan 12 V 100 Ah kapasiteli 2 adet jel aküde depolanmıştır.

Her iki havalandırma sistemi de dalgıç pompa, pompa kontrol cihazı, 4 adet venturi enjektör, boru bağlantı parçaları, PV güneş paneli, 2 adet jel akü, şarj kontrol cihazı, su geçirmez kontrol panosu, elektronik kontrol kartı, oksijen sensörü, su sıcaklık sensörü, galvaniz çelik profillerden oluşmaktadır.

Geliştirilen havalandırma sisteminin performans deneyleri için PVC/PE malzemeden yapılmış 4 m^3 hacmine sahip dairesel plastik havuz kullanılmıştır.

Şekil 6 Yüzer platformun plastik havuzda denemesi (Figure 5.17)

7. STANDARD TEST PROSEDÜRÜ

V1 venturi enjektörler esas alınarak bağlantıları yapılan iki prototip havalandırma sistemi, Prototip I ve Prototip II plastik havuzda test edilmiştir. ASCE (American Society of Civil Engineers) tarafından önerilen standart test prosedürüre göre test edilmiştir. Sayısal veriler için test havuzunda oksijen giderme ve oksijen kazandırma işlemleri sırasıyla gerçekleştirilmiştir. Havalandırma sistemlerine dinamik oksijen kazandırma yöntemi uygulanmıştır. Oksijen transfer katsayılarının saptanması için grafik yöntem kullanılmıştır.

Oksijen transfer katsayıları:

Normal koşullardaki su sıcaklıklarına göre farklı güç tüketimlerinde elde edilen oksijen transfer katsayıları aşağıdaki çizelgede verilmiştir. $(K_{La})_T$ oksijen transfer katsayıları 1.1 ve 5.55 h^{-1} arasında, standart oksijen transfer katsayıları 1.15 ve 5.42 h^{-1} arasında değişmiştir (Çizelge 1).

Çizelge 1 standart oksijen transfer katsayıları

P (W)	T_w (°C)	K_{LaT} (min^{-1})	K_{LaT} (h^{-1})	K_{La20} (h^{-1})
75	18	0.0183	1.10	1.15
100	22	0.0397	2.38	2.27
150	18	0.0630	3.78	3.96
200	18	0.0693	4.16	4.36
250	21	0.0815	4.89	4.78
300	21	0.0925	5.55	5.42

Performans Test Sonuçları : Standart oksijen transfer hızı (SOTR), standart havalandırma etkinliği (SAE) ve standart oksijen transfer etkinliği (SOTE)'den oluşan performans parametreleri aşağıdaki çizelgede (Çizelge 2) gösterildiği gibi farklı güç girdileri için verilmiştir.

Çizelge 2 Venturi havalandırma sistemi performansı

Güç tüketimi (W)	SOTR (kgO_2/h)	SAE (kg O_2/kWh)	SOTE (%)
75	0.042	0.560	4.7
100	0.082	0.820	7.0
150	0.144	0.960	10.7
200	0.158	0.790	10.3
250	0.174	0.696	9.6
300	0.197	0.657	9.4

Pompa farklı güçlerde çalıştırılırken, O_2 ekleme süreçlerinde bazı farklılıklar elde edilmiştir. Havalandırma sistemine ilişkin standart oksijen transfer hızı ve standart havalandırma etkinliği verileri elde edilmiştir. Buna göre, en yüksek standart oksijen transfer hızı 300 W için 0.197 kgO_2/h olarak saptanmıştır. Buna karşın, en yüksek standart havalandırma ekinliği 150 W güç kullanımında 0.96 kg O_2/kWh olarak elde edilmiştir. Deney sonuçlarına göre, farklı venturi bağlantı şekilleri içerisinde en etkili sonuçların alındığı söylenebilir. Güç-SAE verileri karşılaştırıldığında, standart havalandırma etkinliği 0.56–0.96 (kg O_2/kWh) arasında gerçekleşmiştir. Güç ile SAE-SOTR-SOTE'nin değişimleri aşağıdaki şekillerde grafik olarak gösterilmiştir. Bu değerler, (Dong vd. 2012) tarafından 0.06 ile 0.21 kg O_2/kWh olarak verilen performanslardan daha yüksektir. Standart oksijen transfer etkinlikleri 150 ve 200 W güç girdileri için sırasıyla 10.7 ve 10.3 olarak elde edilmiştir.

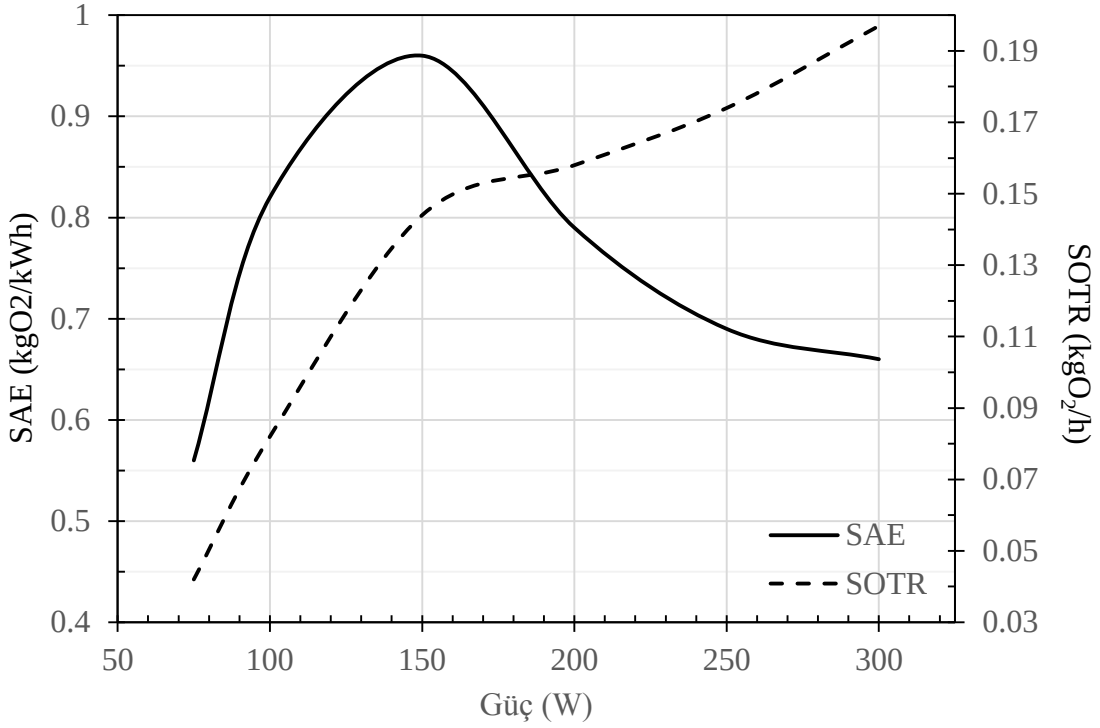

Şekil 7 Pompa güç tüketimi ile SOTR ve SAE'nin değişimi (Figure 5.25)

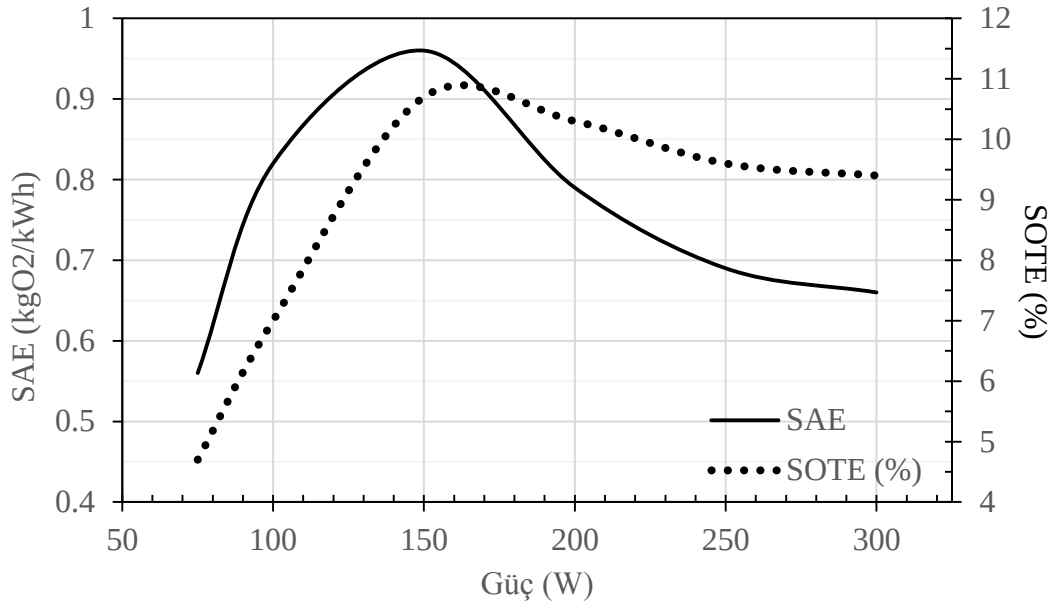

Şekil 8 Pompa güç tüketimi ile SOTR ve SOTE'nin değişimi (Figure 5.26)

ASCE tarafından önerilen test prosedürlerinden farklı olarak, havalandırma sistemi için oksijen transfer modeli tanımlanmıştır. Bu modele göre, aşağıdaki çizelgede verilen sıcaklık (T) ve atmosferik basınç (P_{atm}) koşulları için farklı güç (P), suyun hacimsel debisi (Q_w), oksijenin kütlesel debisi (m_o), oksijen transfer hızı (OTR), oksijen transfer faktörü (OTF), oksijen transfer etkinliği (η) gibi parametreler hesaplanmıştır.

Pompa 300 W güçte çalıştırılırken 5 m^3/h su akışı sağladığında, venturi girişinden geçen hava hızı 2.3 m/s olarak ölçülmüştür. Dört venturinin ürettiği hava kütlesel debisi 9 kg/h, oksijen kütlesel debisi 2.1 kg/h'dir. Havalandırma sisteminin oksijen enjeksiyon etkinliği 7 kg O_2 kWh^{-1}, oksijen transfer faktörü 0.6 kg O_2 kWh^{-1}, oksijen transfer etkinliği %8.5'dir. Kalan oksijen atmosfere transfer edilmektedir.

Çizelge 3 Havalandırma sistemi havuz performans verileri

P (W)	T_w (°C)	P_{atm} (kPa)	Q_w (m^3/h)	m_o (kg O_2/h)	OTR (kg O_2/h)	OTF (kg O_2/kWh)	η (%)
75	18.2	91.9	3.0	0.913	0.0378	0.504	4.14
100	21.9	91.9	3.6	1.188	0.0754	0.754	6.35
150	18.0	91.8	4.0	1.370	0.1299	0.866	9.48
200	18.1	91.9	4.5	1.551	0.1430	0.715	9.22
250	20.9	91.7	4.7	1.827	0.1582	0.633	8.66
300	21.0	91.7	5.0	2.102	0.1796	0.599	8.54

8. HAVALANDIRMA SİSTEMİNİN BALIK ÇİFTLİĞİNDE DENENMESİ

Prototip II havalandırma sistemi Ankara Üniversitesi Ziraat Fakültesi Çifteler Su Ürünleri Araştırma ve Uygulama İşletmesi alabalık havuzlarında 20-24 Temmuz 2015 tarihleri arasında test edilmiştir. Test denemeleri, büyüklükleri 6 × 10 m ve derinlikleri 0.75 m olan benzer iki havuzda yapılmıştır. Bu havuzlardan birisinde havalandırma sistemi çalıştırılmış olup; diğerine herhangi bir havalandırma sistemi yerleştirilmemiştir. Her havuza 140 g ağırlığında 2600 adet gökkuşağı alabalığı konulmuştur. Yemleme rejimleri ve tüm kültürel işlemler eş zamanlı yapılmıştır. Havalandırma sisteminin çalıştırıldığı test havuzunda balık ölümleri ile karşılaşılmamıştır. Ancak, havalandırma sisteminin olmadığı kontrol havuzunda günde 3 ve 12 arası adet balık ölümü tespit edilmiştir.

Şekil 9 havalandırma sistemi test denemeleri (Figure 5.29)